NERO

NUUK ECOLOGICAL RESEARCH OPERATIONS

7th Annual Report 2013

GEM

Greenland Ecosystem Monitoring

Aarhus University
DCE – Danish Centre for Environment and Energy

NUUK ECOLOGICAL RESEARCH OPERATIONS

7th Annual Report 2013

AARHUS
UNIVERSITY
DCE – DANISH CENTRE FOR ENVIRONMENT AND ENERGY

Data sheet

Title: Nuuk Ecological Research Operations
Subtitle: 7th Annual Report 2013

Editors: Lillian Magelund Jensen and Torben Røjle Christensen
Department of Bioscience, Aarhus University

Publisher: Aarhus University, DCE – Danish Centre for Environment and Energy
URL: http://dce.au.dk

Year of publication: 2014

Please cite as: Jensen, L.M. and Christensen, T.R. (eds.) 2014. Nuuk Ecological Research Operations 7th Annual Report, 2013, Aarhus University, DCE – Danish Centre for Environment and Energy. 94 pp.

Layout and drawings: Tinna Christensen, Department of Bioscience, Aarhus University
Front cover photo: Kobbefjord in late June. Photo: Katrine Raundrup
Back cover photo: Arctic fritillary (*Clossiana chariclea*) in late July. Photo: Katrine Raundrup

ISSN: 1904-0407
ISBN: 978-87-93129-21-4

Number of pages: 94

Internet version: The report is available in electronic format (pdf) on www.nuuk-basic.dk/Publications and on www.dce.au.dk

Supplementary notes: Nuuk Basic Secretariat
Department of Bioscience, Aarhus University
P. O. Box 358, Frederiksborgvej 399
DK-4000 Roskilde

E-mail: nuuk-basic@au.dk
Phone: +45 30783161

Nuuk Ecological Research Operations (NERO) is together with Zackenberg Ecological Research Operations (ZERO) operated as a centre without walls with a number of Danish and Greenlandic institutions involved. The two programmes are gathered under the umbrella organization Greenland Ecosystem Monitoring (GEM). The following institutions are involved in NERO:
Department of Bioscience, Aarhus University: GeoBasis, BioBasis and MarineBasis programmes
Greenland Institute of Natural Resources: BioBasis and MarineBasis programmes
Asiaq – Greenland Survey: ClimateBasis programme
University of Copenhagen: GeoBasis programme

The programmes are coordinated by a secretariat at the Department of Bioscience at Aarhus University, and are financed with contributions from:
The Danish Energy Agency
The Environmental Protection Agency
The Government of Greenland
Private foundations
The participating institutions

Contents

Summary for policies makers

Lillian Magelund Jensen and Torben Røjle Christensen

The 2013 field season in the Kobbefjord area started 10 January and continued until 11 December. During this period 47 scientists and logisticians spent 534 and 36 'man-days' in the study area, respectively.

From the beginning of March to mid-April a sea ice campaign in the fjord of Kanajorsuit, a small tributary of Godthåbsfjord was carried out by the Arctic Science Partnership (University of Manitoba, Canada, Aarhus University, Denmark and Greenland Institute of Natural Resources) in collaboration with the University of Washington, USA.

Nuuk Ecological Research Operation is involved in several larger international research projects. Greenland Ecosystem Monitoring (GEM) is involved in the EU projects 'International Network for Terrestrial Research and Monitoring in the Arctic' (INTERACT) and 'Svalbard Integrated Arctic Earth Observing System' (SIOS). In 2013, four projects (nine researchers) received support for 137 bed nights from INTERACT Transnational Access. Researchers from the GEM programme are also involved in/associated with the Arctic Research Centre at Aarhus University and Arctic Science Partnership.

Results from the Nuuk Basic monitoring programme are continuously published in scientific papers and popular science articles. Furthermore, data from the Nuuk Basic programme is freely available and was in 2013 used for reporting purposes in a number of international fora and by a number of externally funded research projects.

In 2013, more than twelve peer-reviewed papers were publish by the researchers from the Nuuk Basic programme and from externally funded research projects.

Executive summary

Jakob Abermann, Birger Ulf Hansen, Peter Aastrup, Thomas Juul-Pedersen and Lillian Magelund Jensen

Introduction

The year 2013 was the seventh year of operation of the fully implemented Nuuk Basic programme (including both a terrestrial and a marine component), and it was the fifth year with complete annual time series for all sub-programmes.

ClimateBasis

The ClimateBasis is dedicated to describing the climatological and hydrological conditions in Kobbefjord. Two automatic climate stations, C1 and C2, two automatic hydrometric stations, H1 and H2, and three diver stations, H3, H4 and H5, monitor the physical parameters related to climate and hydrology. The two climate stations are placed next to each other to ensure data continuity and fill data gaps.

The mean annual air temperature at the climate station in Kobbefjord was 0.2 °C in 2013, which is exactly the average since the programme started in 2008. Generally, winter months above average were balanced by summer months below average and May was unusually cold with –0.5 °C on average. There was no freezing between 9 June and 14 September.

Hydrological measurements in the Kobbefjord basin started in 2006 at H1, at H2, H3 and H4 in 2007 and at H5 in 2008. Manual measurements of discharge were carried out at all sites but H2 in 2012 and only at H1 in 2013. H1 and H2 are measuring throughout the year, while sensors at H3, H4 and H5 are set up in early spring when the rivers are free of snow and ice, and taken down in late autumn before the river freezes.

For H1, which is placed at the main river in Kobbefjord, the total discharge during the hydrological year 2011/2012 was 49.06 mill. m^3, in 2012/2013 it was 42.41 mill. m^3. The peak discharge in 2012 was recorded 6 July, while it was the 1 October in 2013. The two years seasons differ notably, with 2012 being more influenced by snowmelt and 2013 by late-season precipitation.

GeoBasis

The 2013 season was the sixth full season for the GeoBasis programme with a field season between May and late September. However, due to cooperation with other research projects the programme continued until late October. Data collected by the Danish Meteorological Institute shows that in 2013 the annual mean air temperature in Nuuk reached –0.3 °C, i.e. 0.5 °C colder in Kobbefjord (see above), and 1.1 °C warmer than its long-term norm. The warmest month was July with 7.7 °C, which was 1.0 °C warmer than normal but 2.4 °C colder than the previous July, which was the warmest July during the period 1866-2013. The coldest month in 2013 was December with –7.6 °C was 0.9 °C colder than normal.

The ice covering of the lakes in the Kobbefjord drainage basin was formed later in the winter 2012/2013 than in the previous winters. The break-up of the ice cover on the lakes was approximately 7-8 days later than the average for the period 2007-2012. When comparing the snow cover survey 2013 with the snow cover survey in the three previous years, the maximum snow depth of 60 cm makes the winter 2012/13 the second lowest snow depth winter since continuous measurements of snow depth started only exceeded by the winter 2009/2010 with a lesser 25 cm. The average density for the sites was 297 kg m^{-3}, which is a bit lower than previous winters.

At the micrometeorological stations in Kobbefjord, the temperatures during the spring (March to April) were higher than normal and March with –3.4 °C was the highest mean monthly air temperature for March in the period 2007-2013. In 2013 May, June and July with respectively

–0.6, 6.1 and 8.9 °C were the coldest mean monthly air temperatures measured in the period 2007-2013. These measurements are in line with the air temperature measured in Nuuk located 30 km away. For the GeoBasis monitoring period 2007-2013, the minimum monthly mean air temperature was –13.5 °C measured at SoilFen in February 2008 and the maximum monthly mean air temperature was 11.7 °C measured in July 2012. The pattern of high monthly mean air temperature in March 2013 was also seen in the data from M500. In 2008-2012, the mean air temperature in July at the M500 station was between 7.6 °C and 10.4 °C; in 2013, it was only 6.6 °C. At the three automatic soil stations in the area; SoilFen, SoilEmp and SoilEmpSa the soil inter-annual temperature variations in 2013 were quite similar to those documented in previous years and with an average soil temperature of 2.9 °C, 2013 is placed between 2011 with 2.3 °C and 2012 with 3.4 °C.

In 2013, thirty-three water samples were collected from end May to start October, which is a field season one month shorter than previous year due to a very late snow-/icemelt. *In situ* measurements of river water temperature, conductivity and pH were conducted along with the water sampling. The water temperature varies through the season 2013 as it did in field season 2009 and 2011. The minimum river water temperature was 1.0 °C from end May to mid-June which was 1.0 °C lower than the previous years and the water temperature peaked with a maximum temperature of 12.9 °C in the beginning of August which was 3.7 °C lower and three weeks later than 2012. The conductivity measurements showed a normal decrease in conductivity within the snow-melting period from 20 µSc m^{-1} to a level of 14 ± 1.5 µSc m^{-1}. From the beginning of July and through the rest of the field season, the conductivity shows no significant trend, which is normal for the period. pH shows a normal trend from 6.2 in the beginning of the field season to 7.6 in the beginning of August, followed by some variation due to rain event in the autumn.

In early June, when measurements started, average CH_4 fluxes were below 2 mg CH_4 m^{-2} h^{-1}. As the season progressed, emissions increased and reached a peak in early August, amounting to approximately 6.2 mg CH_4 m^{-2} h^{-1}. This CH_4 emission peak level is lower than in 2009 and 2012, but higher than in 2008, 2010 and 2011. The variation between years is likely related to variations in timing of snowmelt, meteorological conditions and primary production in the fen.

After the CH_4 emission peak in early August, CH_4 fluxes decreased steadily and reached approximately 1 mg CH_4 m^{-2} h^{-1} in late September. Overall, the observed temporal CH_4 flux pattern of the Kobbefjord fen displays low shoulder season emissions with a dome-shaped peak during the growing season.

Eddy covariance measurements of the CO_2 and H_2O exchange in the fen were initiated 29 May and lasted until 22 October. Highest daily spring time emission (0.7 g C m^{-2} d^{-1}) was measured 11 June, which coincided with high air temperature. As vegetation developed, photosynthetic uptake of CO_2 started, and 23 June the fen ecosystem switched from being a net source to a net sink of atmospheric CO_2 on a daily basis. The period with net CO_2 uptake in 2013 lasted until 24 August. During this period, the fen accumulated –67.3 g C m^{-2}, which is in the higher end of the measurement record. Maximum daily accumulation rate amounted to –2.7 g C m^{-2} (measured 11 August), which is also in the higher end of the range based on previous years' measurements. By 24 August, respiration processes exceeded the fading photosynthesis and the ecosystem returned to a net source of atmospheric CO_2. In the beginning of this period, there is plenty of fresh litter available and soil temperatures remain relatively high, allowing decomposition processes to continue at a decent rate. Highest daily emission during autumn was measured 6 September (1.2 g C m^{-2} d^{-1}). During the entire measuring period (144 days), the fen constituted a sink for atmospheric CO_2 amounting to –24.2 g C m^2.

In 2011, GeoBasis installed a new energy balance station in cooperation with the INTERACT programme at a new site over the heath vegetation. The remote placing on the heath site and the use of fuel cells have caused numerous breaks in the time series although the station was visited frequently even outside the normal field season. In 2014, a more stable power supply will be installed.

BioBasis

Results of the seventh year of the BioBasis monitoring programme at Nuuk are presented.

Reproductive phenology: In *L. procumbens* and *S. acaulis* vegetative phenology is similar to that of 2012, although there was a tendency to produce larger numbers of flowers in most plots. The timing of 50 % flowering was within the same range as previous years. The flower bud production, the onset of flowering, and the peak flower production of *L. procumbens* occurred at approximately the same time as in 2012. A second bud production was recorded 3 September Day of Year (DOY) 246. All plots produced more flowers in 2013 than in 2012. The first senescent flowers were recorded about the same time as in 2012. Timing of budding, flowering and senescence in *S. acaulis* was later than in 2012. *S. glauca* buds were observed a week later compared to the earliest year 2010. First flowering male catkins were observed 13 June (DOY 164) and first female catkins 18 June (DOY 169). The first female flowers with hair were observed 11 July. A higher number of flowers were produced in 2013 than in 2012.

During April the area was exposed to two weeks of severe snowmelt, followed by heavy snowfall in May, resulting in late snowmelt. A preliminary review of data related to flowering indicates that 2013 was characterized by no larval outbreak of the noctuid moth *E. occulta*, and large numbers of flowers produced in *L. procumbens* and *S. glauca* compared to 2012.

Vegetation greening: *Empetrum nigrum* reached the highest Normalised Difference Vegetation Index (NDVI) values of all the species, and NDVI was consistently high throughout the season. The values were at the same level or higher than in 2012, which was the highest recorded so far. Generally, the vegetation greening in 2013 was very similar to that in 2012. The NDVI values were in many cases higher throughout the season compared to previous years, with an intermediate to late peak. The vegetation seems to have recovered after the outbreak of the noctuid moth larvae.

Carbon dioxide exchange: Since 2008 carbon dioxide exchange has been measured including manipulation experiments simulating higher temperatures and increased cloud cover. Generally, all plots functioned as sinks for atmospheric CO_2 at the time of the measurement (midday). In October, Net Ecosystem Exchange (NEE) was generally close to zero. Similar to previous years the uptake of CO_2 was higher in control plots compared to plots with elevated temperature and shaded plots. The differences between treatments during 2013 were in general similar to previous years. Together with 2012, the flux amplitudes in 2013 were higher compared with previous years.

UV-B exclusion plots: Measurements of chlorophyll fluorescence as a proxy for plant stress were carried out. The total performance index (PI_{total}) integrates the measurements, and the PI_{total} were sensitive to UV-B exclusion in both *V. uliginosum* and *B. nana*. The seasonal plant stress level was reduced when the plants were protected from UV-B radiation.

Arthropods: Pitfall traps were established from 28 May (DOY 148) through 13 June (DOY 164) and they all worked continuously until 7 October (DOY 280) when the liquid began to freeze. In 2013, arthropods were caught during 4511 trap days (including 4057 pitfall-trap days and 454 window-trap days). Parts of the samples are being sorted at Department of Bioscience, Aarhus University, Denmark. The material sampled in the 2013 season is currently stored in 70 % ethanol at Greenland Institute of Natural Resources.

Microarthropods: In the season 2013, the sampling of microarthropods was reduced from the standard of eight samples per plot to four samples per plot. Sampling was carried out three times during the season. The samples have not been analysed yet. The material sampled and extracted is currently stored in 70 % ethanol at the Greenland Institute of Natural Resources. Materials collected from research projects completed in 2012 in Kobbefjord and Zackenberg were further analysed. For project description and results see chapter 6.

Birds: No survey of breeding passerines was carried out in 2013. A breeding pair of white-tailed eagles *Haliaeetus albicilla* was observed on the mountainside northeast of the research house in Kobbefjord. All four species of passerines (Lapland buntings, snow buntings, northern wheatears, and redpolls) were already present at the time of the first census, and the survey was carried out until no more observations were made at any census point.

The total number of passerines has varied between the years. In 2013, the northern wheatear was the most abundantly observed passerine, and the only species to have more observations per census in 2013 than in 2012. Although there is some variance from year to year, the number of observations of northern wheatears is usually at its maximum in August.

Mammals: The Kobbefjord catchment area is only sparsely populated with mammals. In 2013, at least two different foxes have been observed on several occasions; tracks, faeces and barks have been observed/heard throughout the season. One Arctic hare was observed.

Lakes: 2013 was relatively wet, particularly during the winter period. It was the coldest summer registered during the monitored period and the ice-free period lasted less than 132 days in Badesø and less than 124 in Qassi-sø. Average total nitrogen concentration in both lakes was the lowest measured and average total phosphorus was generally low in Badesø. During the last three years, chlorophyll *a* has stabilized around 0.8 µg Chl *a* l^{-1}, following an increasing trend during the 2008-2010 period. Zooplankton biomass is generally higher in Qassi-sø compared to Badesø, which is consistent with the lack of fish in Qassi-sø. During the past three years an increasing zooplankton biomass is observed in Badesø; this can partly be due to reduced predation pressure, corresponding well with reduced fish abundance in 2013 compared to 2008, when the first fish investigation was undertaken.

MarineBasis

The MarineBasis programme in Nuuk was initiated in late 2005 and this report presents data and results from the eight full year of monitoring. The programme represents the marine component of the comprehensive ecosystem monitoring programme Nuuk Basic. The programme samples key oceanographic parameters including sea ice conditions, physical and chemical oceanography, biological components of the water column and sediment as well as observations of whales and sea birds. The collected data provide essential information for understanding and describing the ecosystem. The long-time series also makes it possible to study, identify and quantify seasonal and inter-annual patterns and variability, as well as aiming to identify possible effects of climate related changes. A parallel marine programme has been operating for eleven years at the high Arctic Zackenberg/Daneborg area (MarineBasis-Zackenberg); both programmes collaborate closely and supplement each other.

During 2013 satellite images (AMSR) showed that sea ice ('West Ice') covered most of the Baffin Bay region until May when the ice began retreating, reaching a minimum during July-September. Sea ice formation from the north started in October, covering much of Baffin Bay by late December. Satellite images (MODIS) of the Godthåbsfjord system showed that sea ice was limited to the smaller fjord branches and the innermost part, as observed in previous years. Part of the sea ice and glacial ice is exported from the fjord in bursts, which is monitored by a camera cross section of the fjord. Unfortunately, no images were taken during much of 2013, but the camera system has been reengaged.

The programme includes measurements of abiotic and biotic hydrographical parameters during the monthly sampling programme in the outer sill region, along with a length and cross section of the fjord. These measurements showed a deep coastal inflow of warm and saline water during winter. Tidal forces create vertical mixing in the outer sill region ('Main Station', GF3) during winter and spring; as a result the water column depicts largely homogenous temperatures, salinities and phytoplankton biomass (i.e. chlorophyll *a*) with depth. Still, the length section shows that an early stratification with high surface phytoplankton biomasses exists within the fjord during spring. Primary production and the biomass of phytoplankton increases in spring, due to the improving light conditions. This production lowers nutrients levels, particularly in the photic zone. Increase freshwater run-off from land, along with icemelt, solar heating of the surface layer and air-sea heat exchange, strengthen the pycnocline, thus withstanding vertical mixing in the outer sill region. A second phytoplankton bloom is observed during summer. Decreasing freshwater run-off during autumn weakens the stratification within the fjord and vertical mixing of the water column re-established in the outer sill region.

The phytoplankton community in outer sill region was mainly comprised of haptophytes *Phaeocystis* sp. and diatoms throughout the year, as observed in previous years. *Phaeocystis* sp. dominated the phytoplankton community from March-June and surprisingly again in September, while diatoms such as *Thalassiosira* spp. and *Chaetoceros* spp. were the dominant groups during winter, autumn and in July. The zooplankton abundances were generally lower than in previous year. However, cirripedia nauplii still dominated in spring, while copepod nauplii, copepods and rotifers dominated during summer. The species composition of copepods also resembled previous years dominated by *Microsetella norvegica*, although *Oithona* spp. contributed significantly during summer. The fish larvae show inter-annual variation in abundances. In general, sand eel (*Ammodytes* sp.) larvae dominate the fish larvae assemblage in February/March, Arctic shanny (*Stichaeus punctatus*) larvae dominates in April/May and capelin (*Mallotus villosus*) larvae in July-September. In 2013, the highest concentration of fish larvae in the outer sill region was observed in February, dominated by sand eel larvae, and in July, dominated by capelin larvae. The length section showed the highest fish larvae abundances around the outer sill region, while in certain years the highest numbers has been recorded on Fyllas Banke, mainly due to sand eel larvae. Atlantic cod larvae were only found within the fjord. The shellfish larvae community showed the characteristic peak of *Pandalus* sp. in May, while *Chionoecetes opilio* and *Hyas* spp. also peaked in May, which is one month earlier than in previous years. In the outer sill region *Ctenophora,* jellyfish and/or *Sagitta* spp. dominated the community in all months, except from April to June were *Pandalus* spp., *Chionoecetes opilio* and *Hyas* spp. became more abundant.

Vertical sinking flux of organic material showed one of the highest fluxes of total particulate carbon during the entire monitoring programme. The chlorophyll *a* sinking flux increased in parallel with the phytoplankton biomass during spring, followed by a decrease in fluxes during post-bloom conditions in June. The subsequent summer phytoplankton production resulted high sinking fluxes again in September. Several trap arrays were unfortunately lost or grounded (i.e. samples lost), due to unusually high drift speeds of the trap array and in a direction not common at previous samplings.

The benthic community increased the oxygen uptake into the sediment during spring and summer, when primary production in the photic zone and sinking flux were highest. Elevated oxygen utilization during spring and summer also resulted in a shallower oxic zone. Previous monitoring of benthic fauna and flora has established a solid baseline for future comparisons. Therefore, monitoring of benthic fauna and flora has focused on the intertidal species since 2012, which is expected to response strongly to regional temperature changes. The macroalgae knotted wrack *Ascophyllum* showed a considerably faster tip growth compared to the previous year. The increased growth rate likely reflect that ice cover was extremely limited during the winter 2012/2013 and the inner part of Kobbefjord at the sampling site did not freeze at all. Studies in the intertidal zone have shown that abundance of the blue mussel *Mytilus cf edulis* in the area appears to be regulated by factors such as wave exposure, ice and winter mortality due to low temperatures. Cages with mussels deployed in 2012 were collected in 2013, but deformed metal cages and crushed shells clearly indicated that high mortality was caused by heavy ice scouring during the winter of 2012/2013. This winter stands out from other years by having almost no fast ice in the inner part of the fjord. The cage design and placement in the field has been changed in an attempt to reduce sensitivity to ice scouring.

Two major seabird colonies near Nuuk are monitored for the MarineBasis programme, but additional colonies are also included in this report. The Qeqertannguit bird colony holds the largest diversity of breeding seabirds in the Nuuk area and the colony is influenced by legal and illegal egg harvesting. Arctic tern was not observed at the island and no nests were found. Complete absence of Arctic tern on Qeqertannguit was also recorded in 2008. Small and mid-sized colonies of Arctic tern in Greenland are known to fluctuate considerably in population size. Only one breading pair and one large chick of kittiwake were observed here in 2013. In 2012, kittiwake was not breeding on the island at all. In contrast, the number of Iceland gulls increased in 2013 after a minimum in

2012. Another seabird colony (Nunngarussuit) in the Nuuk area showed the highest numbers of two species of guillemots since 2008. All the monitored colonies showed the lowest recorded numbers of kittiwakes throughout the time series.

A photo-identification programme is used to estimate the number of humpback whales *Megaptera novaeangliae* present and returning to the Godthåbsfjord system. Photos were collected during 2013, but due to temporary lack of personnel they were not analysed in time for this report. However, this study have shown that individual whales has a strong site fidelity for Godthåbsfjord, i.e. returning to the area, and these individuals also stay the longest within the fjord during each year.

Research projects

In 2013; six different research projects were carried out, two of them in cooperation with Nuuk Ecological Research Operations. The research projects focused on different biological topics in the limnic and terrestrial compartment of the ecosystem. The research projects are presented in Chapter 6.

Bog bilberry, Vaccinium uliginosum *(top),* Alpine azalea, Loiseleuria procumbens *(middle) and stiff clubmoss,* Lycopodium annotinum *(bottom). Photo: Katrine Raundrup.*

1 Introduction

Lillian Magelund Jensen and Torben Røjle Christensen

The year 2013 was the seventh year of operation of the fully implemented Nuuk Basic programme (including both a terrestrial and a marine component), and it was the fifth year with complete annual time series for all sub-programmes. The 2013 field season in the Kobbefjord area started 10 January and continued until 11 December. During this period 47 scientists and logisticians spent 534 and 36 'man-days' in the study area, respectively.

Funding

Nuuk Basic is funded by the Danish Energy Agency and the Environmental Protection Agency with contributions from Greenland Institute of Natural Resources, Asiaq – Greenland Survey, Aarhus University and University of Copenhagen. Aage V. Jensen Charity Foundation has generously provided most of the necessary research infrastructure, including boats, research house, boathouse, warehouse and office and accommodation facilities at Greenland Institute of Natural Resources.

Sea ice campaign

From the beginning of March to mid-April a sea ice campaign in the fjord of Kanajorsuit, a small tributary of Godthåbsfjord was carried out by the Arctic Science Partnership (University of Manitoba, Canada, Aarhus University, Denmark and Greenland Institute of Natural Resources) in collaboration with the University of Washington, USA. Different strategies were applied to measure the gas dynamics within the ice and combined with rate measurements of primary production and bacterial processes. Measurements included in the campaign was: sea ice profiles of greenhouse gasses, high-resolution pH profiles, Ikaite concentration, primary production, bacterial uptake of Choline, *in situ* flux measurements using eddy correlation and potential rates of processes involved in the nitrogen cycle.

International cooperation

Nuuk Ecological Research Operation is involved in several larger international research projects. Greenland Ecosystem

Diapensia, Diapensia lapponica. *Photo: Katrine Raundrup.*

Monitoring (GEM) is involved in the EU projects 'International Network for Terrestrial Research and Monitoring in the Arctic' (INTERACT) and 'Svalbard Integrated Arctic Earth Observing System' (SIOS). In 2013, four projects (nine researchers) received support for 137 bed nights from INTERACT Transnational Access. Researchers from the GEM programme are also involved in/associated with the Arctic Research Centre at Aarhus University and Arctic Science Partnership.

Outreach

Results from the Nuuk Basic monitoring programme are continuously published in scientific papers and popular science articles. Furthermore, data from the Nuuk Basic programme is freely available and was in 2013 used for reporting purposes in a number of international fora and by a number of externally funded research projects.

In 2013, more than twelve scientific papers were publish by the researchers from the Nuuk Basic programme and from externally funded research projects.

Further information

Further information about the Nuuk Ecological Research Operations (NERO) programme is collected in previous annual reports, which can be found on the NERO website www.nuuk-basic.dk. Much more information is available on the NERO website: www.nuuk-basic.dk including manuals for the different monitoring programmes, a database holding data from the monitoring, up-to-date weather information, a NERO bibliography and a collection of public outreach papers in PDF-format.

The NERO programme's address is:

Nuuk Basic Secretariat
Department of Bioscience,
Aarhus University
P.O. Box 358
Frederiksborgvej 399
DK-4000 Roskilde
Denmark
Phone: +45 30 78 31 61
E-mail: nuuk-basic@au.dk
Website: www.nuuk-basic.dk

Greenland Institute of Natural Resources provides the logistics in the Nuuk area:

Logistics Coordinator
Greenland Institute of Natural Resources
P.O. Box 570
Kivioq
3900 Nuuk
Greenland
Phone: +299 55 0 562
E-mail: heph@natur.gl
Website: www.natur.gl

Labrador tea, Ledum palustre. *Photo: Katrine Raundrup.*

2 Nuuk Basic

ClimateBasis programme

Jakob Abermann, Per Hangaard, Louise Holm Christensen, Dorthe Petersen and Majbritt Westring Sørensen

The ClimateBasis is dedicated to describing the climatological and hydrological conditions in Kobbefjord. Two automatic climate stations, C1 and C2, two automatic hydrometric stations, H1 and H2, and three diver stations, H3, H4 and H5, monitor the physical parameters related to climate and hydrology. In 2012, a small mountain glacier on the northern side of the basin had been included in the programme as an strategic initiative in order to understand the cryospheric component of the water-cycle.

The location of the different stations can be seen in figure 2.1. ClimateBasis is operated by Asiaq – Greenland Survey.

2.1 Meteorological data

In 2013, the climate stations in Kobbefjord were visited seven times by Asiaq personnel. The maintenance of the stations included reference tests of the parameters. Furthermore, a new UV Sensor has been set up, an Iridium Satellite link has been installed and the temperature sensors have consequently been changed to 4-Wire Bridges. The problem of overcharging the batteries through the wind mill has been solved by including a new regulator, all batteries have been changed, and the malfunctioning ones transported back to Nuuk. A full description of the climate stations is given in Iversen et al. 2008.

This annual report describes the sixth full year of data for all climate parameters and refers to data collected during the period from 1 January to 31 December 2013.

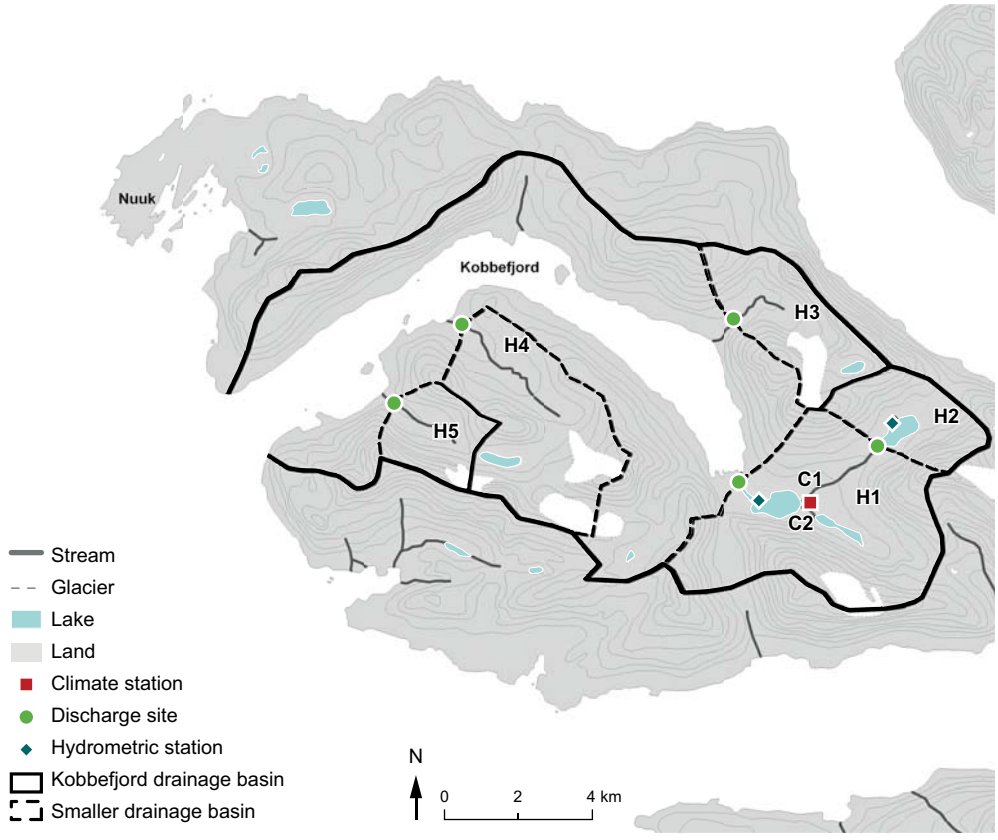

Figure 2.1 Location of the climate station (square), the hydrometric (H1, H2) and diver stations (H3, H4, H5) in Kobbefjord together with the drainage basins of Kobbefjord and the drainage basin for the hydrometric stations and the diver stations.

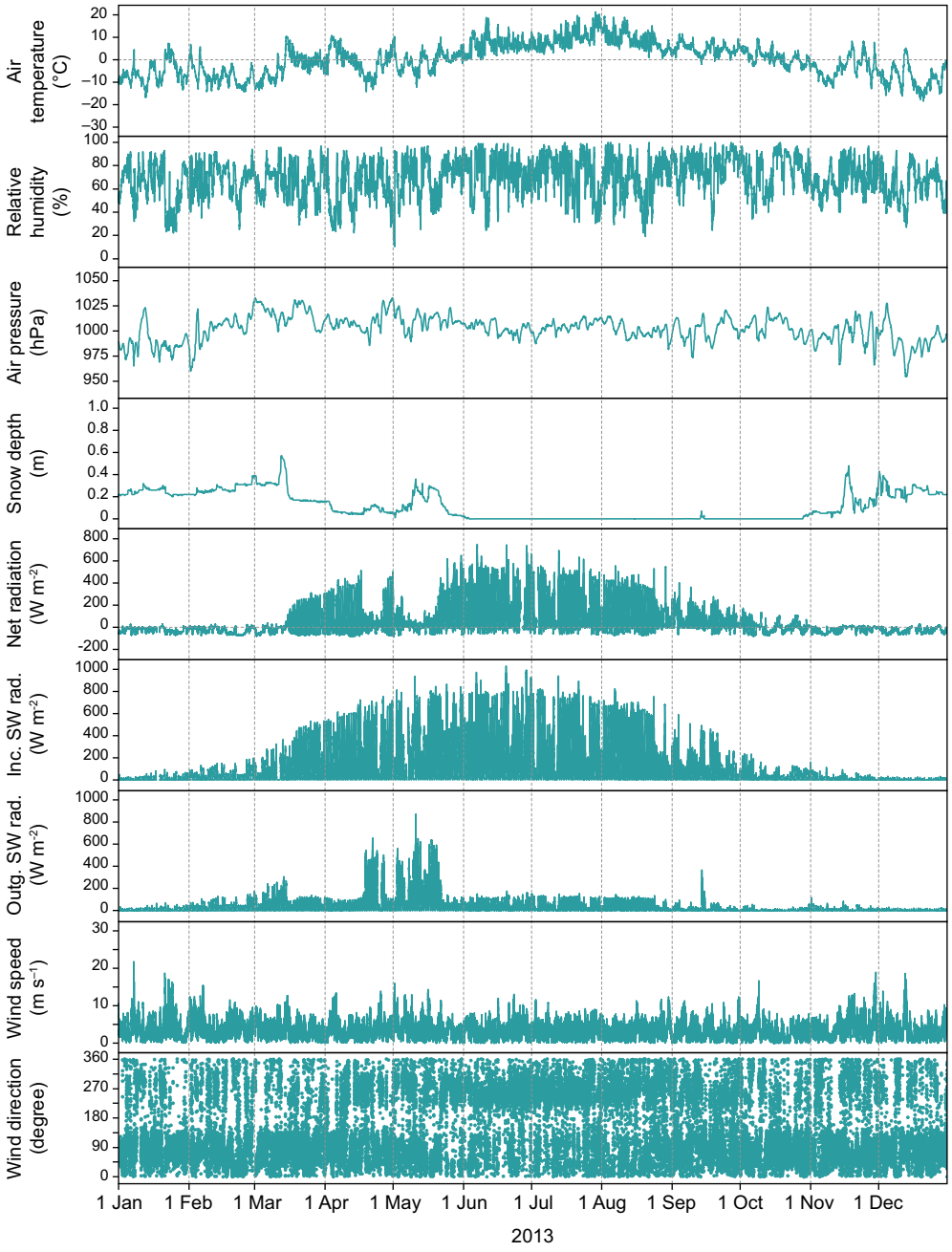

Figure 2.2 Variation of selected climate parameters in 2013. From above: Air temperature, relative humidity, air pressure, snow depth, net radiation, incoming short wave radiation, outgoing short wave radiation, wind speed and wind direction. Wind speed and direction are measured 10 m above terrain; the remaining parameters are measured 2 m above terrain.

Figure 2.2 gives an overview of selected meteorological parameters in 2013.

The mean annual temperature in 2013 was 0.2 °C, which is exactly the average between 2008 and 2013 (table 2.1 and 2.2). The highest temperature was recorded 29 June (21.2 °C) and the lowest 20 December (–18.7 °C). There was no month where not at least once positive temperatures were recorded, while there was no freezing from 9 June until 14 September. The first day with a mean daily temperature below 0 °C after summer was 7 October. While the winter months were above average, the months between May and September showed negative deviations from the mean, with an unusually cold May (–0.4 °C) with significant fresh snow.

The thin snow cover is mirrored in a particular course of the net-radiation, where unusually high positive values were reached early in the season (mid-April – mid-May) and reduced in May by the last significant snowfall events of the season. Air pressure was lowest in January and highest in March, which is in contrast to the usual pattern, the summer months generally showing higher pressure. Generally, it was more variable in winter than in summer.

There are two predominant wind-directions, ENE and WSW (table 2.1.), which

Table 2.1 Monthly mean values of selected climate parameters from January to December 2013 and the annual average.

Month	Rel. hum. (%)	Snow depth (m)	Air temp. (°C)	Air pressure (hPa)	Precip. (mm)	Wind (m s^{-1})	Wind dir. (most frequent)
Jan	63	0.24	-5.9	988	15.8	4.0	ENE
Feb	68	0.27	-7.2	1001	27.9	4.2	E
Mar	67	0.26	-3.1	1018	25.2	3.5	E
Apr	62	0.08	-0.8	1009	63.0	3.5	NE
May	69	0.14	-0.4	1011	101.4	4.1	WNW
June	74	0.00	6.6	1003	12.3	3.5	WSW
July	73	0.00	9.7	1004	60.8	3.4	WSW
Aug	69	0.00	8.8	1001	156.5	3.3	WSW
Sep	80	0.00	4.7	1001	259.4	2.9	ENE
Oct	75	0.00	0.9	1004	109.8	2.8	NE
Nov	69	0.13	-3.5	997	190.6	3.8	ENE
Dec	64	0.25	-8.2	990	23.5	3.4	ENE
2013	69	–	0.2	1002	1046.2	3.5	–

Table 2.2 Comparison of monthly mean air temperatures 2007 to 2013 (italic text represents months with incomplete coverage).

	Air temperature (°C)						
Month	2007	2008	2009	2010	2011	2012	2013
Jan	–	–12.0	–5.4	–3.8	–5.4	–8.7	–5.9
Feb	–	–13.3	–6.1	–1.6	–8.7	–7.7	–7.2
Mar	–	–8.3	–11.7	–4.5	–9.2	–11.0	–3.1
Apr	–	–0.9	–3.2	–0.1	–9.5	–1.7	–0.8
May	*0.6*	3.9	0.3	7.1	0.3	3.2	–0.4
June	*5.3*	7.9	6.4	8.8	6.2	9.4	6.6
July	10.8	10.9	10.6	10.7	10.0	12.1	9.7
Aug	10.6	8.7	9.3	11.7	8.7	10.0	8.8
Sep	4.0	4.4	3.8	7.8	3.9	6.6	4.7
Oct	–0.5	0.0	–0.6	2.9	–2.4	3.0	0.9
Nov	–3.5	–1.7	–7.9	1.2	–6.2	–3.0	–3.5
Dec	–8.7	–7.8	–2.8	0.5	–7.5	–6.1	–8.2
Year	–	–0.7	–0.6	3.4	–1.6	0.5	0.2

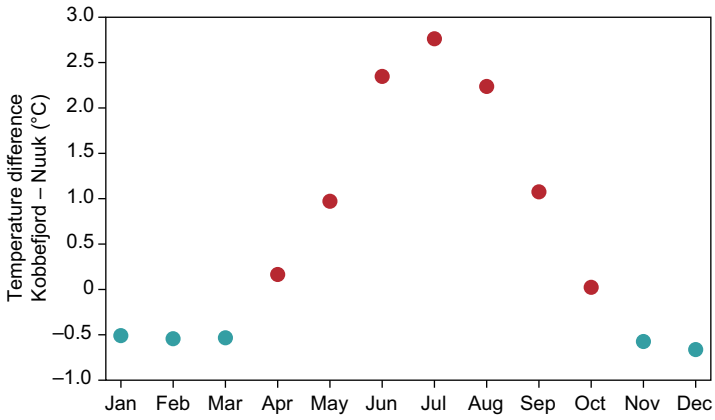

Figure 2.3 Difference in monthly average temperature Kobbefjord – Nuuk: mean for the period 2008-2013.

corresponds to out- and inflow through the valley (figure 2.2.). In summer, the valley-wind system clearly favours up-valley airflow, while in winter radiative cooling triggers stronger out-flow. The land-sea breeze adds an additional mechanism to support this general flow system. Wind speed also follows a general cycle of higher wind speed in winter than in summer and individual storms can well be seen in figure 2.2. Compared to the other years on record, an unusually windy May can be noted.

Precipitation was above average in 2013 although the snow cover of winter 2012/2013 was unusually thin. The late summer and autumn lead to an overall wet year with more than two thirds of the

Table 2.3 Monthly mean values of selected radiation parameters in 2013.

Month	Short wave rad (W m^{-2})		Long wave rad. (W m^{-2})		Net rad. (W m^{-2})	PAR (µmol s^{-1} m^{-2})	UV-B (mW m^{-2})
	in	out	in	out			
Jan	5.3	4.5	239.7	271.8	–31.0	12.6	0.2
Feb	17.7	15.9	235.1	268.6	–33.1	43.6	1.0
Mar	72.3	32.5	243.7	289.0	–6.6	165.6	4.6
Apr	162.6	57.3	252.9	307.9	52.0	368.9	10.1
May	204.6	112.6	275.5	311.1	59.4	492.2	18.2
June	232.4	35.5	305.0	357.5	145.1	544.0	21.9
July	204.7	34.5	318.7	371.7	113.8	475.7	20.0
Aug	155.6	28.1	312.1	362.8	77.5	359.7	13.9
Sep	52.5	9.7	316.2	333.4	21.5	127.0	4.8
Oct	19.1	3.7	280.0	310.8	–15.5	49.5	1.9
Nov	6.4	4.9	259.4	286.2	–26.1	16.1	0.3
Dec	2.1	2.3	232.9	262.2	–30.0	5.3	0.1

annual precipitation between August and November. September was the wettest on record with a total of 259 mm on 21 days.

Figure 2.3 shows the climatologic temperature difference between the station in Nuuk and the one in Kobbefjord. Albeit less than 20 km apart, the two sites differ considerably in terms of continentality. While the annual cycle in Nuuk is attenuated by the more direct exposure to the sea, climate in Kobbefjord follows a stronger annual cycle. This leads to warmer summers (May to October) and to cooler winters (November to March) in Kobbefjord, compared to Nuuk. The differences get as high as 2.8 °C in July and down to –0.7 °C in December.

Table 2.3 summarizes the radiation components on a monthly basis measured in Kobbefjord. The short-wave balance clearly determines the net-radiation in summer, while the long-wave balance does so in winter. Most net radiation input happens in June with 145.1 W m^{-2} being added to the surface while net radiation minimum does not coincide with minimum solar irradiation but in March, when cold surface temperatures lead to a maximal long-wave radiation loss that is not outweighed by the short-wave radiation balance. Photosynthetic active radiation (PAR) and ultra-violet B (UV-B) both peak in June (544 µmol s^{-1} m^{2}) along with the maximum shortwave incoming radiation (232.4 W m^{-2}). Compared to previous years, net-radiation was particularly high in April and May, while from June onwards it was on average. This can be attributed once again to the below-average snow cover, early exposure of snow-free ground and the consequent albedo reduction.

2.2 River water discharge

Hydrometric stations

We present both 2012 and 2013 in this annual report as this was omitted in the previous one. There were hydrological measurements carried out on five locations in the Kobbefjord catchment. Two hydrometric stations were established in 2007 and various divers are set up every year in three minor rivulets to Kobbefjord. The drainage basins of the five locations cover 58 km^2 corresponding to 56 % of the 115 km^2 catchment area of Kobbefjord.

In figure 2.1 the locations of the hydrometric stations (H1, H2) and the diver stations (H3, H4, and H5) are marked. For further descriptions of the stations and their respective drainage area see Jensen and Rasch 2009. For descriptions of the hydrometric stations see Jensen and Rasch 2008.

Q/h-relation

Manual discharge measurements have been carried out at station H1 (2012: 2; 2013: 1), H3 (2012: 7; 2013: 0), H4 (2012: 1; 2013: 0) and H5 (2012: 3; 2013: 0). The purpose is to establish and validate a stage-discharge relation (Q/h-relation). It is generally recommended to base a Q/h-relation on a minimum of 12-15 discharge measurements covering the water levels normally observed at the station (ISO 1100-2, 1998). For H2, H3, H4 and H5 not enough dis-

charge measurements have been made yet to produce a reliable Q/h-relation. Measurements at high water levels are particularly missing. Therefore data from these stations are not presented yet.

A Q/h-relation was established for H1 in 2009 and based upon 17 discharge measurements. The Q/h-relation has been updated in 2011 in order to account for winter conditions with the outlet being affected by ice/snow. The measurements from 2012 and 2013 fit well to the previous Q/h-relation, which has therefore been used. Details on that can be found in Pernosky et al. 2012.

River water discharge at H1

Figure 2.4a and b show the discharge at H1 for 2012 and 2013, respectively, and illustrate the different dominating processes that determine the run-off. In 2012, high discharge values were already reached in mid-March, and the maximum discharge that has been recorded during this year happened in early July. The early season run-off peaks are clearly associated with snowmelt and additional precipitation events. Some autumn storms lead to peaks late in the season but after July the discharge never exceeded 10 $m^3 s^{-1}$ again. In 2013, in contrast (figure 2.4b), the spring-discharge was comparably modest, which is a consequence of the thin snow cover. During rain events early in September, and in October 10 $m^3 s^{-1}$ were reached again. More than half of the total annual run-off occurred therefore from September onwards, with snowmelt being an unusually small contributor in 2013.

Table 2.4 Total discharge and mean water loss for hydrological years 2007-2008 to 2012-2013.

Hydrological year	Total discharge (million m^3)	Water loss (mm)
2007-2008	32.79	1058
2008-2009	40.83	1317
2009-2010	23.21	749
2010-2011	34.34	1108
2011-2012	49.06	1583
2012-2013	42.41	1368

Table 2.5 summarizes the total discharge for the hydrological years from 2007/2008 until 2012/2013. The two latest seasons are the wettest on record (49.06 mill. m^3 and 42.41 mill. m^3), while 2009/2010 was the driest. Inter-annual variations are high, the maximum year showing more than double the run-off than the minimum year. Taking the drainage basin of 31 km^2 into account, the overall water loss was 1583 mm in 2011/2012 and 1368 mm in 2012/2013.

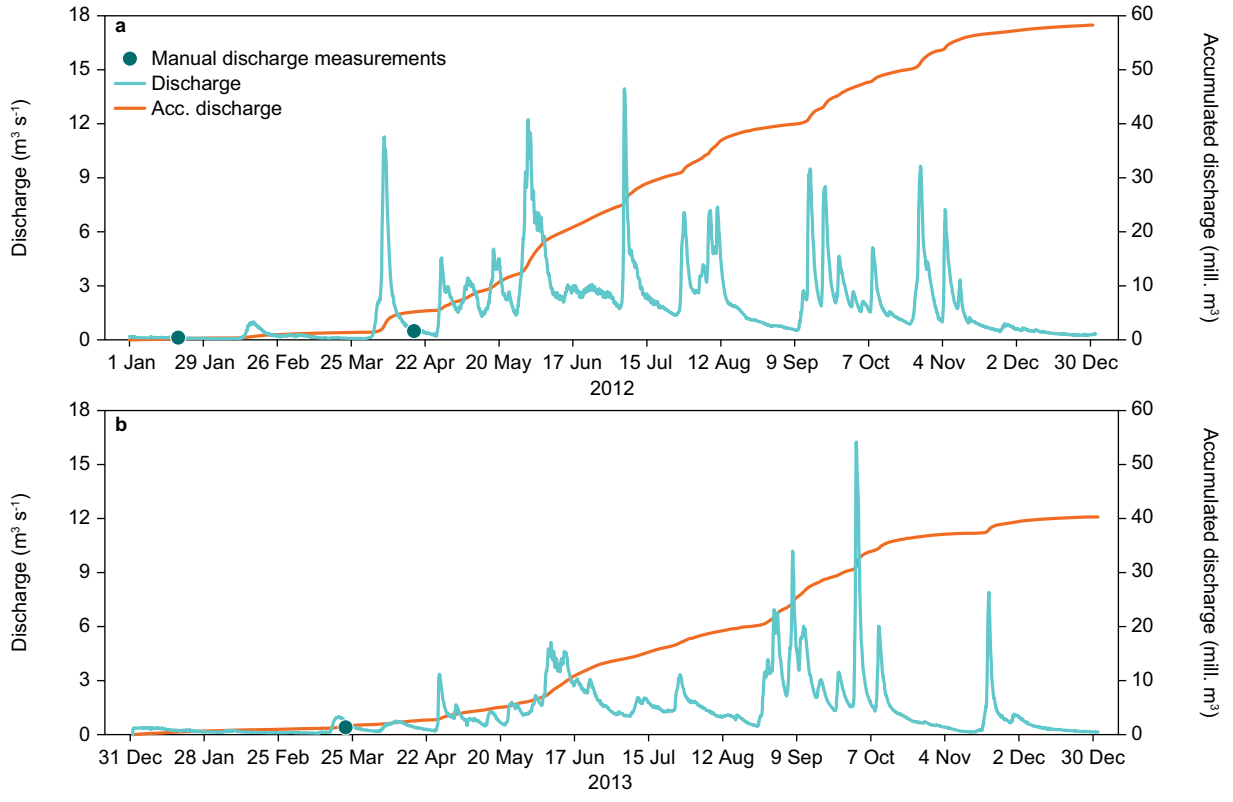

Figure 2.4 River water discharge at H1 during (a) 2012 and (b) 2013.). The blue line is the instantaneous discharge, refers to the left axis, the red line the accumulated discharge over the calendar year, and refers to the right axis.

3 Nuuk Basic

GeoBasis programme

Birger Ulf Hansen, Louise Holm Christensen, Mikkel P. Tamstorf, Magnus Lund, Stine Højlund Pedersen, Maria Libach Burup, Katrine Raundrup, Mikhail Mastepanov, Andreas Westergaard and Torben Røjle Christensen

The GeoBasis programme provides long-term data of climatic, hydrological and physical landscape variables describing the environment in the Kobbefjord drainage basin close to Nuuk. GeoBasis was in 2013 operated by the Department of Geosciences and Natural Resource Management, University of Copenhagen in collaboration with the Department of Bioscience, Aarhus University. In 2013, GeoBasis was funded by Danish Ministry for Climate and Energy as part of the environmental support programme DANCEA – Danish Cooperation for Environment in the Arctic. A part-time position is placed in Nuuk at Asiaq - Greenland Survey. The GeoBasis programme includes monitoring of the physical variables within snow and ice, soils, vegetation and carbon flux. The programme runs from May to the end of October with some year round measurements from automated stations.

The 2013 season is the sixth full season for the GeoBasis programme. In 2007, the field programme was initiated during a three-week intensive field campaign in August where most of the equipment was installed, although some installations had to be postponed until 2008. Methods and sampling procedures are described in detail in the manual 'GeoBasis – Guidelines and sampling procedures for the geographical monitoring programme of Nuuk Basic', which can be downloaded from www.nuuk-basic.dk.

In 2011, GeoBasis installed two new energy balance stations (figure 3.1) in cooperation with the INTERACT programme. One station is located at a new site over heath vegetation (figure 3.2) and the second station was installed at the existing fen site (Hansen et al. 2013). The remote placing of the heath site and the use of fuel cells caused numerous breaks in the time series although the station was visited frequently even outside the normal field season. In 2013, a more stable power supply was installed combining a wind

Figure 3.1 A new Snow Pack Analyzing System was installed at the heath site in August 2013. In the background the new wind generator and solar panel for the power supply can be seen.

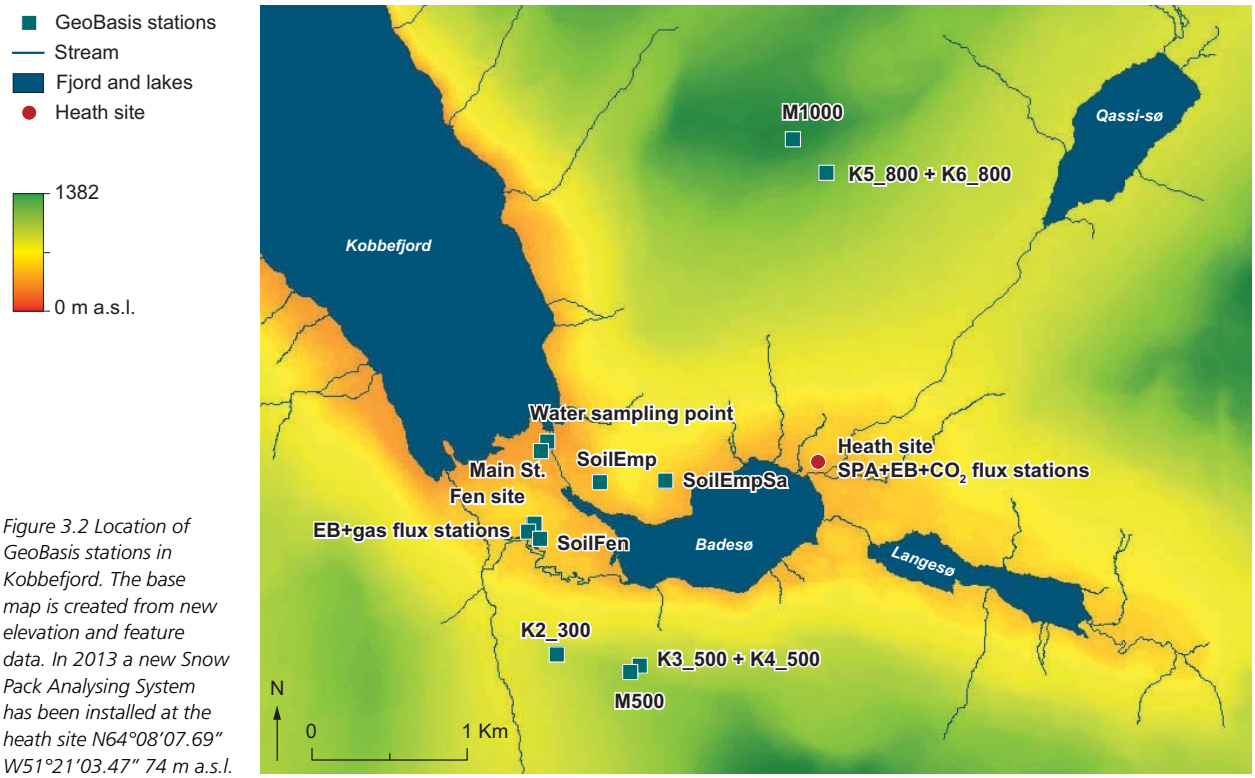

Figure 3.2 Location of GeoBasis stations in Kobbefjord. The base map is created from new elevation and feature data. In 2013 a new Snow Pack Analysing System has been installed at the heath site N64°08'07.69" W51°21'03.47" 74 m a.s.l.

generator with a nominal effect of 350 W and a 18 W solar panel. With that the time-series recording at both the energy balance and the Snow Pack Analysing System (SPA) stations have been more stable with only a few minor breaks.

In 2013, GeoBasis installed a SPA on the heath site close to the energy balance and CO_2 stations (figure 3.1). The heath site was chosen as it is the dominating ecosystem within the drainage basin. The SPA constitutes an innovation in snow measurements as it automatic and continuous measure all relevant snow parameters such as snow depth and at three levels (10, 35 and 55 cm) snow density, snow water equivalent and contents of liquid water and ice are measured.

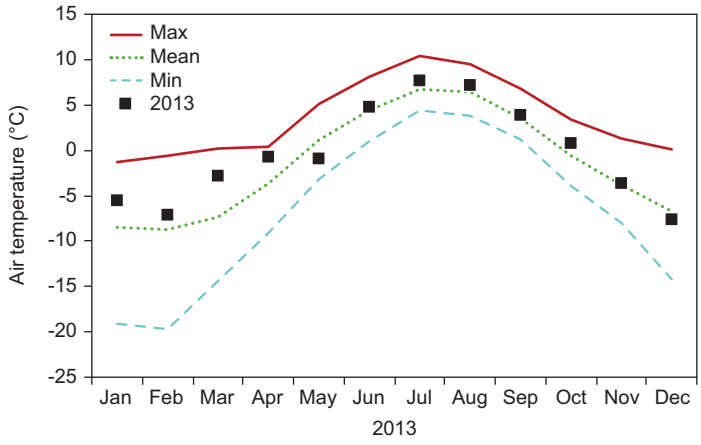

Figure 3.3 The monthly minimum, mean and maximum air temperature for the period 1866-2013 measured at Nuuk and monthly mean air temperature for 2013 (points) (Cappelen, 2013).

Data collected by the Danish Meteorological Institute (figure 3.3) shows that 2013 the annual mean air temperature in Nuuk reached –0.3 °C, which is 1.1 °C warmer than normal (Cappelen, 2013). All months except May and December were warmer than normal. The warmest month was July with 7.7 °C, which was 1.0 °C warmer than normal but 2.4 °C colder than the previous July, which was the warmest July in the period 1866-2013. The coldest month in 2013 was December with –7.6 °C, which was 0.9 °C colder than normal.

3.1 Snow and ice

Snow cover extent

The first four automatic cameras were installed in 2007 at 300 and 500 m a.s.l. to monitor the snow cover extent in the central parts of the Kobbefjord drainage basin (Tamstorf et al. 2007). In September 2009 two snow monitoring cameras K5 and K6 were installed. Both cameras were installed at position N64°9'06.25" W51°20'46.47" 770 m a.s.l. (figure 3.2). K5 is facing to the south monitoring the central parts of the drainage basin with Badesø and Langsø while K6 monitors Qassi-sø-lake in the northern valley of the drainage basin (figure 3.4). In 2011, a new camera was reinstalled at

K1_300 (N64°7′26″ W51°22′55″) overlooking the fen area. This automatic camera takes photos three times daily March through November, and once daily during the winter months.

One of the main advantages of camera-based snow monitoring is that it is relatively insensitive to cloud cover (in contrast to satellite-based techniques). Only low clouds and foggy conditions can make the image data unsuitable for mapping purposes. A new updated and more user friendly algorithm for snow cover monitoring has been developed in MatLab, so it is now possible, for each melting season, to construct snow cover depletion curves for user specified regions of interest (ROI) on the basis of image data obtained at daily frequency. In the previous year's depletion curves for 3 regions of interest seen from K2_300 have been shown (Hansen et al. 2012), but due to technical problems it will not be possible to show any depletions curves from these ROI.

Instead two new ROI are shown in figure 3.5. They cover the vegetation types copse (willow with a maximum height of 1 meter) and fen. Fen is very similar to the footprint for the CO_2-station in the fen. Both ROI are covered by K1_300 and K3_500 so a future monitoring of the two ROI should be more stable. Figure 3.5 show that 50 % of the snow cover was melted on DOY 150 for copse and four days later for fen in 2013, which for both places are 12 days later than the average for the four years of registration. In 2013, the melting season for both locations started on DOY 140 and lasted for two weeks at the copse location and 26 days at the fen area, which is the latest for the four years of registration.

Figure 3.4 Camera K5_800 (to the right) and K6 (to the left). (N64°7′26″ W51°22′55″). The background is showing the field of view for camera K5 which monitor Langsø (to the left) and Badesø (to the right).

Snow cover

To support the studies under the Nuuk Basic monitoring programme, a snow cover survey using ground penetrating radar (GPR), and taking manual stake measurements was carried out in the main parts of Kobbefjord drainage basin 20-22 March, 2013. A comparison of average snow depth for the three GeoBasis sites can be seen in table 3.1. A snow depth of 36 cm as an average for the three sites is 29 cm below the average for the three sites in the period 2009-2013. An average of 303 kg m^{-3} in density is also well below the average of 327 kg m^{-3} for the five years period.

Even though the snow survey is carried out at nearly the same time every year, snow depth has large variations from year to year and the maximum snow cover date is also strongly variable from year to year, see figure 3.6. The snow cover in the winter 2012/2013 started early October but lasted only eight days. On 11 November, a new snow cover started to build up and over the following month reached 25 cm and then settled at this depth for the next two months. During February, the snow depth

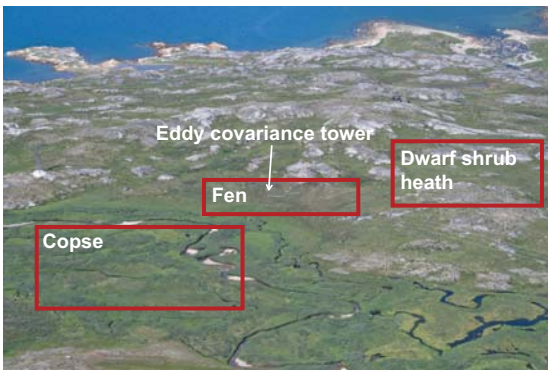

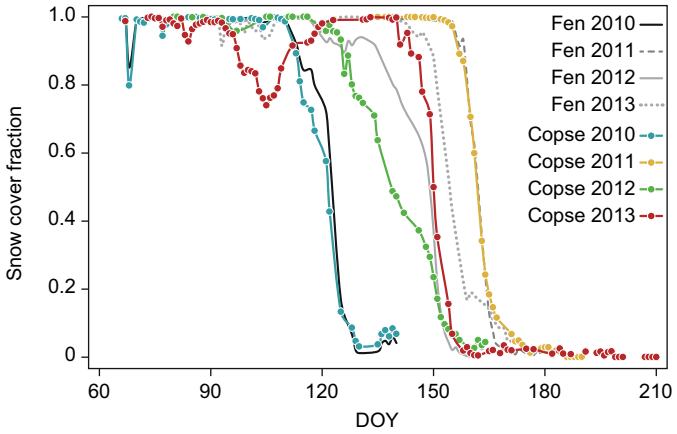

Figure 3.5 Snow cover depletion for two regions of interest copse and fen at 50 m a.s.l. have been analysed using a new snow cover algorithm. The regions are specified on the image to the left, and the depletion curves for each region in the period 2010-2013 are shown in the diagram to the right. DOY (day of year).

Table 3.1 Comparison of snow depth/densities (in brackets) at GeoBasis sites A-C, 2009-2013. No snow pit was dug at SoilEmpSa in 2010.

Snow survey dates	Soil Fen (A) Average depth (m) Density (kg m^{-3})	Soil Emp Salix (B) Average depth (m) Density (kg m^{-3})	Soil Emp (C) Average depth (m) Density (kg m^{-3})
15-16 April, 2009	0.91 (237)	0.90 (275)	1.02 (329)
15-16 April, 2010	0.20 (339)	0.19 (n.a.)	0.17 (366)
7-9 April, 2011	0.87 (364)	0.92 (297)	0.91 (383)
17-18 April, 2012	0.96 (373)	0.74 (353)	0.92 (320)
20-22 March, 2013	0.42 (316)	0.35 (311)	0.32 (282)

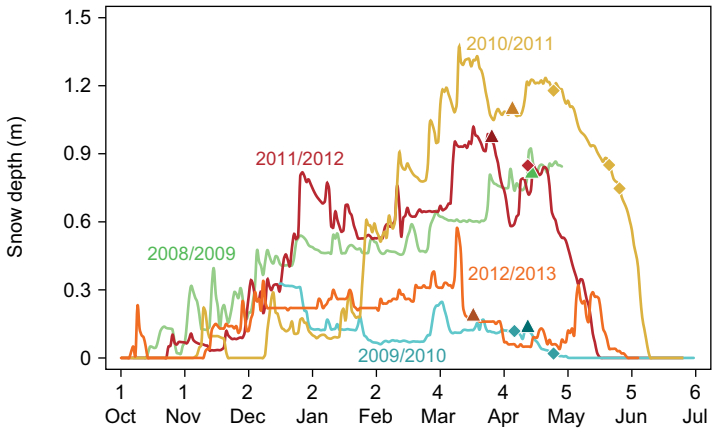

Figure 3.6 Snow depth measured at the ClimateBasis station and placement of snow surveys, 2009-2013. Triangles represent the main survey for the year and the small diamonds represent additional snow surveys.

steadily increased to 30 cm. Minor snow falls in March caused a short increase of snow depth to approximately 60 cm before a steady snowmelt started only interrupted by a brief snow falls in mid-May causing a temporally increase in the snow depth to 30 cm. The 2012/2013 snow cover had finally melted away at the ClimateBasis station 5 June. Since continuous measurements of snow depth started in 2008 only the winter 2009/2010 had lesser snow than the winter 2012/2013, which lasted nearly one month longer.

Table 3.2 describes snow depths and densities at the three GeoBasis soil microclimate stations SoilFen, SoilEmpSa and SoilEmp using ground penetrating radar (GPR) and manual stake measurements (figure 3.7). The snow survey strategy used in Kobbefjord is outlined in the 3rd Annual Report (Hansen et al. 2010). In order to document the properties of the snowpack snow pits were dug at SoilFen in point A1, at SoilEmpSa in point B1 and at SoilEmp in point C1 (figure 3.7). The examination of the snowpack included temperature profiling, density measurements and texture description. Table 3.2 summarizes the snow depth, density and temperature results from the three stations. The texture of the snow profile at all three sites is characterized as homogenous coarse-grained snow, with densities between 282-316 kg m^{-3}. Although the variation in densities are smaller than previous years (Hansen et al. 2012) the huge variation in snow depths ranging from 0 cm to 109 cm causes huge variations in snow water equivalents ranging from zero to 339 mm within few meters at SoilEmpSa.

Ice cover

The ice cover of the lakes in the Kobbefjord drainage basin was generally formed late in the winter 2012/2013 compared to previous winters (table 3.3). The break-up of the ice cover on the lakes was 7-8 days later than the average for the period 2007-2013. Sea ice cover in Kobbefjord developed as late as 24 February 2013, which is the latest registration in the six years of monitoring in Kobbefjord. The fjord was ice-free 26 April, which is the earliest registration in the six years and nearly 20 days earlier than the average for the five previous years. In 2013 the ice cover was formed four days earlier on Qassi-sø (250 m a.s.l.) than on Badesø (30 m a.s.l.) while it the three previous years has been formed 2-3 weeks earlier. As usually the ice cover on Qassi-sø broke up eight days later than the ice cover on Badesø. The difference is due to the difference in elevation of the two lakes.

Table 3.2 Snow pit depth, average density, snow depth, standard deviation of snow depth, average snow temperature and average water equivalent in three soil stations (SoilFen, SoilEmpsa and SoilEmp) measured 22-23 March 2013.

Site	Snow pit depth (cm)	Avg. density (kg m^{-3})	Snow depth (min-avg.-max) (cm)	Standard dev. of snow depth (cm)	Avg. snow temperature (°C)	Avg. water eq. (mm)
SoilFen (A1)	33	316	14-42-99	11	-3.7	100
SoilEmpSa (B1)	21	311	0-37-109	23	-0.3	65
SoilEmp (C1)	28	282	18-39-87	17	-1.0	79

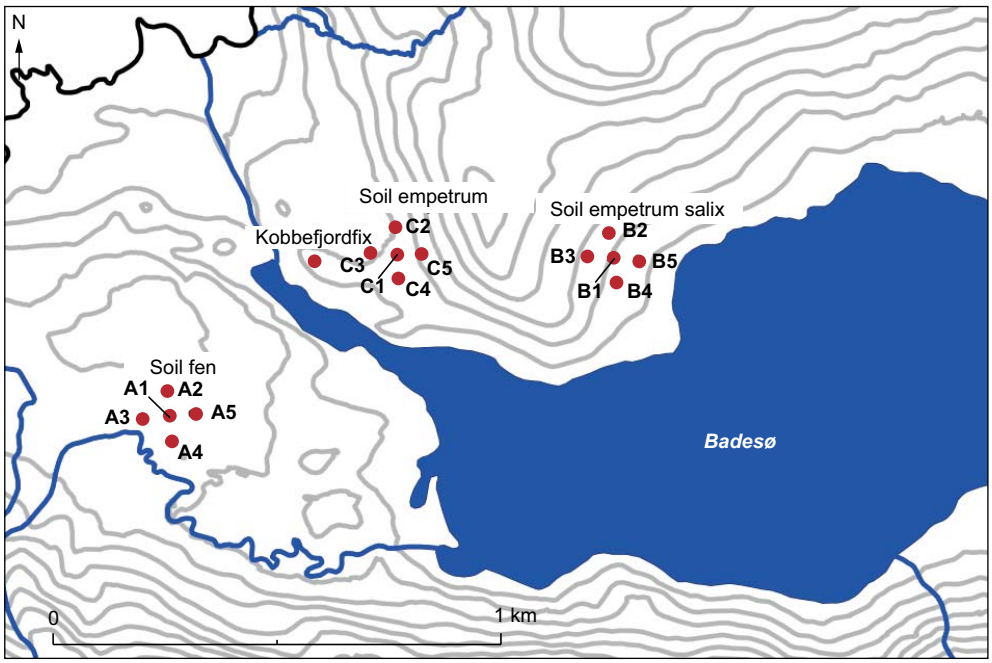

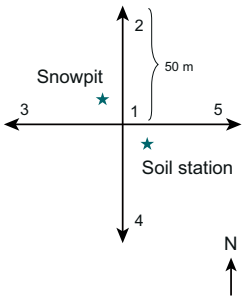

Figure 3.7 Map showing the three snow survey sites. The figure on the right outlines the strategy at each site.

Table 3.3 Visually estimated dates for perennial formation (50%) of ice cover and date for break-up of ice cover on selected lakes within the Kobbefjord drainage basin and on Kobbefjord from 2007 to 2013. Dates are reported for perennial formation of ice cover in the fall and for the break-up of ice cover in the spring. Badesø is the main lake in the area and Qassi-sø is the lake at 250 m a.s.l. in the northern valley of the drainage basin.

	Badesø		Langsø		Qassi-sø		Kobbefjord	
Year	Break-up	Formation	Break-up	Formation	Break-up	Formation	Break-up	Formation
2007		23 Oct		22 Oct		22 Oct		27 Dec-12 Feb*
2008	2 Jun	5 Nov	13 May	5 Nov	9 Jun	4 Nov	17 May	no data
2009	13 Jun	1 Nov	11 June	no data	22 Jun	10 Oct	4 Jun	12 Feb
2010	14 May	22 Nov	no data	no data	24 May	6-11 Nov	2 Jun	23 Nov
2011	18 Jun	22 Oct	no data	no data	28 Jun	20 Oct	23 May	16 Nov
2012	9 Jun	15 Nov	no data	no data	18 Jun	11 Nov	22 May	24 Feb
2013	14 Jun	24 Oct	no data	no data	22 Jun	26 Oct	26 Apr	15 Oct

Micrometeorology

Table 3.4 reports the monthly mean air temperature, relative humidity, surface temperature and soil temperature measured at SoilFen 2010-2013 (monthly data for the period 2007-2009 can be found in Hansen el al. 2013). In 2013, the temperatures in the spring – March to April – were higher than average and March with –3.4 °C was the highest mean monthly air temperature for March in the period 2007-2013, while May, June and July with respectively –0.6, 6.1 and 8.9 °C were the coldest mean monthly air temperatures measured in the period 2007-2013. These measurements are in line with the air temperature measured in Nuuk located 30 km away (figure 3.3).

For the GeoBasis monitoring period 2007-2013, the minimum monthly mean air temperature was –13.5 °C measured at SoilFen in February 2008 and the maximum monthly mean air temperature was 11.7 °C measured in July 2012.

The micrometeorological stations M500 and M1000, measuring air temperature, relative humidity, surface temperature and shortwave irradiance, are presented in table 3.5 and table 3.6 (monthly data for the period 2007-2009 can be found in Hansen el al. 2013). M500 is placed approximately 500 m a.s.l. south of Badesø and M1000 is

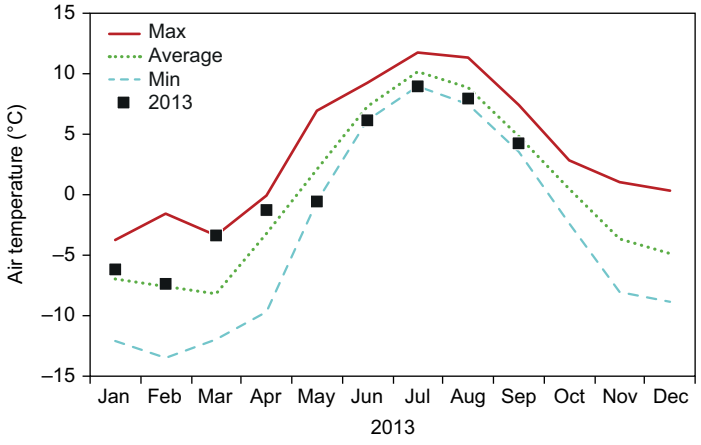

Figure 3.8 Monthly mean air temperatures in 2013, and maximum, average and minimum monthly mean air temperatures from 2007-2013. Measured at the SoilFen station 2,5 meter above ground.

Table 3.4 Air temperature, relative humidity, surface temperature and soil temperature at five depths (1 cm, 10 cm, 30 cm, 50 cm and 75 cm) from the SoilFen station in the fen area from January 2010 to September 2013 (data from October, November and December are not retrieved yet).

Month-year	Air temp. 2.5 m (°C)	Rel. hum. 2.5 m (%)	Surface temp. 0 m (°C)	Soil temp. –1 cm (°C)	Soil temp. –5 cm (°C)	Soil temp. –10 cm (°C)	Soil temp. –30 cm (°C)	Soil temp. –50 cm (°C)	Soil temp. –75 cm (°C)
2010									
January	–3.8	71.1	–7.0	–1.9	–1.6	–1.0	0.5	0.7	1.1
February	–1.6	67.7	–5.4	–3.2	–2.8	–2.3	0.1	0.3	0.8
March	–4.5	69.8	–7.9	–2.2	–2.1	–1.8	–0.2	0.1	0.5
April	–0.1	74.1	–3.0	–0.5	–0.5	–0.5	–0.1	0.1	0.4
May	6.9	68.8	6.9	6.2	4.3	2.3	0.0	0.1	0.4
June	8.6	73.6	10.7	10.9	9.6	7.8	1.0	0.8	0.7
July	10.2	78.2	12.6	13.8	13.0	12.1	7.9	6.9	5.5
August	11.3	79.8	11.7	12.6	12.4	11.9	9.7	9.0	7.9
September	7.4	73.4	6.5	7.3	7.6	7.7	7.7	7.6	7.2
October	2.8	71.1	0.7	1.5	1.9	2.4	3.9	4.2	4.6
November	1.0	69.7	–2.4	–0.4	–0.2	0.1	1.6	2.0	2.5
December	0.3	75.5	–2.5	–0.1	–0.1	0.0	1.0	1.3	1.8
2011									
January	–5.6	70.6	–8.7	–0.7	–0.5	–0.2	0.7	1.0	1.4
February	–9.1	73.2	–12.0	–0.4	–0.4	–0.2	0.5	0.7	1.1
March	–9.5	73.6	–11.6	–0.2	–0.2	–0.2	0.5	0.7	1.0
April	–9.7	69.5	–12.6	0.0	0.0	0.0	0.5	0.7	1.0
May	0.5	71.5	–1.2	0.0	0.0	0.1	0.5	0.7	1.0
June	6.1	77.0	5.4	4.8	3.5	2.5	1.2	1.1	1.2
July	9.6	78.5	11.2	12.4	11.8	11.0	7.4	6.6	5.3
August	8.2	81.3	9.4	11.0	10.8	10.5	8.6	8.1	7.1
September	3.5	77.8	3.2	4.1	4.5	4.8	5.9	6.0	5.9
October	–2.4	70.5	–4.3	0.0	0.3	0.7	2.3	2.6	3.1
November	–6.2	65.8	–8.7	–2.3	–1.8	–1.1	0.8	1.1	1.7
December	–7.6	74.3	–9.5	–0.7	–0.7	–0.5	0.2	0.5	1.0
2012									
January	–8.8	70.6	–11.2	–0.7	–0.7	–0.6	0.1	0.4	0.8
February	–7.8	74.0	–9.8	–0.4	–0.4	–0.4	0.1	0.3	0.7
March	–11.1	73.2	–12.2	–1.2	–1.1	–0.9	0.0	0.2	0.6
April	–1.7	81.0	–2.7	–0.1	–0.1	–0.1	0.1	0.3	0.6
May	3.2	78.8	2.7	1.0	0.3	0.0	0.2	0.3	0.6
June	9.2	74.4	11.2	11.3	9.3	6.6	1.3	1.1	1.0
July	11.7	78.7	13.2	14.7	14.1	13.0	8.6	7.5	5.9
August	9.3	80.2	9.8	11.4	11.3	11.0	9.3	8.7	7.7
September	6.0	76.3	5.7	6.2	6.4	6.6	6.8	6.8	6.5
October	2.6	72.4	1.6	1.6	1.8	2.2	3.4	3.7	4.1
November	–3.3	71.2	–4.4	–0.4	–0.2	0.2	1.7	2.0	2.5
December	–6.2	68.8	–8.3	–0.4	–0.3	–0.1	0.9	1.2	1.6
2013									
January	–6.2	65.2	–7.7	–0.7	–0.6	–0.3	0.6	0.8	1.3
February	–7.4	69.7	–8.4	–0.9	–0.7	–0.5	0.4	0.6	1.0
March	–3.4	67.9	–4.3	–0.5	–0.4	–0.3	0.3	0.5	0.9
April	–1.3	63.8	–1.4	–0.2	–0.2	–0.1	0.4	0.5	0.8
May	–0.6	69.9	0.0	0.0	0.0	0.0	0.3	0.5	0.8
June	6.1	76.3	7.6	7.3	5.6	3.7	1.3	1.2	1.1
July	8.9	74.4	10.2	11.9	11.3	10.3	6.7	5.8	4.7
August	7.9	71.5	8.5	10.0	10.0	9.8	8.5	8.0	7.0
September	4.2	81.0	4.2	4.6	4.7	4.8	5.2	5.2	5.2
October									
November									
December									

Table 3.5 Air temperature, relative humidity, surface temperature and shortwave irradiance measured at the M500 station from January 2010 to October 2013 (data from November and to December are not yet retrieved).

Month-year	Air temp. 2.5 m (°C)	Rel. Hum. 2.5 m (%)	Surface irradiance temp. 0 m (°C)	Shortwave irradiance 2.5 m (W m^{-2})
2010				
January	–5.5	73.8	–9.1	5.9
February	–2.7	65.4	–7.5	29.6
March	–6.7	73.1	–9.6	80.4
April	–2.9	79.9	–5.4	170.4
May	4.6	71.3	3.8	205.6
June	5.7	79.9	7.9	211.4
July	8.5	76.3	11.2	217.8
August	9.0	81.3	8.8	132.6
September	5.0	73.5	3.0	89.1
October	0.5	73.1	–2.8	35.8
November	–1.3	73.1	–4.6	8.8
December	–1.7	78.7	–4.3	2.3
2011				
January	–7.6	73.8	–11.0	6.8
February	–11.5	78.1	–13.9	27.8
March	–11.7	80.7	–13.9	76.8
April	–12.6	82.3	–14.5	187.5
May	–3.0	81.0	–3.5	239.2
June	4.6	77.9	7.2	238.7
July	7.6	79.2	8.6	165.8
August	6.8	77.0	7.3	149.8
September	0.7	80.2	–0.8	77.9
October	–4.8	73.1	–8.2	43.4
November	–8.8	70.7	–12.7	11.8
December	–10.8	84.1	–12.3	2.4
2012				
January	–11.3	74.8	–13.7	6.5
February	–10.2	81.7	–12.3	29.0
March	–13.1	78.3	–14.9	72.8
April	–4.0	90.0	–5.1	134.6
May	1.2	82.5	0.2	192.3
June	8.7	68.2	11.1	265.9
July	10.4	74.9	12.2	194.6
August	7.5	79.5	7.4	131.6
September	2.7	85.2	1.8	60.4
October	–0.4	78.5	–2.9	31.3
November	–6.1	77.2	–8.4	8.7
December	–7.3	68.7	–11.7	3.0
2013				
January	–8.4	66.9	–12.1	6.8
February	–10.3	77.8	–12.9	28.5
March	–4.7	64.5	–8.3	80.2
April	–4.0	68.5	–6.1	155.4
May	–4.3	82.3	–5.0	204.8
June	3.8	80.2	5.7	230.6
July	6.6	76.2	7.7	201.5
August	5.6	73.1	6.2	155.3
September	0.9	90.0	–0.6	58.6
October	–1.3	77.1	–4.4	35.3
November				
December				

Table 3.6 Air temperature, relative humidity, surface temperature and shortwave irradiance measured at the M1000 station from January 2010 to January 2012. The station M1000 has been out of order since February 2012.

Month-year	Air temp. 2.5 m (°C)	Rel. hum. 2.5 m (%)	Surface irradiance temp. 0 m (°C)	Shortwave irradiance 2.5 m (W m^{-2})
2010				
January	–6.90	71.15	–9.84	7.10
February	–4.30	62.87	–8.26	32.80
March	–8.70	73.10	–10.01	88.40
April	–7.00	90.86	–7.92	135.50
May	–	–	–	–
June	3.20	94.75	9.27	173.10
July	7.10	75.65	11.83	230.30
August	7.30	82.82	8.67	138.00
September	2.80	75.21	2.79	103.80
October	–1.80	75.23	–3.48	45.20
November	–3.80	79.26	–5.46	9.00
December	–3.60	81.54	–5.44	2.20
2011				
January	–9.70	72.71	–11.47	8.20
February	–13.70	76.27	–14.33	29.60
March	–14.20	83.92	–13.60	80.30
April	–15.00	77.93	–14.69	191.90
May	–5.20	79.95	–3.16	245.90
June	3.80	73.31	7.60	256.90
July	5.60	81.87	7.81	177.30
August	5.20	76.31	6.73	157.10
September	–1.60	81.02	–2.36	97.90
October	–6.80	71.40	–8.71	50.10
November	–11.20	72.58	–13.4	15.8
December	–14.00	91.32	–13.38	2.2
2012				
January	–13.50	74.12	–14.49	6.8

In order to minimize the number of gaps in the time series from the climate stations one 350W wind generator and four 110W solar panels were installed at the heath site and two 350W wind generators were added to the existing power installation at the fen site early in the field season, Kobbefjord June 2014. Photo: Louise Holm Christensen .

placed approximately 1000 m a.s.l. north of Badesø. The pattern of high monthly mean air temperature in March 2013 was also seen in the data from M500. In 2008-2012 the mean air temperature in July at the M500 station was between 7.6 °C and 10.4 °C, in 2013 it was only 6.6 °C. The humidity measured at the M500 station in 2012 generated a new maximum record in September (90.0 %) and new minimum records for January (66.9 %) and March (64.5 %), while the monthly mean incoming shortwave irradiance in 2013 in general was lower than normal. Unfortunately, M1000 has been out of order since February 2012 although it has been repaired several times frequently strong winds and icing have damaged all sensors shortly after each repair.

3.2 Soil

Physical soil properties

The results of selected parameters for the soil stations SoilFen, SoilEmp and SoilEmpSa are presented in tables 3.4, 3.7 and 3.8 (monthly data for the period 2008-2009 can be found in Hansen el al. 2013). The difference in soil properties between the three locations, which were detected in previews years are also seen in the data, collected in 2013. Those being higher winter soil temperatures at SoilFen than at SoilEmp and SoilEmpSa, as the snow depth at SoilFen is significant higher. During summer, the soil temperatures at SoilFen are significant higher, as the site is more protected from cold winds from Kobbefjord and Badesø. The temperature in 30 cm depth is at SoilFen less affected by fluctuations in surface temperature than at SoilEmp and SoilEmpSa where the soil is well-drained. The results of the measured soil water content show markedly lower values for the well-drained soil at SoilEmp than at SoilEmpSa. The monthly mean soil moisture is 16 % at SoilEmp and 34 % at SoilEmpSa during the 2013 field season. At all three soil stations the soil was 4 °C colder in June than the previous years due to a colder and more prolonged winter season in 2012/2013.

Throughout the season, soil water was collected from two depths at three characteristic soil profiles representing the dominating plant communities in the drainage basin. During the period 20 June to 1 October 2013, thirty-four soil water samples were collected from the soil water stations at SoilEmp (10 and 30 cm), SoilFen (10 and 80 cm) and SoilHeath (10 and 50 cm).

At the research house in Kobbefjord, measurements of pH, temperature and conductivity were carried out on each sample. In August 2011, laboratory equipment was installed in the research house, which enabled analyses of soil water alkalinity. After the field season, the soil water samples have been analysed for all major anions and cations as well as for dissolved organic carbon content.

River water

In 2013, thirty-three water samples were collected from end May to start October which is a field season one month shorter than previous year due to a very late snow-/icemelt. *In situ* measurements of river water temperature, conductivity and pH were carried out along with the water sampling. The measured values are presented in figure 3.9. The water temperature varies through the season 2013 as it did in field seasons 2009 and 2011 (Hansen et al. 2013). The minimum river water

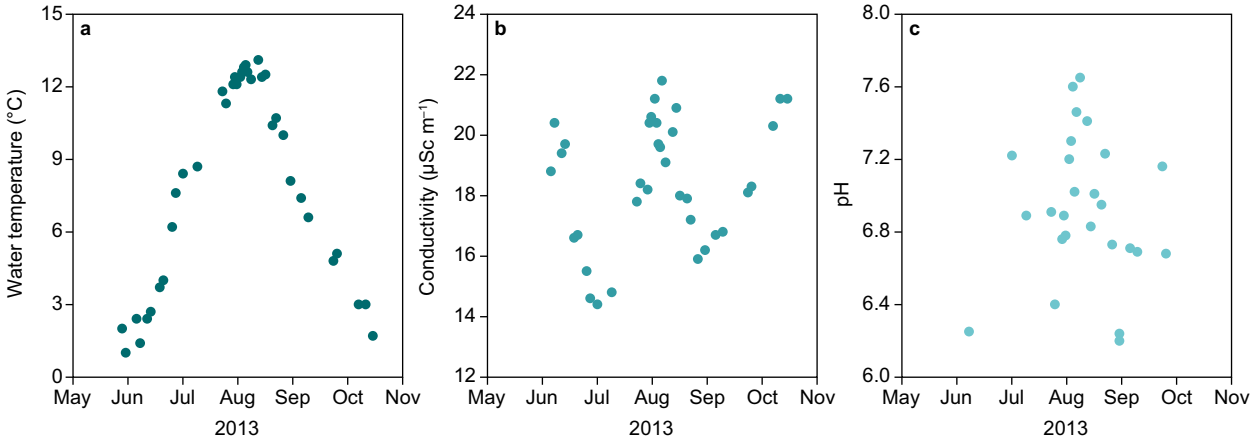

Figure 3.9 a) water temperatures, b) conductivity and c) pH measured in 2013 in Kobbefjord river at the water sampling point near the research house.

Table 3.7 Soil temperature and soil moisture at four depths measured at SoilEmp from January 2010 to November 2013 (data from December is not yet retrieved).

Month-year	Soil temp. –1 cm (°C)	Soil temp. –5 cm (°C)	Soil temp. –10 cm (°C)	Soil temp. –30 cm (°C)	Soil moist. –5 cm (%)	Soil moist. –10 cm (%)	Soil moist. –30 cm (%)	Soil moist. –50 cm (%)
2010								
January	–5.2	–5.1	–4.9	–3.9	0.6	8.0	1.5	1.8
February	–5.3	–5.1	–5.0	–4.1	0.6	7.7	1.5	1.6
March	–4.5	–4.4	–4.4	–3.9	0.6	7.6	1.4	1.6
April	–0.6	–0.8	–0.8	–0.8	6.3	16.2	10.1	8.3
May	6.4	5.6	5.1	3.8	19.5	42.0	33.6	31.2
June	10.1	9.4	9.0	7.7	5.4	35.1	7.6	5.0
July	12.4	11.8	11.4	10.4	4.1	27.8	5.2	4.1
August	11.6	11.3	11.2	10.6	10.6	36.6	15.5	15.2
September	7.0	7.3	7.4	7.6	9.2	38.0	14.1	11.2
October	1.6	2.1	2.4	3.0	6.6	36.4	6.6	4.7
November	–0.7	–0.5	–0.4	0.2	4.6	16.2	6.7	4.9
December	–0.2	–0.2	–0.1	0.2	13.6	35.6	25.7	24.5
2011								
January	–1.7	–1.5	–1.2	–0.4	3.2	13.6	5.2	4.4
February	–1.3	–1.1	–1.0	–0.6	2.4	9.9	3.6	3.5
March	–1.3	–1.2	–1.1	–0.8	2.4	9.7	3.4	3.4
April	–0.7	–0.6	–0.5	–0.3	2.5	10.0	3.4	3.4
May	0.0	0.0	0.1	0.1	11.1	17.9	14.1	15.5
June	5.3	4.7	4.3	3.2	27.1	38.6	26.0	31.8
July	10.9	10.5	10.2	9.1	7.9	37.5	8.9	6.2
August	10.1	10.0	9.8	9.3	7.3	36.3	8.3	6.7
September	3.8	4.2	4.4	4.9	12.6	39.8	22.8	20.0
October	–0.7	–0.3	–0.1	0.7	6.4	25.3	7.7	6.0
November	–4.7	–4.4	–4.0	–2.5	2.8	8.4	3.6	4.9
December	–2.6	–2.5	–2.4	–2.1	2.9	8.5	3.5	4.1
2012								
January	–2.5	–2.4	–2.3	–2.0	2.9	8.7	3.6	4.1
February	–1.7	–1.6	–1.6	–1.5	3.2	10.3	3.7	4.2
March	–3.8	–3.7	–3.5	–3.1	2.8	8.5	3.4	4.0
April	–0.1	–0.2	–0.2	–0.3	3.6	12.9	3.8	4.3
May	1.0	0.9	0.7	0.2	19.5	27.9	19.0	17.5
June	11.3	10.5	10.0	8.2	17.3	40.1	25.7	22.9
July	13.3	12.8	12.4	11.3	7.7	32.5	16.3	13.0
August	10.6	10.4	10.3	9.9	16.3	39.6	23.6	20.3
September	5.9	6.1	6.2	6.4	25.4	41.7	25.6	23.5
October	2.0	2.1	2.3	2.6	31.7	46.1	35.6	32.9
November	–1.2	–0.9	–0.7	0.0	11.9	20.5	21.4	19.0
December	–1.7	–1.5	–1.4	–0.8	4.6	10.8	7.5	5.8
2013								
January	–3.3	–3.2	–3.0	–2.5	4.1	9.1	6.5	4.4
February	–3.4	–3.3	–3.2	–2.8	4.0	9.0	6.4	4.2
March	–2.3	–2.3	–2.3	–2.2	4.1	9.6	6.3	4.1
April	–0.7	–0.6	–0.6	–0.5	4.4	11.5	7.7	6.0
May	0.5	0.3	0.1	0.0	22.9	30.5	10.4	13.7
June	8.9	8.0	7.5	5.8	18.5	39.8	28.7	24.8
July	10.8	10.2	9.9	8.9	7.1	31.7	9.5	6.9
August	9.3	9.2	9.2	8.8	8.9	22.1	12.0	10.0
September	4.3	4.3	4.4	4.4	38.8	48.1	40.9	37.2
October	0.0	0.4	0.6	1.2	20.4	33.3	28.5	22.8
November	–2.6	–2.3	–2.0	–1.0	6.6	13.2	12.6	9.2
December								

Table 3.8 Soil temperature and soil moisture at four depths measured at SoilEmpSa from January 2010 to November 2013 (data from December is not yet retrieved).

Month-year	Soil temp. –1 cm (°C)	Soil temp. –5 cm (°C)	Soil temp. –10 cm (°C)	Soil temp. –30 cm (°C)	Soil moist. –5 cm (%)	Soil moist. –10 cm (%)	Soil moist. –30 cm (%)	Soil moist. –50 cm (%)
2010								
January	–1.7	–1.0	–1.4	–0.5	22.6	13.6	19.5	33.9
February	–2.6	–1.8	–2.2	–1.3	21.2	13.0	12.4	22.0
March	–1.9	–1.7	–1.8	–1.4	20.0	12.3	11.0	12.4
April	–0.2	–0.3	–0.3	–0.3	26.4	15.4	12.2	13.3
May	3.1	1.3	1.7	1.0	59.2	47.3	26.3	16.5
June	8.3	6.0	6.8	5.5	59.6	45.9	46.6	46.3
July	11.4	9.7	10.6	9.2	56.0	32.2	41.8	37.7
August	11.0	10.2	10.4	10.1	59.2	48.8	44.5	45.0
September	7.6	7.7	7.6	7.7	59.7	48.8	46.1	49.3
October	2.7	3.7	3.1	4.0	58.1	36.0	44.2	43.0
November	–0.2	0.6	0.2	0.9	57.0	36.3	44.2	40.7
December	0.4	0.7	0.6	0.7	60.2	54.4	46.3	46.6
2011								
January	–1.1	–0.2	–0.5	0.0	32.7	25.9	44.5	43.3
February	–0.6	–0.3	–0.5	–0.2	23.5	14.8	41.8	37.0
March	–0.6	–0.4	–0.5	–0.3	23.6	14.5	25.0	33.5
April	–0.7	–0.5	–0.6	–0.4	23.8	14.4	19.3	31.5
May	0.1	0.1	0.1	0.2	30.5	21.5	20.0	32.7
June	3.9	3.2	3.4	3.0	53.4	47.0	35.9	45.1
July	10.3	9.0	9.2	8.9	60.0	51.9	47.4	49.9
August	10.2	9.3	9.6	9.1	58.0	39.9	45.0	44.2
September	4.7	5.1	5.0	5.2	60.1	53.3	46.9	49.4
October	0.2	1.0	0.6	1.3	52.0	40.2	45.2	45.5
November	–1.9	–0.8	–1.4	–0.3	21.9	15.1	40.5	39.4
December	–0.9	–0.7	–0.8	–0.5	21.3	13.5	15.7	35.1
2012								
January	–0.9	–0.7	–0.9	–0.5	21.3	13.4	15.6	32.2
February	–0.6	–0.5	–0.6	–0.4	23.1	14.0	15.8	22.2
March	–1.6	–1.3	–1.5	–1.0	20.0	12.5	14.5	17.0
April	0.0	0.0	0.0	0.0	27.2	14.9	16.2	17.3
May	0.6	0.2	0.3	0.1	45.1	26.4	18.0	18.8
June	8.6	6.3	7.1	5.7	58.8	45.5	44.4	37.6
July	11.9	10.6	11.2	10.2	57.6	42.3	44.9	42.7
August	10.2	9.7	9.8	9.6	59.5	49.7	46.1	47.7
September	6.6	6.8	6.7	6.9	58.9	48.5	45.6	45.7
October	2.8	3.1	3.0	3.1	60.4	56.7	46.8	50.0
November	–0.1	0.4	0.3	0.5	52.8	50.9	46.4	49.2
December	–0.8	–0.2	–0.4	0.0	27.0	30.0	44.3	41.9
2013								
January	–1.4	–0.8	–1.2	–0.4	21.6	14.1	35.6	35.3
February	–2.2	–1.6	–2.0	–1.1	19.6	13.2	14.7	25.8
March	–1.3	–1.0	–1.1	–0.8	21.1	14.4	14.8	16.1
April	–0.1	–0.1	–0.1	–0.1	25.8	15.4	16.0	16.9
May	0.2	0.0	0.0	0.0	30.5	16.8	17.3	17.8
June	4.4	1.6	2.5	1.1	58.7	40.7	32.3	23.9
July	9.1	7.2	8.0	6.7	57.6	39.9	45.2	44.0
August	9.0	8.4	8.7	8.2	55.2	35.1	43.8	38.9
September	4.5	4.5	4.5	4.5	60.4	56.7	46.5	46.4
October	1.2	1.5	1.5	1.6	60.3	53.3	46.8	49.9
November	–1.1	–0.3	–0.5	–0.1	31.1	21.7	45.1	43.4
December								

temperature was 1.0 °C from end May to mid June which was 1.0 °C lower than the previous years and the water temperature peaked with a maximum temperature of 12.9 °C in the beginning of August which was 3.7 °C lower and three weeks later than 2012. The conductivity measurements showed a normal decrease in conductivity within the snow melting period from 20 µSc m^{-1} to a level of 14 ± 1.5 µSc m^{-1}. From the beginning of July and through the rest of the field season, the conductivity shows no significant trend, which is normal for the period. pH shows a normal trend from 6.2 in the beginning of the field season to 7.6 in the beginning of August, followed by some variation due to rain events during the autumn.

3.3 Vegetation

Vegetation in the Kobbefjord area is monitored by both the BioBasis and GeoBasis programmes. While BioBasis monitors individual plants and plant phenology using plot scale sites and transects, the GeoBasis programme monitors the phenology of the vegetation communities from satellite.

Satellite imagery

Unlike the previous years it has not been possible to acquire QuickBird, WorldView or Aster image data, due to cloudy conditions in the requested period (optimum of growing season in end of July). Instead, a SPOT6-scene was acquired from 28 July at around 14:30 GMT. The scene was geometrically corrected with Rational Polynomial Coefficients (RPC) methods and known ground control points from former campaigns in Kobbefjord (30 Ground Control Points (GCP) also used to correct previous QuickBird scenes). Moreover, it is orthorectified using the 10 m digital elevation model. Furthermore, it is atmospherically corrected using a dark object subtraction approach and data is converted from digital numbers to top of atmosphere reflectance. Finally, Normalised Difference Vegetation Index (NDVI) is derived from the reflectance (see figure 3.10) and average NDVI is extracted from regions of interest covering a fell field, an open mixed heath, an *Empetrum nigrum* dominated heath, a fen, a copse and the heath monitored by the INTERACT station (see figure 3.11). Over the six years Fell field had significant lower NDVI-

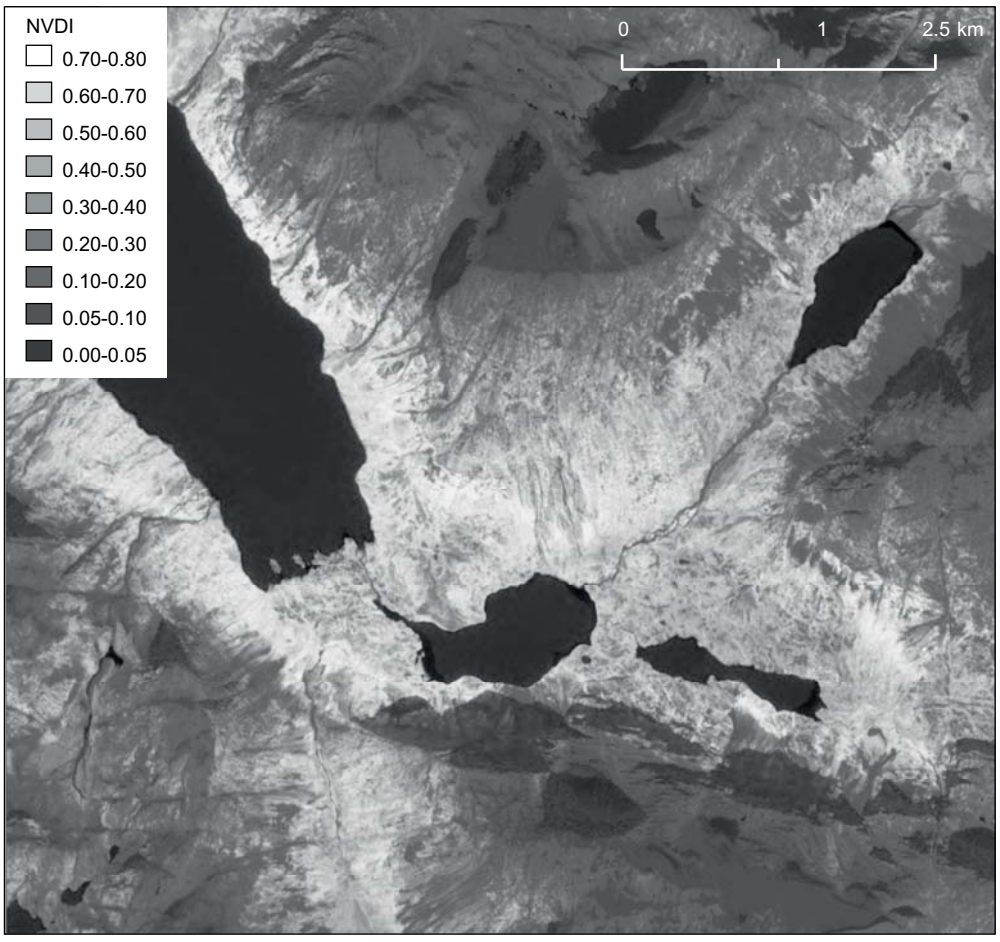

Figure 3.10 Normalised Difference Vegetation Index (NDVI) based on a SPOT6 scene from 28 July 2013. Data are dark subtracted as atmospheric correction and lack the topographic correction.

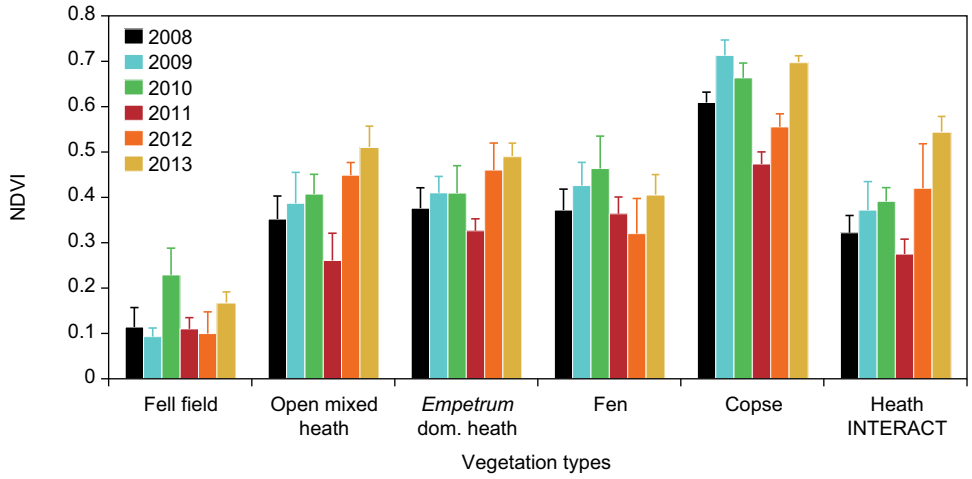

Figure 3.11 NDVI from 17 July 2008 and 2009, 10 July 2010, 14/30 July 2011, 25 July 2012 and 28 July 2013 for the six different vegetation types. NOTE that changes between greenness are due not only to phenology differences between years but also seasonal phenology as the images are acquired approximately two weeks around the maximum greenness dates.

values around 0.13 ± 0.14, while copse had significant higher values around 0.60 ± 0.13 all six years. The four other vegetation classes had NDVI values around 0.36-0.40 ± 0.05. As also noticed from ground truth measurements of NDVI (BioBasis, 2013), higher NDVI values are observed in 2013 than in 2011 and 2012, probably as a result of the shrubs recovering from the *Eurois occulta* larvae attack in 2011, combined with a more dominating understory resulting from the decreased competition from shrubs during the attack. The higher NDVI values are most prominent in heaths as expected.

Digital camera imagery

Phenology studies of Arctic ecosystems are still dependent on spatial scale and quality (e.g. percent cloud cover) of the image data. Furthermore, the sparse vegetation and heterogeneous surface can be difficult to trace with coarse spatial resolution NDVI. Higher spatial and temporal resolution can be achieved by monitoring the ecosystems with automated digital cameras. Better still, image data can thus be acquired under cloudy conditions, which is advantageous in Arctic ecosystems with short intense growing seasons where a high frequency of data is important. Major challenges when using of digital cameras is to compensate for changes in incoming radiation, as well as having the limitation of low spectral resolution. Even so, indices based on visual bands available from unmodified digital cameras have been found to correlate with NDVI over numerous types of ecosystems. However, of the few existing studies, none investigates the performance in Arctic environments with high variability in species composition. The use of conventional Red Green Blue (RGB) cameras as a tool to monitor landscape wide phenology has gained a lot of attention over the last few years. Mostly a measure of canopy greenness for a region of interest (ROI) is used to produce yearly time series, reflecting canopy phenology. The use of RGB prevents the use of established vegetation indices such as NDVI or Ratio Vegetation Index (RVI). However, since photosynthesis by vegetation is related to chlorophyll

Figure 3.12 Greenness index for three ecosystems copse, fen and heath at 50 m a.s.l. have been analysed using a new greenness index, %G. The regions are specified on figure 3.5 left and the fen area is very similar to the footprint for the CO_2-station in the fen. The %G for all three ecosystem during the period 2010-2013 is shown in the figure. The triangles represent the days for the satellite measurements (table 3.11). DOY (day of year).

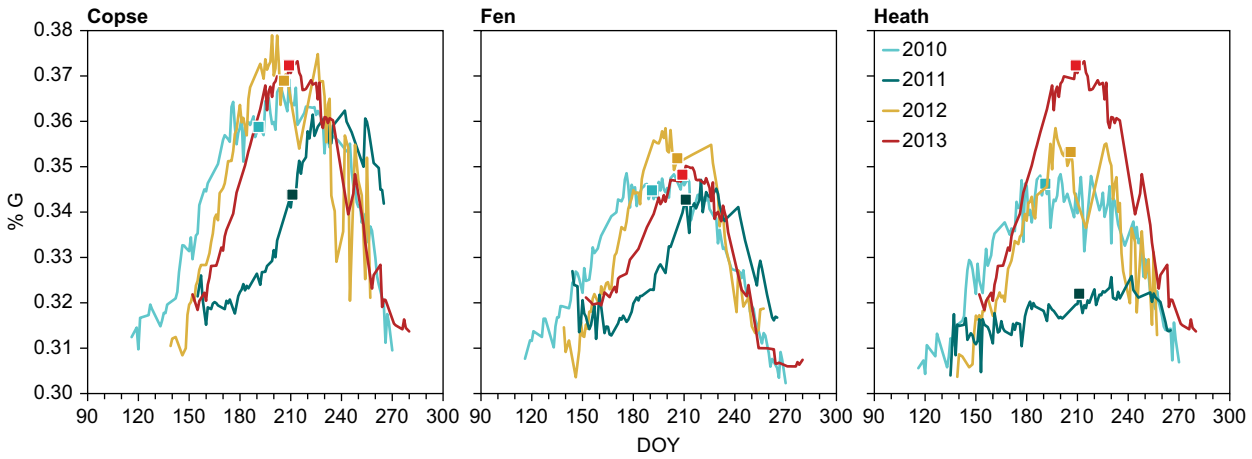

content and biomass in various vegetation types, we hypothesize that indices based on the excess of the green channel can describe seasonal growth patterns in vegetation. The most common is a greenness index, calculated as percent greenness, %G = DN(G)/(DN(R)+DN(G)+DN(B)), where DN is the digital value in each of the RGB channels. Figure 3.12 shows the significant lower %G-values in 2011 due to the outbreaks of *Eurois occulta* larvae, but the figure also shows that all three ecosystems in 2013 seems to have recovered from the outbreak. Figure 3.12 also shows that copse has a fast and earlier greenness compared to fen and heath, but all three ecosystems reached the maximum within the same week in ultimo July.

3.4 Carbon gas fluxes

Carbon gas fluxes are monitored on plot and landscape level in a fen area in Kobbefjord using two techniques:

- Automatic chamber measurements of CH_4 and CO_2 exchange on plot scale
- Eddy covariance measurements of CO_2 and H_2O exchange on landscape scale

Automatic chamber measurements

An automatic chamber system consisting of six flux chambers for monitoring the exchange of CH_4 and CO_2 was installed in the fen in August 2007 (Tamstorf et al. 2008). In 2013, measurements started 7 June and lasted until 27 September, with only few interruptions in the data record (figure 3.13). During this period, approximately 18% of data was lost due to maintenance, calibration and preventive system closedowns (i.e. due to expected high winds that may break the auto-chamber lids).

The spatial and temporal variation in CH_4 emissions is primarily related to temperature, water table depth and primary production. The fen in Kobbefjord is a source of CH_4 due to the permanently wet conditions that promote anaerobic decomposition, by which CH_4 is an end product.

In early June, when measurements started, average CH_4 fluxes were below 2 mg CH_4 m^{-2} h^{-1}. As the season progressed, emissions increased and reached a peak in early August, amounting to approximately 6.2 mg CH_4 m^{-2} h^{-1}. This CH_4 emission peak level is lower than in 2009 and 2012, but higher than in 2008, 2010 and 2011. The variation between years is likely related to variations in timing of snowmelt, meteorological conditions, and primary production in the fen.

After the CH_4 emission peak in early August, CH_4 fluxes decreased steadily and reached approximately 1 mg CH_4 m^{-2} h^{-1} in late September. Overall, the observed temporal CH_4 flux pattern of the Kobbefjord fen displays low shoulder season emissions with a dome-shaped peak during the growing season.

Eddy covariance measurements

In order to describe the inter-annual variation of the seasonal CO_2 budget, the land-atmosphere exchange of CO_2, H_2O and energy in the fen has been monitored using the eddy covariance technique since 2008. The eddy covariance system consists of a 3D sonic anemometer and closed path infrared CO_2 and H_2O gas analyser (Tamstorf et al. 2009). Raw data from the eddy covariance system was calculated using the software package EdiRe (Robert Clement, University of Edinburgh). For more details on the flux calculation procedures see Hansen et al. (2010).

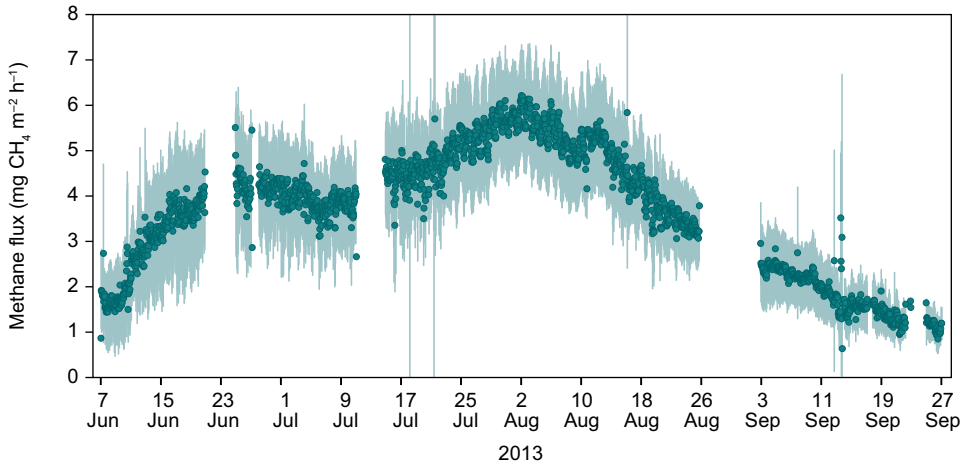

Figure 3.13 Methane (CH_4) emissions from the fen during 2013.

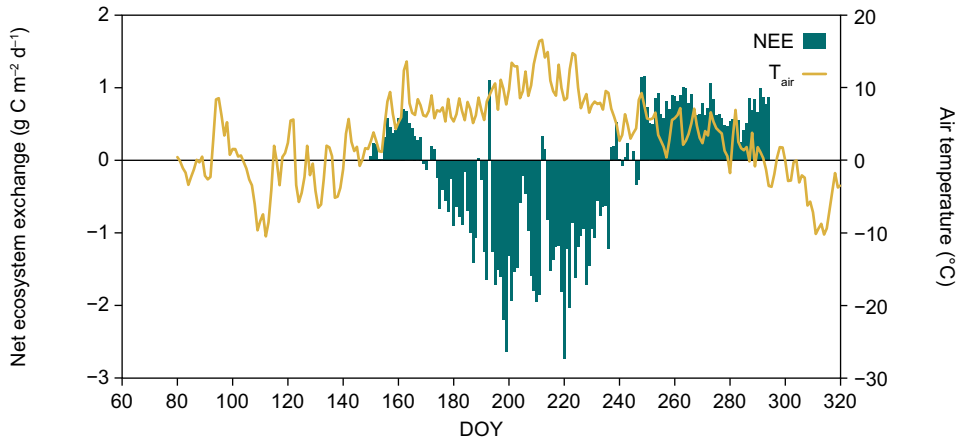

Figure 3.14 Diurnal net ecosystem exchange (NEE) and air temperature (T_{air}) measured in the fen in 2013.

The temporal variation in mean daily net ecosystem exchange of CO_2 (NEE) and air temperature during 2013 for the fen site is shown in figure 3.14 and various variables summarized in table 3.9. NEE refers to the sum of all CO_2 exchange processes at the ecosystem scale; including photosynthetic CO_2 uptake by plants, plant respiration and microbial decomposition. The CO_2 exchange is controlled by climatic conditions, mainly temperature and photosynthetic active radiation (PAR), along with amount of biomass and soil moisture content. The sign convention used in figures and tables is the standard for micrometeorological measurements; fluxes directed from the surface to the atmosphere are positive whereas fluxes directed from the atmosphere to the surface are negative.

Eddy covariance measurements of the CO_2 and H_2O exchange in the fen were initiated 29 May and lasted until 22 October. During this period, 9.3 % of data were lost due to malfunction, maintenance and calibration. Highest daily spring emission (0.7 g C m^{-2} d^{-1}) was measured 11 June, which coincided with high air temperature (figure 3.14). As the vegetation developed, photosynthetic uptake of CO_2 started, and 23 June the fen ecosystem switched from being a net source to a net sink of atmospheric CO_2 on a daily basis.

The period with net CO_2 uptake in 2013 lasted until 24 August. During this period, the fen accumulated –67.3 g C m^{-2}, which is in the higher end of the measurement record (table 3.9). Maximum daily accumulation rate amounted to –2.7 g C m^{-2} (measured 11 August), which is also in the higher end of the range based on previous years' measurements. By 24 August, respiration processes exceeded the fading photosynthesis and the ecosystem returned to a net source of atmospheric CO_2. In the beginning of this period there is plenty of fresh litter available and soil temperatures remain relatively high, allowing decomposition processes to continue at a decent rate. Highest daily emission during autumn was measured 6 September (1.2 g C m^{-2} d^{-1}). During the entire measuring period (144 days), the fen constituted a sink for atmospheric CO_2, amounting to –24.2 g C m^2.

Table 3.9 Summary of the eddy covariance measurement periods and CO_2 exchanges 2008-2013 at the fen site. Please notice that the measurement period varies from year to year.

Year	2008	2009	2010	2011	2012	2013
Measurements start	05 Jun	15 May	4 May	15 May	06 Jun	29 May
Measurements end	29 Oct	31 Oct	9 Oct	14 Oct	31 Oct	22 Oct
Start of net uptake period	–	01 Jul	29 May	28 July	16 Jun	23 Jun
End of net uptake period	16 Aug	27 Aug	18 Aug	7 Sep	31 Aug	24 Aug
NEE for measuring period (g C m^{-2})	–45.5	–14.0	–20.9	42.6	–33.4	–24,2
NEE for net uptake period (g C m^{-2})	–	–42.5	–65.4	–14.3	–73.1	–67.3
Max. daily accumulation (g C m^{-2} d^{-1})	–2.27	–1.48	–3.14	–1.58	–2.73	–2,74

4 Nuuk Basic

BioBasis programme

Maia Olsen, Josephine Nymand, Katrine Raundrup, Peter Aastrup, Paul Henning Krogh, Torben L. Lauridsen, Magnus Lund and Kristian Albert

This chapter presents the results of the seventh year of the BioBasis monitoring programme at Nuuk. The chapter gives an overview of the activities and presents examples of the results. The programme aims at providing long-term data series on biotic variables from the Kobbefjord area, approximately 20 km southeast of Nuuk. Methods and sampling procedures are described in detail in the manual 'Conceptual design and sampling procedures of the biological programme of Nuuk Basic' (Aastrup et al. 2009).

The programme was initiated in 2007 by the National Environmental Research Institute (now Department of Bioscience), Aarhus University in cooperation with the Greenland Institute of Natural Resources. BioBasis is funded by the Environmental Protection Agency as part of the environmental support programme DANCEA – Danish Cooperation for Environment in the Arctic. The authors are solely responsible for all results and conclusions presented in this chapter, which do not necessarily reflect the position of the Environmental Protection Agency.

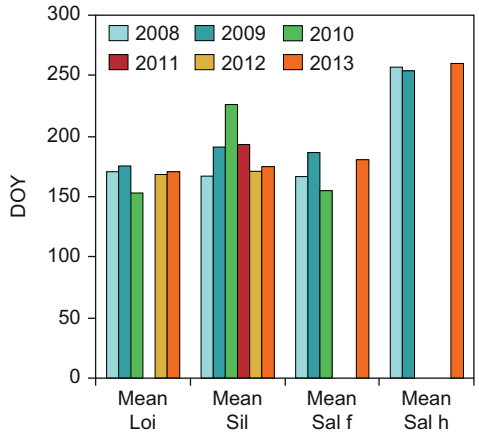

Figure 4.1 Mean value for days of year (DOY) of 50% flowers/catkins for each of the species (Loiseleuria procumbens, Silene acaulis, *and* Salix glauca*) in the plant reproductive phenology plots for 2008-2013. Also included are the senescent catkins of* S. glauca *(Sal h).* Erratum*: Please note that the similar figures in annual reports from 2008-2011 are incorrect.*

4.1 Vegetation

Reproductive phenology

The reproductive phenology has been studied since 2008 on three vascular plant species: The evergreen dwarf shrub *Loiseleuria procumbens*, the herb *Silene acaulis*, and the shrub *Salix glauca.* For each species, four phenology plots cover an ecological amplitude with respect to snow cover, soil moisture and altitude. In 2013, the recording of phenology started 22 May (DOY 142) and ended 15 October (DOY 288). Examples of the results from 2008-2013 are shown and commented in the following text. In *L. procumbens* and *S. acaulis* vegetative phenology in 2013 is comparable to that of 2012. However, there was a tendency to produce larger numbers of flowers in most plots, which may be due to plants having recovered from previous impacts of noctuid moths. The timing of 50 % flowering was within the same range as previous years (figure 4.1).

The flower bud production, the onset of flowering, and the peak flower production of *L. procumbens* occurred at approximately the same time this year as in 2012 (figures 4.2a and 4.2b).

A second bud production was recorded 3 September (DOY 246) 30 days earlier than in 2012 and 10 days later than in 2010. All plots produced more flowers in 2013 than in 2012, but not as many as before the outbreak of the noctuid moth, *Eurois occulta* in the seasons 2010 and 2011. The first senescent flowers were recorded only one day earlier (18 June, DOY 169) than in 2012 (figure 4.2c). The sudden drop in senescent flowers was caused by the second bud production.

With respect to timing of budding, flowering and senescence, *S. acaulis* was late by 5-6 days, compared to 2012 (figures 4.3a-c). First budding recorded occurred 11 June (DOY 162), as was the onset of flowering; senescence occurred 25 June

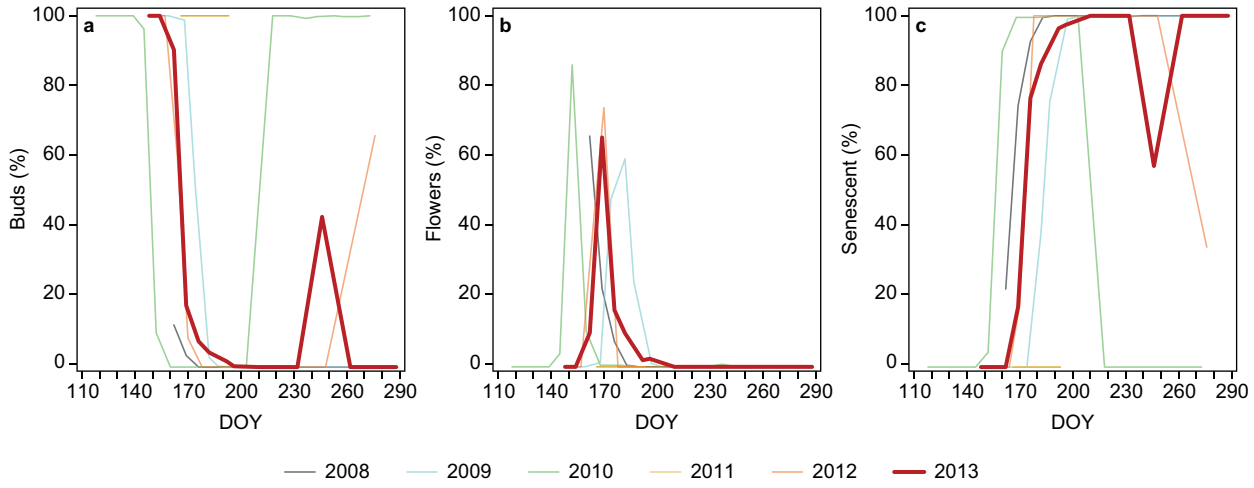

Figure 4.2 Percentage of Loiseleuria procumbens *in plot 1 during the growing seasons of 2008-2013 of a) buds, b) flowers and c) senescent flowers.*

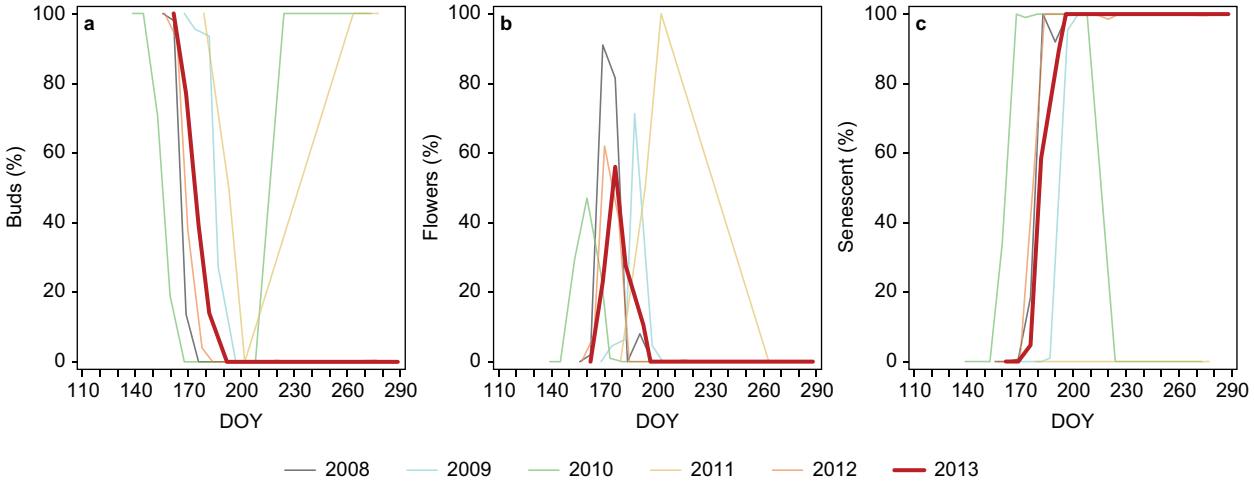

Figure 4.3 Percentage of Silene acaulis *in plot 3 during the growing seasons of 2008-2013 of a) buds, b) flowers and c) senescent flowers.* Erratum*: Figure 4.3a-c in NERO 6th Annual Report is not correct. Data has been recalculated and is shown in the present report.*

(DOY 176), making 2013 an intermediate year with respect to timing. The flowering peaked 26 June (DOY 177) which is considered early, compared to previous years.

The first flower buds of *S. glauca* were observed 11 June (DOY 162), a week later than the earliest year 2010 (2 June, DOY 153). First flowering male catkins were observed 13 June (DOY 164) and first female catkins 18 June (DOY 169). The first female flowers with hair were observed 11 July (DOY 192). A higher number of flowers were produced in 2013 than in 2012, which indicates that *S. glauca* has recovered from the impact of the noctuid moths in 2010 and 2011.

Furthermore, in the C-flux plots *S. glauca* produced a higher number of flowers than observed in previous years (table 4.1), with several plots reaching more than 100 female flowers (C4: 154, T1: 100 and T3: 131). On average, all plots produced a higher number of catkins in 2013 than in previous years, except for plots in the 'Long Growing Season' treatment. Nineteen C-flux plots out of 30 produced catkins in 2013, the highest recorded so far.

Summing up reproductive plant phenology

During April the area was exposed to two weeks of severe snowmelt, followed by heavy snowfall in May, resulting in a late snowmelt. A preliminary review of data related to flowering indicates that 2013 was characterized by:

- No larval outbreak of the noctuid moth *E. occulta*.
- Large numbers of flowers produced in *L. procumbens* and *S. glauca* compared to 2012 indicate full recovery from the impact of the noctuid moth.

Table 4.1 Average number of female catkins in Salix glauca *for each treatment in the C-flux plots for 2008-2013. Average number of female catkins with hair in* S. glauca *for each treatment in the ITEX plots for 2008-2013. For explanations of treatments see section in carbon dioxide exchange p. 37.*

		C	LG	S	SG	T
No. catkins	2008	5.17	3.33	2.33	2.83	16.17
	2009	5.33	3.33	1.17	2.5	2
	2010	1	1.67	0.33	1.5	0.33
	2011	0	0	0	0	0
	2012	0.33	0.17	0	2.33	5.5
	2013	40.83	3	8.17	8.17	60.83
No. catkins with hair	2008	1	0.67	0.5	2.17	1.83
	2009	0	1.67	0	1.17	0.17
	2010	0	0.5	1	0	0
	2011	0	0	0	0	0
	2012	0	0	0	2.17	2.83
	2013	24.5	2.37	2.67	6	36.5

Vegetation greening, NDVI

The seasonal greening of the vegetation was monitored in plots with 1) *Empetrum nigrum* ssp. *hermaphroditum* and *Eriophorum angustifolium*, 2) the plant phenology plots, and 3) along the NERO line (Bay et al. 2008). We used a handheld Crop Circle TM ACS-210 Plant Canopy Reflectance Sensor, which calculates the greening index (Normalized Difference Vegetation Index – NDVI). Measurements were made weekly in the *Empetrum nigrum*-plots, *Eriophorum angustifolium*-plots, and the plant phenology plots, and monthly along the NERO line.

NDVI in the *Empetrum nigrum-, Eriophorum angustifolium*-plots and plant phenology plots

Empetrum nigrum reached the highest NDVI values of all the species (figure 4.4a), and NDVI was consistently high throughout the season, with very little variation. The values were at the same level or higher than 2012, which otherwise was the highest year recorded so far. In three out of four plots the NDVI values measured at the beginning of the season were the highest ever recorded this time of year, even though 2013 had a late snowmelt. No real peak was recorded.

Eriophorum angustifolium peaked intermediate to late in 2013, compared to other years (figure 4.4b). Plots 1 and 4 peaked around 14 August (DOY 226) and plots 2 and 3 around 3 September (DOY 246).

The NDVI values for *L. procumbens* were similar to previous years (figure 4.4c), except 2011 which in general had low values. *L. procumbens* tends to have intermittent values, compared to the other species measured in Kobbefjord, and has little variation throughout the

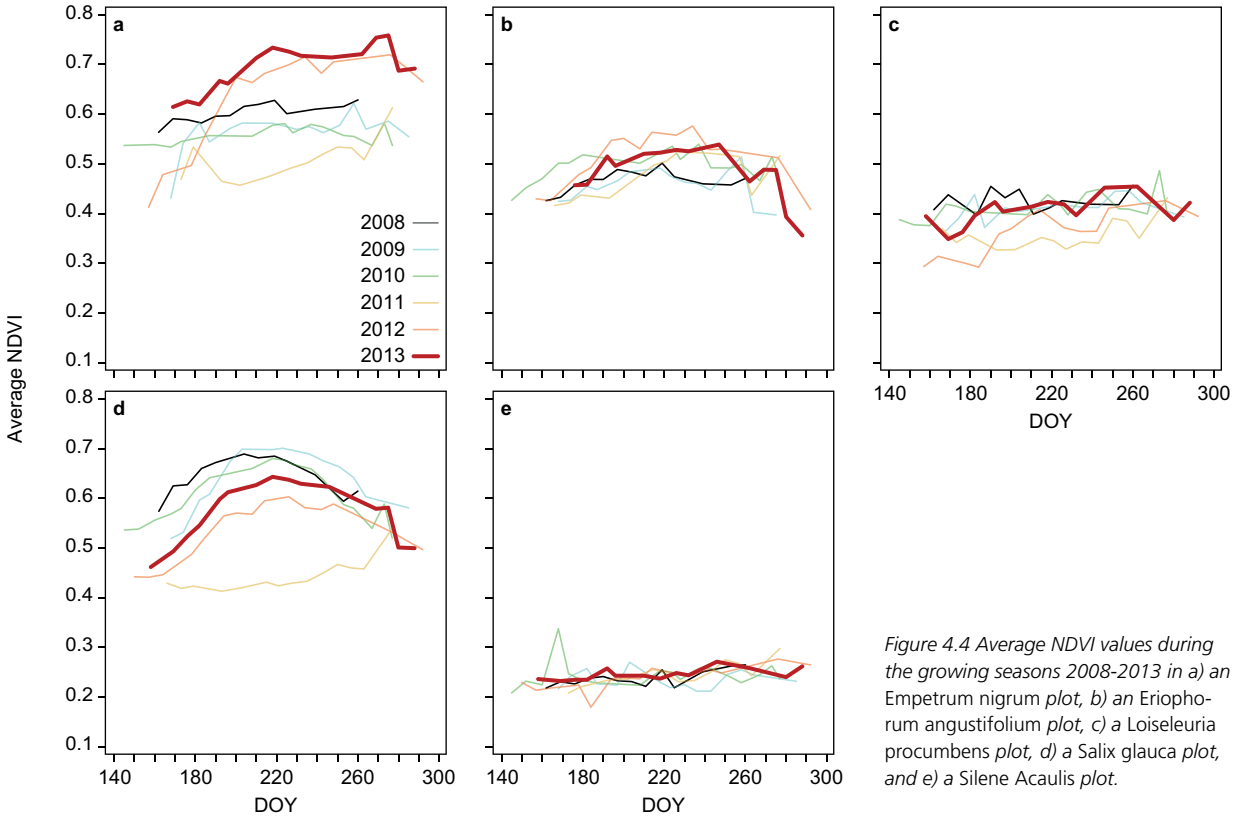

Figure 4.4 Average NDVI values during the growing seasons 2008-2013 in a) an Empetrum nigrum *plot, b) an* Eriophorum angustifolium *plot, c) a* Loiseleuria procumbens *plot, d) a* Salix glauca *plot, and e) a* Silene Acaulis *plot.*

season. The peak on DOY 269 and 275 is presumably due to wet vegetation and must be interpreted with caution. Plot 3 had higher NDVI values in 2012 and 2013 than in previous years, but the density of *L. procumbens* has been decreasing (comparing photos and distribution from 2009 to today). In 2013 there was very little *L. procumbens* left; today the plot mostly consists of *E. nigrum* and graminoids.

In 2013, the NDVI values in *S. glauca* plots were comparable to previous years, except in plot 2 (figure 4.4d), which has more year-to-year variation. The peak occurred 6 August (DOY 218), approximately 10 days earlier than in 2012 but later than in 2009. In 2013, all plots were back at previous NDVI levels, that is, before the outbreak of noctuid moth larvae in 2010 and 2011.

S. acaulis generally has the lowest NDVI values of all the species monitored, and there appears to be very little year-to-year variation, with the values in 2013 at the same level as the previous four years (figure 4.4e). *S. acaulis* is found in very sandy patches, with sparse vegetation cover, which could explain the very stable values. The peak on DOY 269 and 275 is presumably due to wet vegetation and must be interpreted with caution.

NDVI along the NERO line

The seasonal development of NDVI along the NERO line in 2013 is comparable to 2012. The values tended to be higher than most years (figures 4.5a-d), with a maximum occurring late in the season at approximately 14 August (DOY 226); except for the snow patch, in which greening occurred not only earlier (approximately DOY 200) than recorded in previous years, but also at higher levels throughout most of the season (figure 4.5d). In the heath and copse (figures 4.5a-b), the NDVI values stayed consistently high through most of the season with a peak occurring late, compared to previous years. The NDVI values recorded for the fen (figure 4.5c) reached a slightly higher maximum than in previous years (except for 2012).

Summing up the vegetation greening

Generally the vegetation greening in 2013 was very similar to that in 2012. The NDVI values were in many cases higher throughout the season compared to previous years, with an intermediate to late peak. The vegetation seems to have recovered after the outbreak of the noctuid moth larvae.

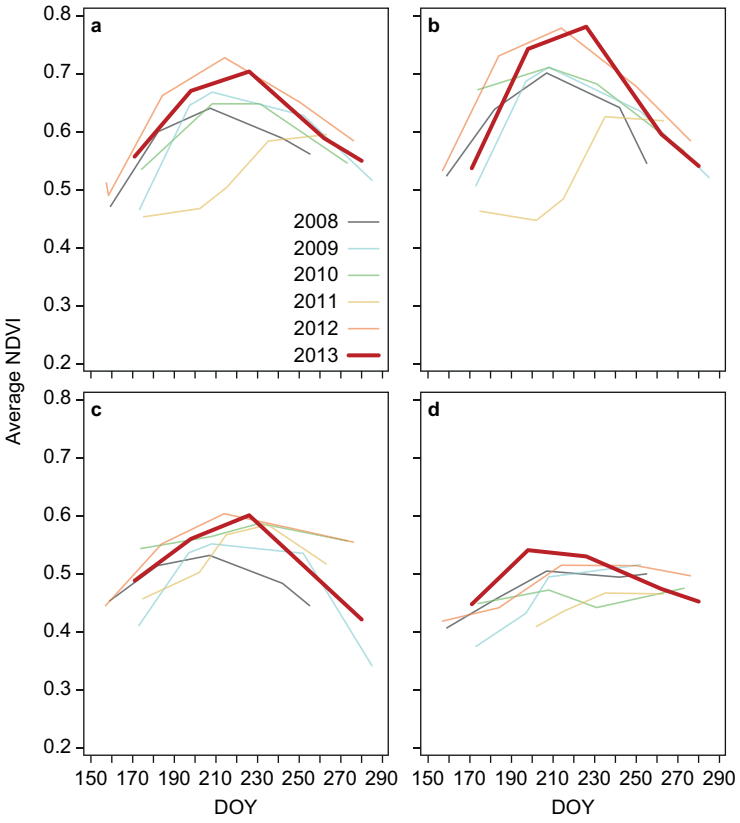

Figure 4.5 Average NDVI values along the NERO line from the vegetation types a) dwarf shrub heath, b) copse, c) fen, and d) snow patch.

Carbon dioxide exchange

In 2008, a manipulation experiment was initiated with five treatments, each with six replicates. The experiment is located in a mesic dwarf shrub heath dominated by *Empetrum nigrum* with *Salix glauca* as a subdominant species. Treatments include control (C), shortened growing season (SG: addition of snow in spring), prolonged growing season (LG: removal of snow in spring), shading (S: hessian tents) and increased temperature (T: ITEX plexiglas hexagons). We have conducted measurements of land-atmosphere exchange of CO_2, once a week using the closed chamber technique; soil temperature, soil moisture and phenology of *Salix glauca* were measured simultaneously during June-September in each year. The net ecosystem exchange (NEE) was measured with transparent chambers while the ecosystem respiration (R_{eco}) was measured with darkened chambers. Gross primary production (GPP) was calculated as the difference between NEE and R_{eco}. The SG and LG treatments have not been applied in 2008-2013, therefore results from these plots can be considered as controls.

The first CO_2 flux measurement day in 2013 was 25 June (DOY 176). Until the last

measurement day, 19 October (DOY 292), CO_2 fluxes were measured on 19 occasions (figure 4.6). Generally, all plots functioned as sinks for atmospheric CO_2 at the time of the measurement (midday). In October, NEE was generally close to zero. Similar to earlier years, NEE was more negative (i.e. higher CO_2 uptake) in C plots compared with T and S plots. The ecosystem respiration showed a pattern of higher emissions in T plots compared with other treatments, especially during June through September, which can be explained by warmer and drier conditions resulting in increased respiration rates. Highest rates of GPP were generally observed in C plots, while especially S plots had lower GPP rates compared with other treatments. As photosynthesis is driven by solar radiation, shading decreases GPP and build-up of biomass.

The differences between treatments during 2013 were in general similar to earlier years. Together with 2012, the flux amplitudes in 2013 were higher compared with previous years.

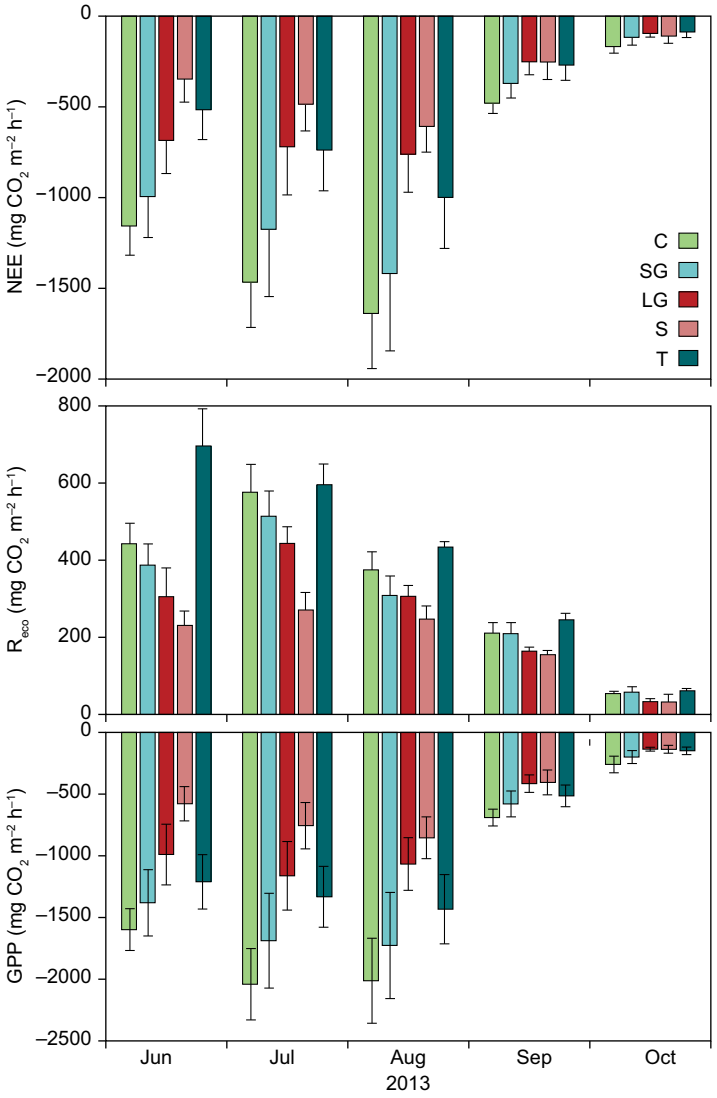

Figure 4.6 Monthly means of net ecosystem exchange (NEE: upper panel), ecosystem respiration (R_{eco}: middle panel) and gross primary production (GPP: lower panel) in 2013 in the manipulation experiment. Error bars refer to standard error in spatial variability (six replicates). For explanation of treatment abbreviations, see text.

UV-B exclusion plots

Measurements of chlorophyll fluorescence as a measure of plant stress were carried out in 2013. The impact of ambient UV-B radiation on the vegetation is studied in a mesic dwarf shrub heath dominated by *Empetrum nigrum* and with *Betula nana* and *Vaccinium uliginosum* as subdominant species. The plots were set up between 5 and 7 June (DOY 156 and DOY 158) except for Teflon F1, which was set up 19 June (DOY 170). In general, the frames were very resistant towards strong winds; only on five occasions from the end of August to the frames were removed by 7 October (DOY 280) the set up was affected by the strong winds. The frames were re-established shortly after disruption.

The ambient UV-B radiation on fluorescence parameters was monitored on *V. uliginosum* and *B. nana*. The total performance index (PI_{total}) is an indicator of the viability of a sample. PI_{total} were sensitive to UV-B exclusion in both *V. uliginosum* and *B. nana*. The seasonal average PI_{total} was improved by around 20 % in *V. uliginosum* and around 16 % in *B. nana* when reduced UV-B was compared to near ambient UV-B (table 4.2). For *B. nana* the PI_{total} was significantly decreased by ambient UV-B by the time of the last measurement (7 August, DOY 219), but not on the first two measurements, 25 July (DOY 206) and 30 July (DOY 211), respectively (figure 4.7). UV-B reduction improved *V. uliginosum* PI_{total} on all dates measured, although only slightly on the final day of measurement (figure 4.2).

4.2 Arthropods

In Kobbefjord, all four pitfall trap stations established in 2007 and the two window trap stations (each with two traps) established in 2010 were open during the 2013 season. Parts of the samples are being sorted by Department of Bioscience, Aarhus University, Denmark. The material sampled during the 2013 season is currently stored in 70 % ethanol at Greenland Institute of Natural Resources.

Pitfall traps were established from 28 May (DOY 148) through 13 June (DOY 164) and they all worked continuously until 7 October (DOY 280) when the liquid began to freeze. In 2013, arthropods were caught during 4511 trap days (including 4057 pitfall-trap days and 454 window-trap days).

Table 4.2 The chlorophyll fluorescence parameters were analyzed with the OJIP test approach (Strasser et al. 2004) and the parameters are: The ratio of PSII reaction centre's (RC) and absorbance flux, [RC/ABS]; The maximum quantum yield, [$\phi P_o = F_V/F_M$)] which corresponds to the efficiency an absorbed photon will be trapped by PSII RC leading to QA reduction; The fraction of electrons transported beyond QA – per exiton trapped by the open reaction PSII RC, [$\psi E_o = ET_o/TR_o$]; The efficiency with which an electron can move from the reduced intersystem electron acceptors to the PSI end acceptors, [$\delta R_o = RE_o/ET_o$]; The performance index [PI_{abs} = (RC/ABS) × [$\phi P_o/(1-\phi P_o)$] x [$\psi E_o/(1-\psi E_o)$] × [$\delta R_o/(1-\delta R_o)$]]; The total performance index integrating the responses of antenna, reaction centre, electron transport and end acceptor dependent parameters [PItotal = (RC/ABS) × [$\phi P_o/(1-\phi P_o)$] × [$\psi E_o/(1-\psi E_o)$] × [$\delta R_o/(1-\delta R_o)$]]. The presented values are the seasonal mean ± standard error for open control (No filter), Filter Control (near ambient UV-B, Transparent filter, Teflon), UV-B reduction (UV-B absorbing filter, Mylar). Analysis of variance included effects of block, campaign (C), treatment (T) and the interaction CxT and the P-values for treatment are given. Tukey test ($p<0.05$). Means that are not sharing a letter are significantly different.

2013		C		F		B		P-value
Betula nana	PI_{total}	3.396±0.594	B	4.076±0.320	AB	4.873±0.448	A	0.0257
	PI_{abs}	3.131±0.212	C	3.638±0.279	B	4.268±0.280	A	0.0003
	RC/ABS	0.675±0.011	B	0.712±0.015	A	0.712±0.016	A	0.0140
	F_v/F_m	0.750±0.006	B	0.761±0.007	B	0.783±0.008	A	0.0210
	ET_o/TR_o	0.531±0.010	B	0.545±0.010	AB	0.564±0.010	A	0.0092
	RE_o/ET_o	0.547±0.014	A	0.538±0.016	A	0.558±0.013	A	0.4410
Vaccinium uliginosum	PI_{total}	6.206±0.243	B	5.598±0.257	B	7.090±0.293	A	0.0001
	PI_{abs}	5.591±0.201	B	4.967±0.215	C	6.530±0.237	A	0.0001
	RC/ABS	0.670±0.010	B	0.664±0.012	B	0.703±0.012	A	0.0025
	F_v/F_m	0.787±0.005	B	0.785±0.006	B	0.809±0.004	A	0.0001
	ET_o/TR_o	0.680±0.005	A	0.648±0.006	B	0.673±0.004	B	0.0001
	RE_o/ET_o	0.525±0.006	A	0.529±0.006	A	0.519±0.006	A	0.4213

Microarthropods

In the season 2013 the sampling of microarthropods was reduced from the standard of eight samples per plot to four samples per plot. Sampling was carried out three times during the season. The samples have not been analyzed yet. The material sampled and extracted are currently stored in 70% ethanol at the Greenland Institute of Natural Resources.

Materials collected from research projects completed in 2012 in Kobbefjord and Zackenberg were further analyzed. See project description and results in chapter 6.

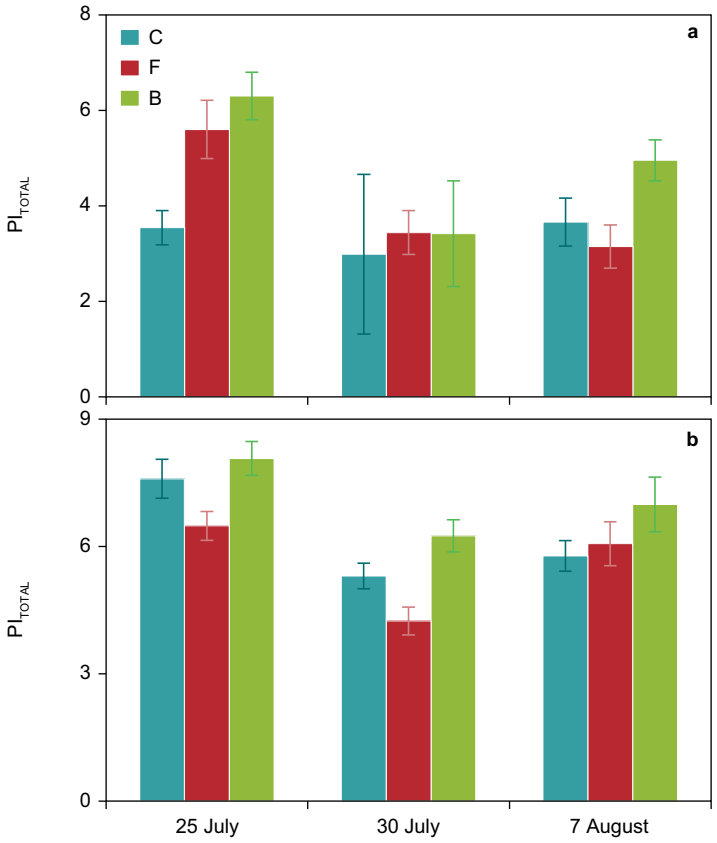

Figure 4.7 Seasonal variations in total performance index for a) Betula nana *and b)* Vaccinium uliginosum. *Treatments are C-Open control (no filter) – F-filter control (transparent filter, Teflon), and B – UV-B reduction (UV-B absorbing filter, Mylar).*

4.3 Birds

Survey for breeding passerines

No formal survey was carried out in 2013.

Breeding eagles

A breeding pair of white-tailed eagles *Haliaeetus albicilla* was observed on the mountainside northeast of the research house in Kobbefjord. The nest was observed for the first time 20 June (DOY 171) and one juvenile eagle was seen on the

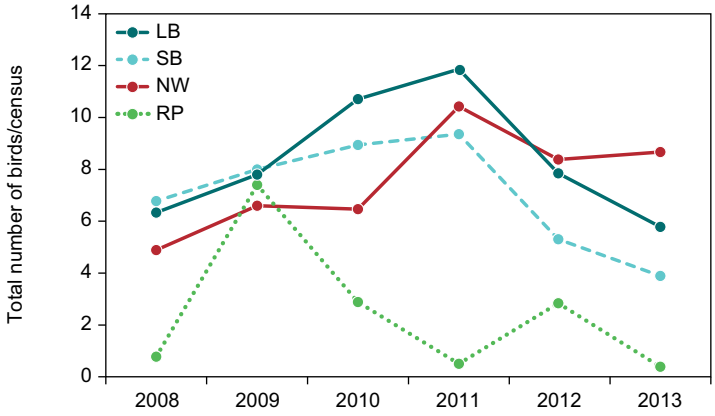

Figure 4.8 Total number of birds counted per census in 2008-2013. For explanation of the bird abbreviations, see text. The lines connecting the dots are only used for illustrative purposes.

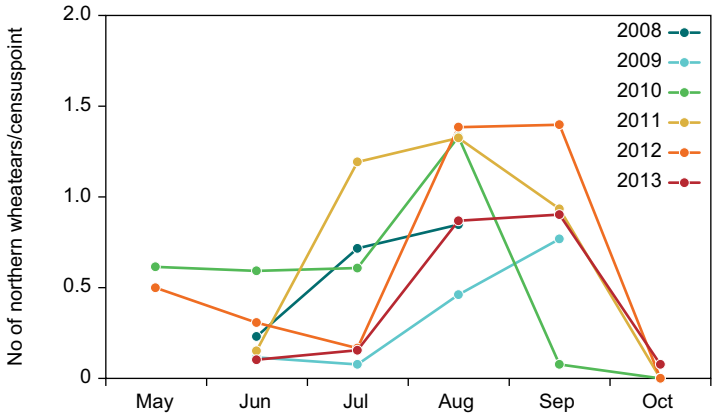

Figure 4.9 Number of northern wheatears per census during the season in 2008-2013. The lines connecting the dots are only used for illustrative purposes.

beach at several occasions after first flight. On 29 August (DOY 241) an adult eagle was seen feeding the juvenile. The last recorded sighting of the juvenile eagle was 2 October (DOY 275).

Bird census points

Passerines were counted at 13 census points within the 32 km^2 Kobbefjord catchment area. A total of 18 censuses were carried out from 7 June (DOY 158) to 15 October (DOY 288) 2013. When arriving at a census point five minutes were used as a 'settling period' (initial period) and a following five minute period (observation period) was used for counting the birds. If none was seen during the 'observation period', the observations from the 'initial period' are used. All four species of passerines were already present at the time of the first census, and the survey was carried out until no more observations were made at any census point.

The total number of Lapland buntings (LB), snow buntings (SB), northern wheatears (NW), and redpolls (RP) has varied between the years (table 4.3). In 2013, the northern wheatear was the most abundantly observed passerine, and the only species to have more observations per census in 2013 than in 2012. 2013 also had fewer observations of LB, SB and RP per census than in any previous years. Figure 4.8 shows the number of passerines counted per census from 2008-2013.

Although there is some variance from year to year, the number of observations of northern wheatears is usually at its maximum in August. This is due to juveniles appearing at the end of July. The northern wheatears start migrating in September and continue in October. Observations of Lapland buntings tend to be more frequent in the beginning of the season, but this is likely due to the very obvious territorial displays by the males.

Figure 4.9 shows the number of northern wheatears counted per census.

4.4 Mammals

The Kobbefjord catchment area is only sparsely populated with mammals. In other years, we have seen Arctic fox, Arctic hare, and caribou. In 2013 at least two different foxes have been observed on several occasions; tracks, faeces and barks have been observed/heard throughout the season. Additionally, only one hare was observed.

Table 4.3 Total number of passerines counted and the number of censuses per year. Also shown is the number of passerines per census. For explanation of bird abbreviations, see text.

Year/birds	LB	SB	NW	RP	No of census's	LB/census	SB/census	NW/census	RP/census
2008	57	61	44	7	9	6.3	6.8	4.9	0.8
2009	39	40	33	37	5	7.8	8.0	6.6	7.4
2010	182	152	110	49	17	10.7	8.9	6.5	2.9
2011	166	131	146	7	14	11.9	9.4	10.4	0.5
2012	102	69	109	37	13	7.8	5.3	8.4	2.8
2013	104	70	156	7	18	5.8	3.9	8.7	0.4

Table 4.4 Meteorological data from the official DMI station in Nuuk, which is the closest official station to the Kobbefjord catchment. A precipitation day is defined as a day with >1 mm precipitation.

	Climate data from Nuuk					
	2008	2009	2010	2011	2012	2013
Annual precipitation (mm)	1041	537	733	748	1201	962
Precipitation May-Aug (mm)	214	122	400	220	411	270
Annual precipitation days	134	82	102	123	129	124
Average temp May-Aug	6.5	4.9	7.3	5.2	7.5	4.7
Average temp May/June	4.7	2.3	5.9	2.8	5.5	2

4.5 Lakes

In the Kobbefjord catchment area two lakes have been monitored since 2008. Both lakes are deep with maximum depths of 35 and 27 metres, respectively. Badesø, which is the deepest, is situated downstream at 50 m a.s.l. and Qassi-sø upstream at approximately 250 m a.s.l. Qassi-sø is the most wind exposed of the two lakes; a small glacier drains into the lake resulting in silt input to the system. Due to the higher altitude, Qassi-sø has generally a longer ice covered period than Badesø. In 2013 fish were monitored for the second time since 2008, consequently fish data are included in this year's report and are compared to the data from 2008.

Climate

Regarding precipitation 2013 was dryer than 2012, but still a wet year compared to the norm (753 mm) (table 4.4). During the summer months, 2013 was very close to an average year of 289 mm precipitation, which means the winter months were particular wet. Precipitation days of 2013 were slightly above the norm of 114 days (table 4.4). The summer 2013 was the coldest of the monitored years; slightly colder than 2009 and 2011, both when looking at the pre-summer period (May-June) and the entire summer/growing season (May-August, table 4.4).

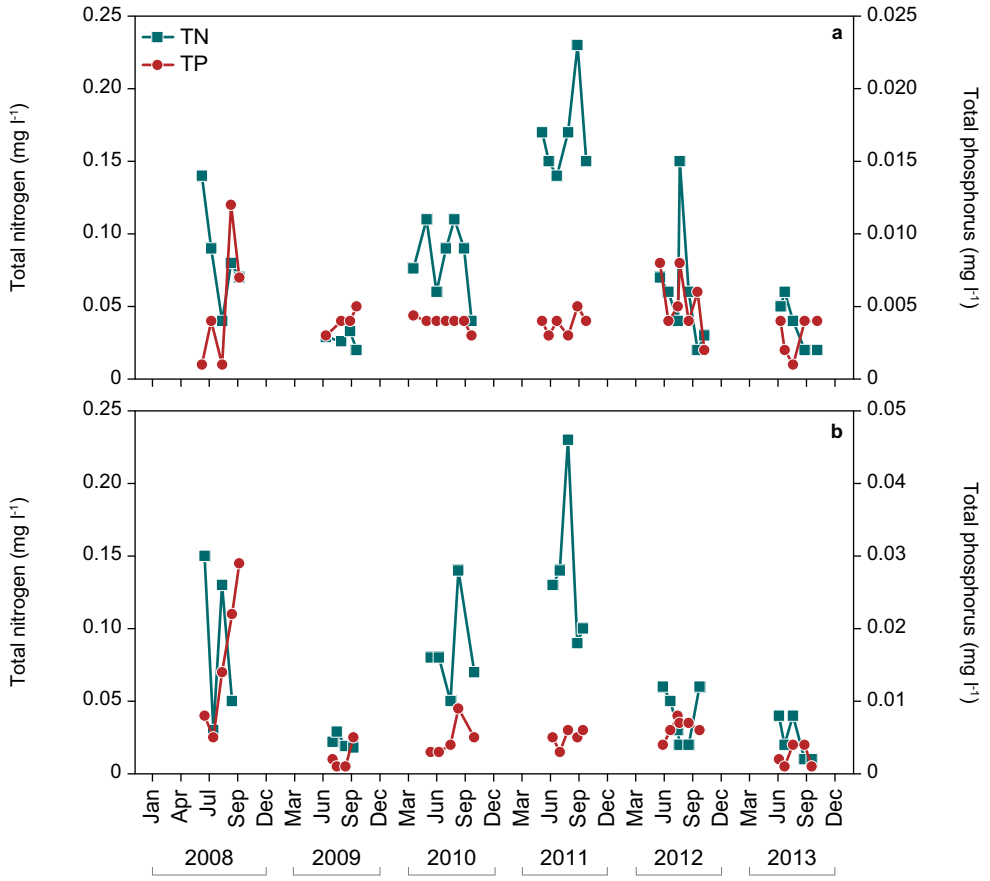

Figure 4.10 Total nitrogen (TN) and total phosphorus (TP) in Badesø (a) and Qassi-sø (b) during 2008-2013.

Table 4.5 Morphometric data, time weighted mean values of water chemistry (min-max values) and physical data measured in Badesø and Qassi-sø during the ice free periods from 2008-2013.

Badesø						
Area (ha)	80					
Maximum depth (m)	35					
Mean depth (m)	9.2					
	2008	**2009**	**2010**	**2011**	**2012**	**2013**
Total phosphorus (mg l^{-1})	0.005 (0.001-0.012)	0.004 (0.003-0.005)	0.004 (0.003-0.004)	0.004 (0.003-0.005)	0.006 (0.002-0.008)	0.003 (0.001-0.004)
Total nitrogen (mg l^{-1})	0.084 (0.040-0.140)	0.027 (0.020-0.033)	0.08 (0.04-0.11)	0.17 (0.14-0.23)	0.06 (0.03-0.15)	0.037 (0.02-0.06)
pH	6.92 (6.59-7.13)	6.85 (6.46-7.14)	6.62 (6.09-7.3)	7.1 (6.51-7.85)		
Conductivity (µS cm^{-1})	20 (19-22)	22 (21-23)	21 (18-26)	21 (15-27)	18 (14-19)	25 (20-42)
Ice free (date)	03 Jun	15 Jun	20 May	23 Jun	09 Jun	14 Jun
Ice covered (date)	24 Oct	30 Oct	13 Dec	25 Oct	14 Nov	24 Oct
Ice free period (days)	143	137	207	124	158	132
Qassi-sø						
Area (ha)	52					
Maximum depth (m)	27					
Mean depth (m)	7.8					
	2008	**2009**	**2010**	**2011**	**2012**	**2013**
Total phosphorus (mg l^{-1})	0.015 (0.005-0.029)	0.002 (0.001-0.005)	0.005 (0.003-0.009)	0.005 (0.003-0.006)	0.006 (0.004-0.008)	0.003 (0.001-0.004)
Total nitrogen (mg l^{-1})	0.09 (0.30-0.150)	0.022 (0.019-0.029)	0.084 (0.050-0.14)	0.138 (0.09-0.23)	0.03 (0.02-0.06)	0.026 (0.01-0.04)
pH	6.72 (6.44-6.96)	6.87 (6.79-6.93)	6.84 (6.37-7.31)	7.59 (6.79-7.97)		
Conductivity (µS cm^{-1})	20 (15-24)	16 (16-17)	17 (15-18)	18 (15-20)	15 (10-20)	20 (17-26)
Ice free (date)	12 Jun	28 Jun	31 May	1 Jul	18 Jun	22 Jun
Ice covered (date)	18 Oct	17 Oct	10 Nov	20 Oct	1 Nov	24 Oct
Ice free period (days)	128	111	163	112	136	124

Ice cover and water chemistry

The ice out date was 14 June (DOY 165) in Badesø and eight days later, 22 June (DOY 173) in Qassi-sø. Both lakes were ice covered again before 24 October (DOY 297), resulting in an ice free period of less than 132 days in Badesø and less than 124 days in Qassi-sø (table 4.5). The exact dates cannot be identified before snow photos are available for the last part of the season. Based on the first six years of observations there is a slight tendency for a decreasing length of the ice free period. However, the year 2010 is characterised by a very long ice free period (207 days and 163 days for Badesø and Qassi-sø, respectively) due to a late freeze at the end of the year. Badesø and Qassi-sø are nutrient poor lakes and therefore the inter-annual variation cannot be prominent, although the relative variation may be large. In 2013 the average total nitrogen concentration in both lakes, was close to the lowest measured during the monitored period, 0.037 and 0.026 mg TN l^{-1}, in Badesø and Qassi-sø, respectively (table 4.5, and figures 4.10a-b). Average total phosphorus was also low compared to previous years, particularly in Badesø (0.003 mg l^{-1}).

Chlorophyll and Secchi depth

Chlorophyll *a* (Chl *a*) is correlated to nutrient levels and the Chl *a* levels of the two lakes are therefore low (figure 4.11a). Chl *a* varied notably between the years, but compared to more nutrient rich lakes the variation remains within a very narrow range due to the low nutrient levels. Over the six-year period Chl *a* exhibited an increasing trend in both Badesø and Qassi-

sø; however, during the period 2011-2013 the increase has been reduced compared to the increase during the first three years; 2008-2010 (figure 4.11a). In general, there is a slightly higher Chl *a* level in Badesø compared to Qassi-sø, which can be explained by the slightly higher temperature in combination with less silt in Badesø and consequently better transparency (Secchi depth) (figure 4.11b).

In Badesø 2013, Secchi depth was on average 8.06 m, and at a level similar to 2008-2009. This was following a period where the Secchi depth decreased from 8.2 m to 4.6 m from 2010-2012 (figure 4.11b). In Qassi-sø, an increased Secchi depth was also observed in 2013 compared to the previous years (figure 4.11b) despite reduced or similar chlorophyll *a* levels compared to previous years.

In certain periods/years reduced Secchi depth can occur despite unchanged nutrient levels. This can be explained by more frequently occurring warm periods causing warmer surface water and stronger stratification in Badesø or a beginning stratification in Qassi-sø. In such periods phytoplankton will concentrate in the photic layer and, due to higher temperatures, increase the primary production and thus reduce Secchi depth, particularly in the surface water. This phenomenon is comparable to the fact that at certain nutrient levels and temperatures, shallow lakes on average will have higher chlorophyll levels compared to deeper lakes.

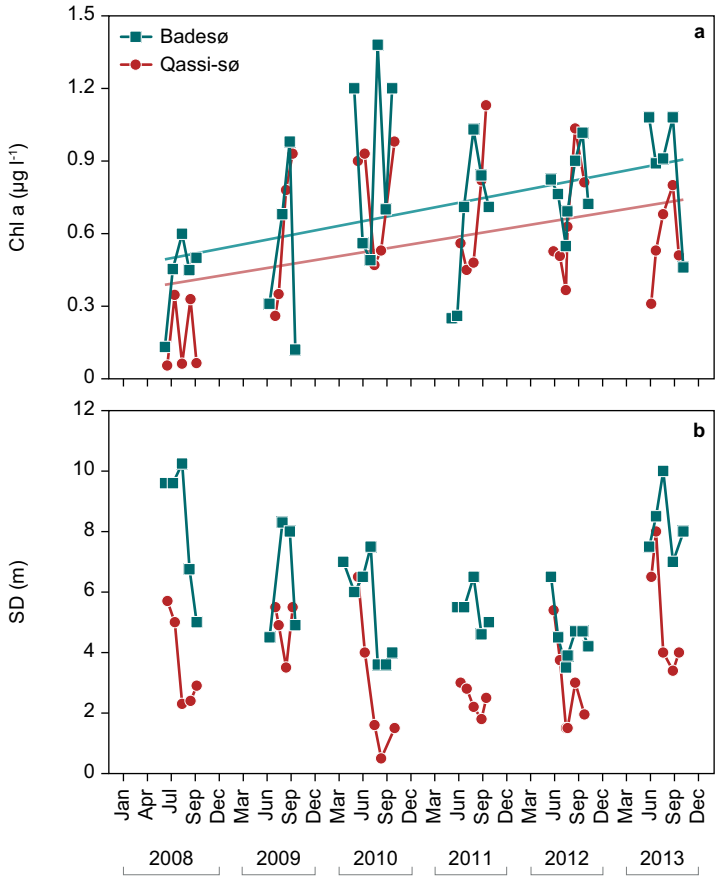

Figure 4.11 Chlorophyll a levels (a) and Secchi depth (b) in Badesø and Qassi-sø during 2008-2013.

Zooplankton

In general, there is no consistent pattern of which lake has the highest total zooplankton biomass. The first three years (2008-2010) Qassi-sø had the highest maximum biomass (figure 4.12), and the following three years the biomass in the two lakes were at similar levels, around 10-20 µg dw l^{-1} (figure 4.12). However, zooplankton communities were slightly different in the two lakes, with complete dominance of calanoid *Leptodiaptomus minutus* and cyclopoid copepods in Qassi-sø, whereas Badesø is dominated by calanoid copepods *Leptodiaptomus minutus* together with either rotifers and/or cladocerans (figure 4.12). When rotifers occur in high biomasses in Badesø they consist of the large *Asplanchna* sp., but also smaller rotifers (like *Keratella* spp. and *Polyarthra* spp.) were found in large numbers. Cladocerans were represented in both lakes (figure 4.12), but in Badesø they consist of the small *Bosmina* sp. together with *Holopedium*, which is in contrast to Qassi-sø where cladocerans are dominated by *Holopedium* sp. together with the large *Daphnia pulex*. The zooplankton composition in Badesø, with fewer and smaller cyclopoid copepods, smaller cladocerans, and more rotifers, reflects that Badesø contains zooplankton-eating fish, contrary to Qassi-sø, which is without fish. During the last three years zooplankton biomass has slightly increased in Badesø (figure 4.12), which may indicate less predation pressure on the zooplankton during this period.

In 2010, additional zooplankton samples were collected in Badesø during April and May before ice out. During this ice covered period zooplankton composition was completely dominated by the calanoid copepods, which is also the group dominating in all years at the first sampling occasion following the ice out (figure 4.12a). Besides rotifers, cyclopoid copepods contribute to the total zooplankton biomass, although to a minor extent. The small biomass before ice out is presumably due to a combination of low temperature and low primary production.

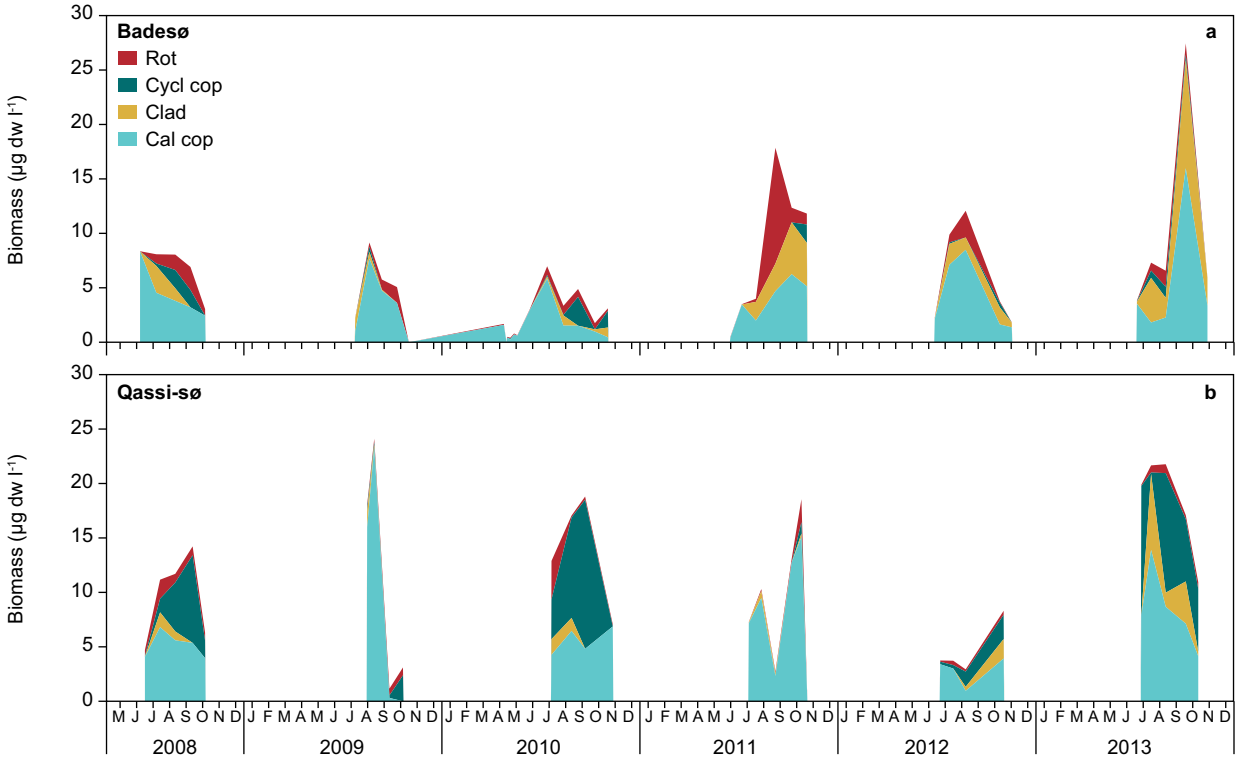

Figure 4.12 Zooplankton biomass in Badesø (a) and Qassi-sø (b) during 2008-2013. Zooplankton is divided into four groups: Cladocerans (Clad), cyclopoid copepods (Cycl cop), calanoid copepods (Cal cop) and rotifers (Rot).

Fish

In 2013 fish were sampled for the second time during the monitored period. Fish are collected overnight in a standardized way using three littoral (near shore), three benthic (bottom standing) and three pelagic (in the water column at approximately 8-10 m depth) multi mesh sized (6.25-75 mm) nets. This method gives a representative sample of the fish community and size distribution. The term Catch Per Unit Effort (CPUE), covers the average number of fish per net.

The $CPUE_{total}$ was dramatically reduced from 2008 to 2013, basically due to a reduction in the Arctic char *Salvelinus alpinus* abundance, which was reduced from 15.9 to 8.6 fish per net, whereas the three-spined stickleback *Gasterosteus aculeatus* was observed in similar numbers in both years (table 4.6). From 2008 to 2013 Arctic char abundance was reduced in both the littoral and the benthic part of the lake; however, only in the benthic part a significant reduction occurred (figure 4.13). In general the catch/abundance is lowest in the pelagic open water habitat, assumably due to lowest food concentration in this habitat compared to the littoral and the benthic habitats where macroinvertebrates are available.

The length frequency distribution of the Arctic char is very similar when comparing the two years. There is a clear

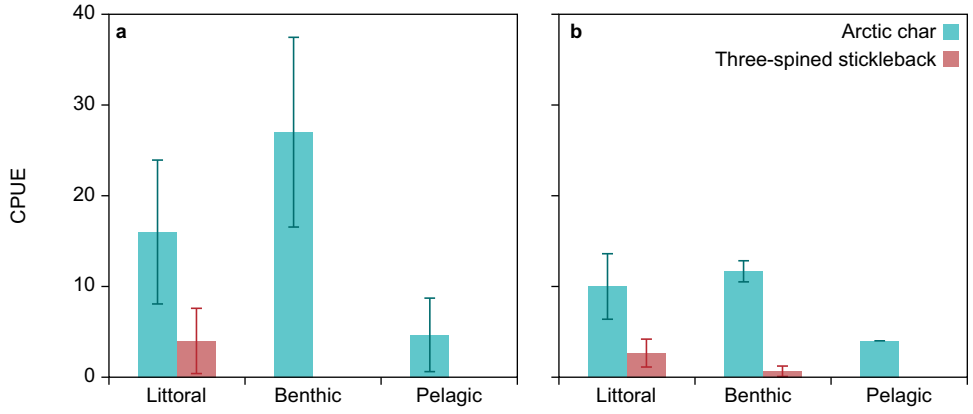

Figure 4.13 Catch Per Unit Effort (CPUE) in Badesø, 2008 (a) and 2013 (b) in the littoral, benthic and pelagic habitats, respectively. Arctic char: blue bars; three-spined stickleback: red bar. Error bars are Standard Deviation.

*Table 4.6 Catch Per Unit Effort (CPUE) as total catch per net and divided into catch of Arctic char (*Salvenus alpinus*) and three-spined stickleback (*Gasterosteus aculeatus*); plus total number of Arctic char divided into size classes ≤10 cm, >10 ≤20 cm and >20 cm, in Badesø 2008 and 2013.*

	2008	2013
$CPUE_{total}$	17.2	9.7
$CPUE_{char}$	15.9	8.6
$CPUE_{3\text{-}sp}$	1.3	1.1
Arctic char <10 cm	11	2
Arctic char >10 <20 cm	92	63
Arctic char >20 cm	41	13

dominance of the 12 to 18 cm char and the decline in abundance is valid for all size classes (figure 4.14).

Particularly the large char can be piscivores and the smaller specimens are omnivores or planktivores. Isotope results from the biological components in the trophic web can help verifying this since the $^{15}N/^{14}N$ ratio ($\delta^{15}N$) increases for every increase in trophic level or step in the food chain. Isotope data from 2008 confirm the piscivory by large char, showing a higher $\delta^{15}N$ number compared to smaller sized char (figure 4.15). For the group of char <20 cm, ^{15}N was around six showing they were basically planktivores or benthivores; for char between 20 and 30 cm, $\delta^{15}N$ increased from six to 10 as char was changing from benthivory to omnivory/piscivory, and above 30 cm chars was basically piscivores with $\delta^{15}N$ values between 8.5 and 10.5 (figure 4.15). Irrespective if the Arctic chars were littoral, benthic or pelagic living fish, they were primarily piscivores in 2008, when larger than 30 cm (figure 4.15).

Due to clear cascading effects of fish in Arctic/Greenlandic lakes, the general reduction in fish abundance from 2008 to 2013 can therefore have had positive effects on the invertebrate community in Badesø, explaining the increasing zooplankton biomass in 2013 caused by the predator sensitive cladocerans and calanoid copepods (figure 4.12).

Summing up – lakes

The year 2013 was relatively wet, particular during the winter period. It was the coldest summer registered during the monitored period and the ice free period lasted less than 132 days in Badesø and less than 124 in Qassi-sø. Average total nitrogen concentration in both lakes was the lowest measured and average total phosphorus was generally low in Badesø. During the last three years chlorophyll *a* has stabilized around 0.8 µg Chl *a* L^{-1}, following an increasing trend during the 2008-2010 period. Zooplankton biomass is generally higher in Qassi-sø compared to Badesø, which is consistent with the lack of fish in Qassi-sø. During the past three years an increasing zooplankton biomass is observed in Badesø; this can partly be due to reduced predation pressure, corresponding well with reduced fish abundance in 2013 compared to 2008, where the first fish investigation was undertaken.

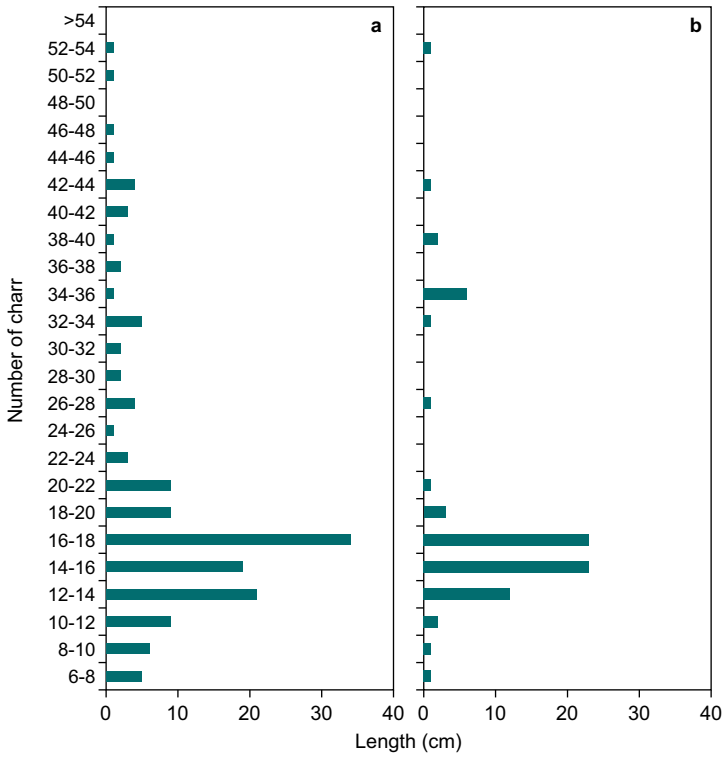

Figure 4.14 Length frequency distribution of Arctic char in 2008 (a) and 2013 (b).

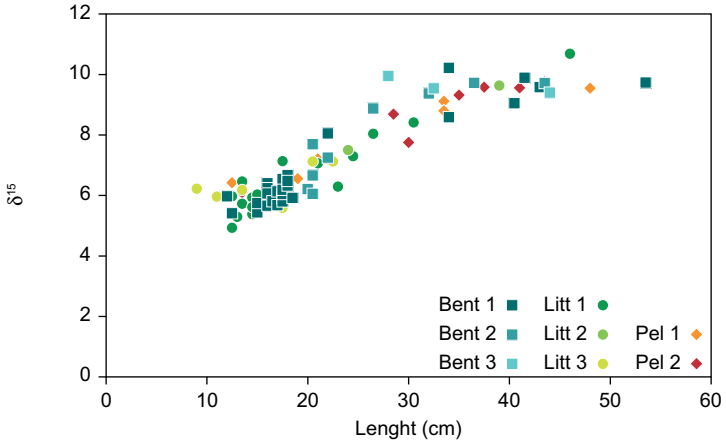

Figure 4.15 $\delta^{15}N$ in muscle tissue vs. the length of the Arctic char caught in the benthic (bent), littoral (litt) and pelagic (pel) part of Badesø in 2008. $\delta^{15}N$ increases with increasing trophic level (see the text for further explanation).

5 Nuuk Basic

MarineBasis programme

Thomas Juul-Pedersen, Kristine E. Arendt, John Mortensen, Diana Krawczyk, Søren Rysgaard, Anja Retzel, Rasmus Nygaard, AnnDorte Burmeister, Dorte Krause-Jensen, Núria Marbà, Birgit Olesen, Mikael K. Sejr, Martin E. Blicher, Lorenz Meire, Ole Geertz-Hansen, Aili L. Labansen, Tenna Boye and Malene Simon

The MarineBasis programme collects and delivers long-term oceanographic data on key physical, chemical and biological parameters of Godthåbsfjord. The programme was initiated in late 2005 and this report describes the eighth year of data collection. The aim is to achieve a better understanding of this low Arctic marine ecosystem and identify, and describe effects of climate change. The sampling programme is comprised of monthly pelagic samplings, seasonal sampling of sediment-water exchange, an annual pelagic section studies of Godthåbsfjord and the adjacent coastal area, annual studies of macroalgae and macrobenthos, counting of seabirds, photo identification of marine mammals and collection of daily satellite and camera images of sea ice conditions in Godthåbsfjord and Baffin Bay. The collected data describes the seasonal, annual and inter-annual patterns and variation in key elements of the marine ecosystem. The time series facilitate identification and quantification of effects of climatic changes. Pelagic sampling is conducted at a permanent sampling station ('Main Station' (GF3); 64°07'N, 51°53'W; bottom depth approximately 350 m) located close to the fjord entrance, while the other parameters are sampled in and around the Godthåbsfjord system (figure 5.1). The methods used are described below, but more details can be obtained from the MarineBasis-Nuuk manual (www.nuuk-basic.dk).

5.1 Sea ice

Sea ice conditions in Baffin Bay were monitored using microwave-radiometer (AMSR-E, 3-6 km resolution) satellite images, while ice conditions in Godthåbsfjord were monitored by MODIS satellite images (250 m resolution). In addition,

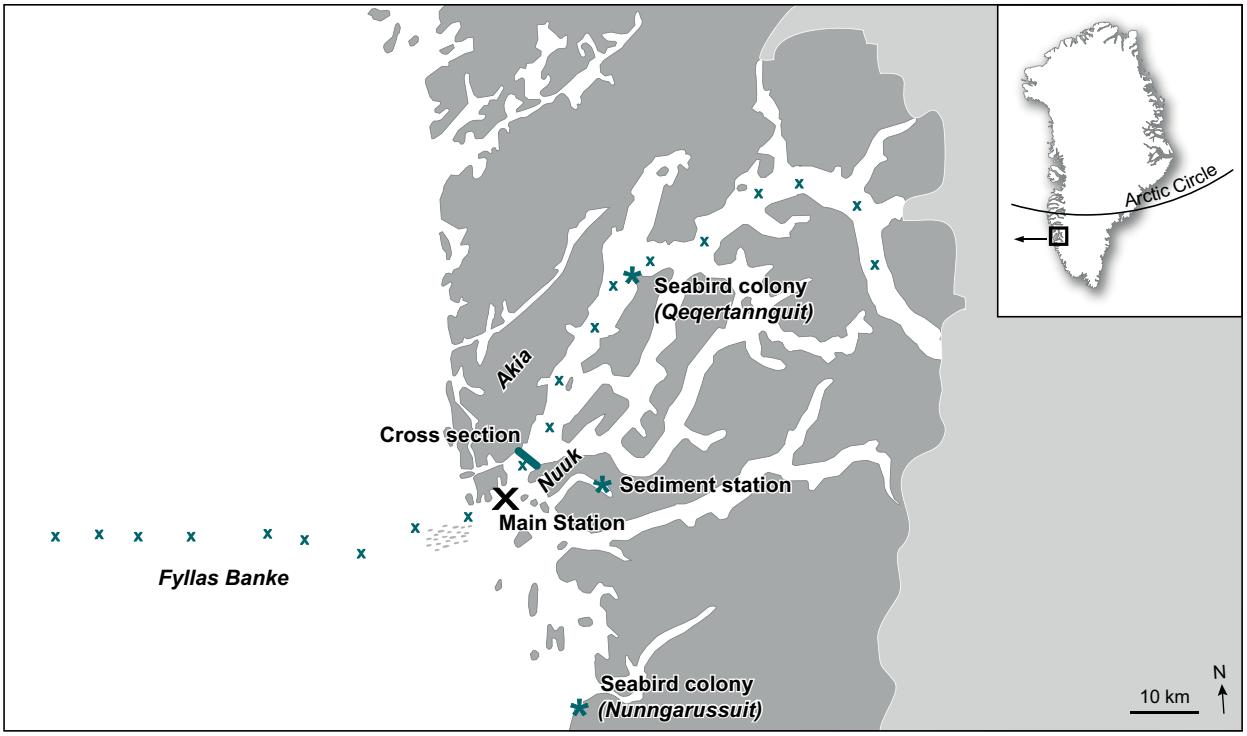

Figure 5.1 Map of sampling stations in and around the Godthåbsfjord system. X represent sampling stations along the hydrographical length section.

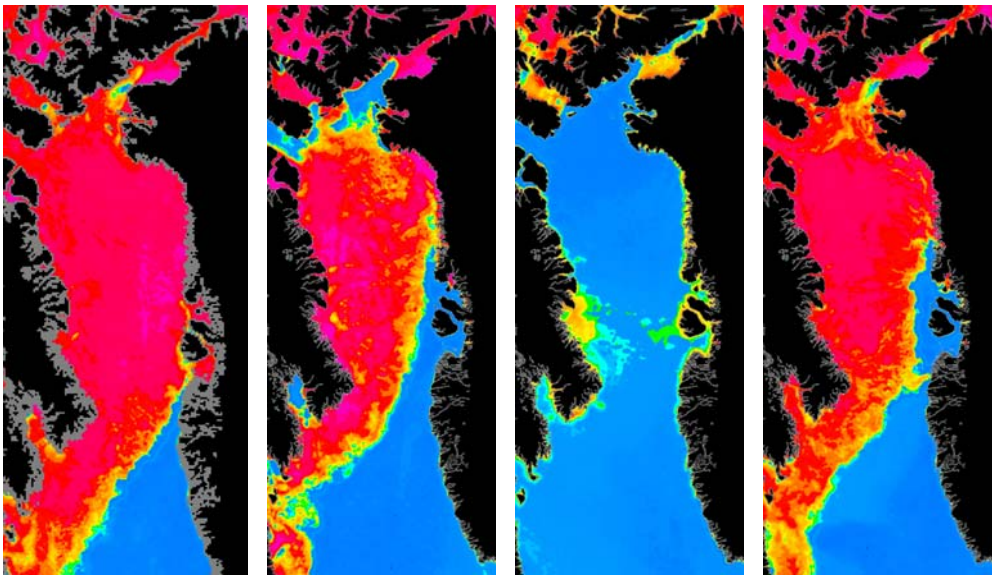

Figure 5.2 Satellite images (AMSR) showing sea ice conditions in Baffin Bay during February, May, July and December 2013.

camera images covering a cross section of Godthåbsfjord were collected daily. Sea ice ('West Ice') in Baffin Bay covered much of the Baffin Bay until May, retreating only during June and reaching a minimum in July-September (figure 5.2). Sea ice formation started in October and covered much of Baffin Bay by late December. Godthåbsfjord remained largely ice free throughout the year and sea ice being restricted to the smaller fjord branches and innermost parts (figure 5.3). Sea ice and glacial ice is exported out of the fjord in bursts, as observed by the MODIS images. The camera system covering a cross section of the fjord normally captures these bursts of exported ice in greater detail, but unfortunately, images were limited to the first and last month of the year with no significant ice export (figure 5.4).

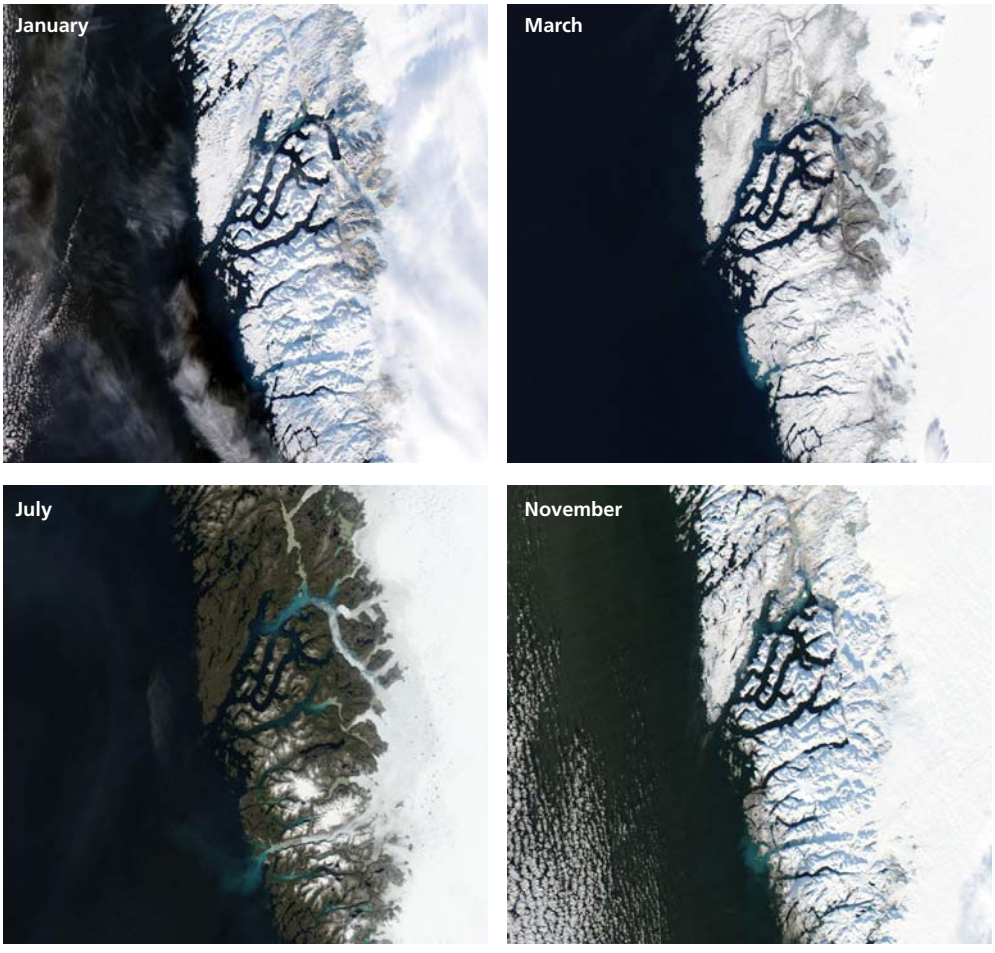

Figure 5.3 Satellite images (AQUA-MODIS) showing sea ice conditions in Godthåbsfjord during January, March, July and November 2013.

Figure 5.4 Digital images from Godthåbsfjord in January and December 2013.

Analyses of satellite data on sea ice coverage are currently conducted as collaboration between Greenland Institute of Natural Resources, the Danish Meteorological Institute and Greenland Climate Research Centre (www.natur.gl). Daily satellite images covering Greenland are available at http://www.dmi.dk/groenland/maalinger/satellit/. Ongoing research at the Greenland Climate Research Centre and the Danish Meteorological Institute are working on improving remote sensing data of the region.

5.2 Length and cross sections

The annual pelagic sampling programme includes a hydrographic length section in May from Fyllas Banke to the ice edge at the innermost part of the fjord and a cross section in May of the fjord. The length section (approximately 200 km long, figure 5.1) was sampled onboard the R/V Sanna in early May. A stratification comprised of colder and slightly fresher surface water was observed inside the fjord, whereas the weak pycnocline in spring was broken down by tidal mixing at the outer sill region near the standard sampling station (figure 5.5). Vertical mixing at the outer sill region is responsible for spreading the phytoplankton biomass to the entire water column (i.e. fluorescence). Similar to previous years, elevated phytoplankton biomass was also observed on top of Fyllas Banke.

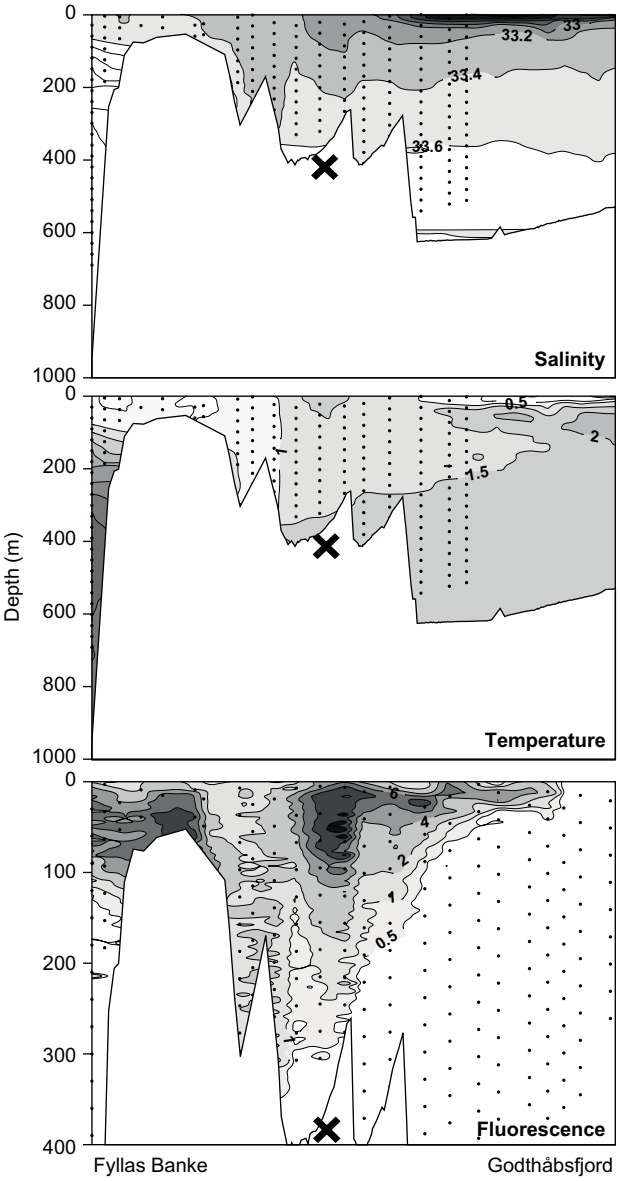

Figure 5.5 Salinity, temperature (°C) and fluorescence along the length section from Fyllas Banke to the inner part of Godthåbsfjord in May 2013. Vertical dotted lines represent sampling stations and depths in increments. X marks the location of the Main Station.

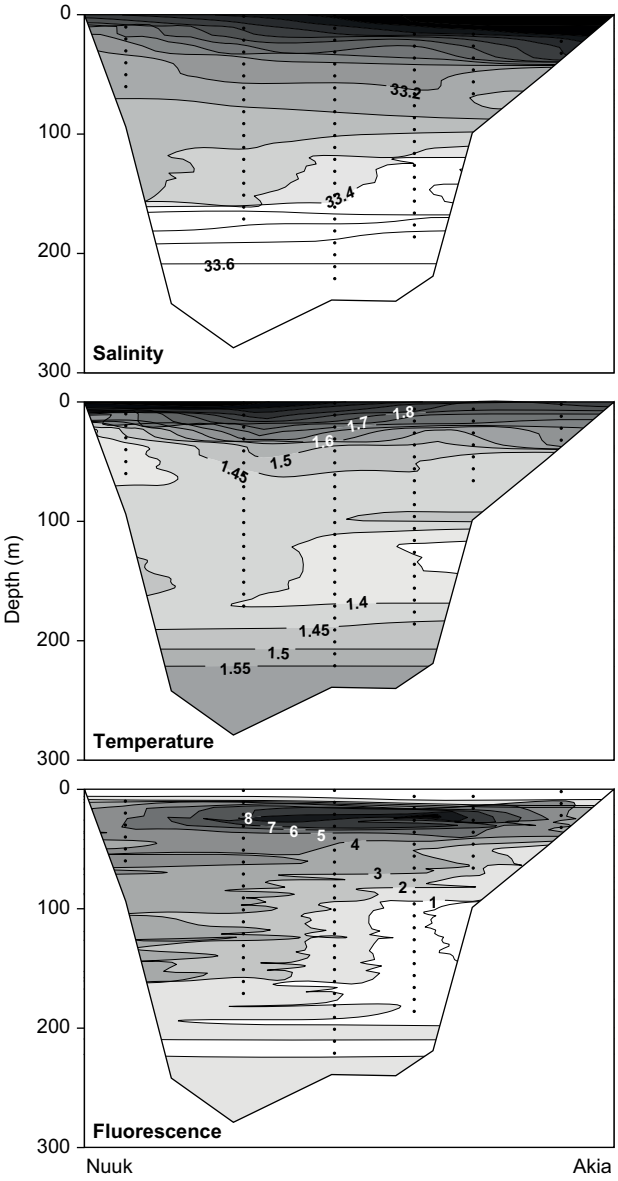

Figure 5.6 Salinity, temperature (°C) and fluorescence along the cross section from Nuuk to Akia in May 2013. Vertical dotted lines represent sampling stations and depths in increments.

The cross section of Godthåbsfjord sampled in late May is located at a narrow point near Nuuk (figure 5.1). The cross section showed a clear pycnocline, which was strongest towards Akia, the north-western side of Godthåbsfjord (figure 5.6). Phytoplankton biomass (i.e. fluorescence) was concentrated mainly within the surface layer, but some vertical mixing of biomass was also present in late May.

5.3 Pelagic sampling

The monthly sampling programme at the 'Main Station' (GF3) near the fjord entrance (approximately 360 m; figure 5.1) includes vertical profiles of salinity, temperature, density, turbidity, irradiance (PAR) and fluorescence is measured using a SBE19+ CTD profiler. In addition, water samples are collected for analyses of concentrations of pigments (chlorophyll *a* and phaeopigments), nutrients (NO_x, PO_4^{3-}, SiO_4 and NH_4^+) at standard depths 1, 5, 10, 15, 20, 30, 40, 50, 100, 150, 250 and 300 m. Samples are also taken for measurements of dissolved inorganic carbon (DIC) and total alkalinity (TA) at 1, 5, 10, 20, 30 and 40 m, representing the euphotic zone. Due to technical problems, there is a delay in analysing TA and DIC samples; hence, we are unable to include pCO_2 values from the monthly sampling programme taken

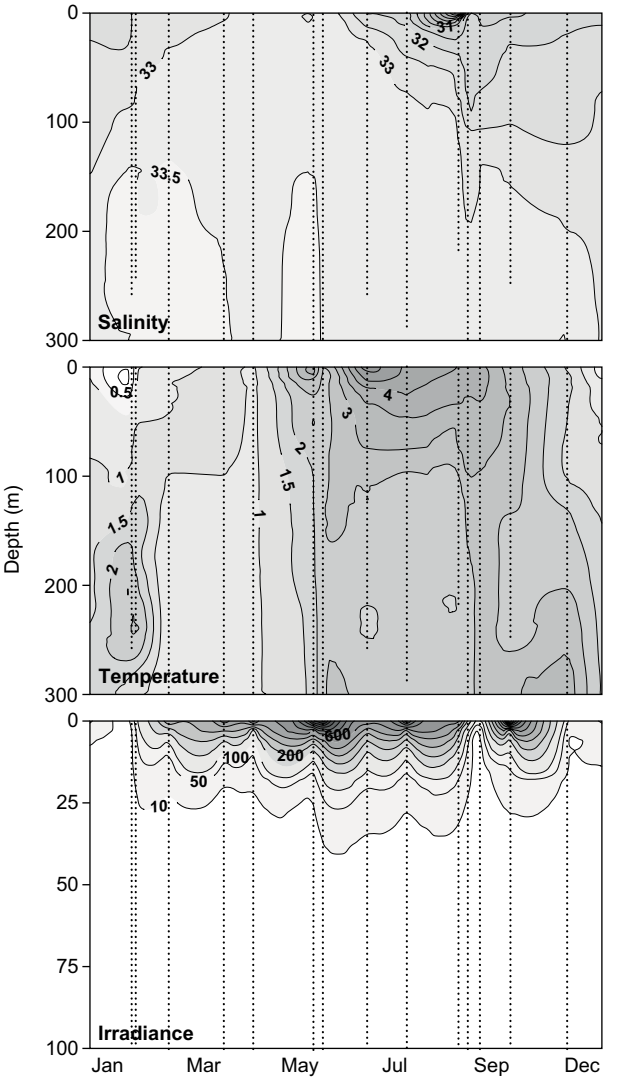

Figure 5.7 Annual variation in salinity, temperature (°C) and irradiance (PAR) at the Main Station in 2013. Vertical dotted lines represent sampling days and depths in increments.

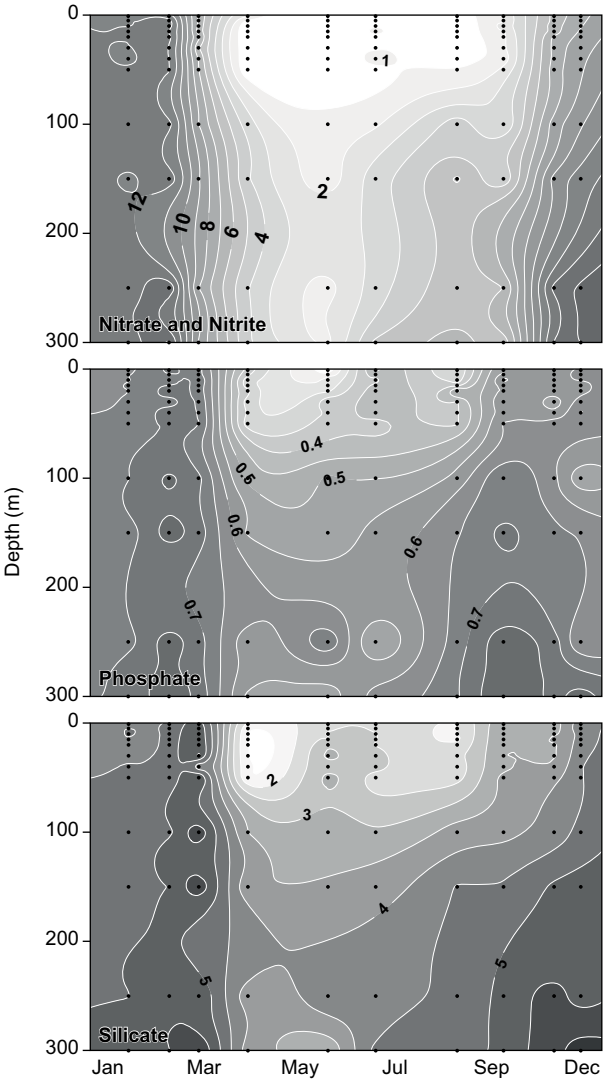

Figure 5.8 Annual variation in nitrate and nitrite (µM), phosphate (µM) and silicate (µM) concentrations at the Main Station in 2013. Vertical dotted lines represent sampling days and depths.

in 2013, which is derived from DIC and TA data. Particulate primary production was measured using the *in situ* C^{14} incubation method corrected for *in situ* light conditions, thus incubation bottles were deployed 5, 10, 20, 30 and 40 m on a free-drifting mooring array for approximately two hours. Vertical sinking flux was measured using four particle interceptor traps also deployed on a free-drifting mooring array at 60 and 65 m (considered the same depth) for approximately two hours. The collected material was analysed for pigments (chlorophyll *a* and phaeopigments), total particulate carbon and nitrogen and a sample saved for identification. Triplicate plankton net tows were also taken for zooplankton (45 µm WP2 net from 0-100 m) and phytoplankton (20 µm net from 0-60 m). To assess shellfish as well as fish larvae at the 'Main Station' (GF3), single oblique sampling with a bongo net (335 µm) was used each month during 2008 (except June), 2009 (except October) and from 2010-2013 (except for February in 2012). Additional samplings with a double oblique bongo net (335 and 500 µm) were carried out along a length section from offshore Fyllas Banke to the inner part of the fjord from 2006 to 2013. Number of collected stations along the length section varies among years, but typically the stations FB3.5, FB2.5, GF3, GF5, GF7 and GF10 are attempted to be sampled each year. In 2013 collections also included FB 2.5, FB 1.5 and a new station 'ice edge' close to the ice edge in the inner part of the fjord.

Abiotic parameters

The monthly sampling programme at the 'Main Station' (GF3) showed the presence

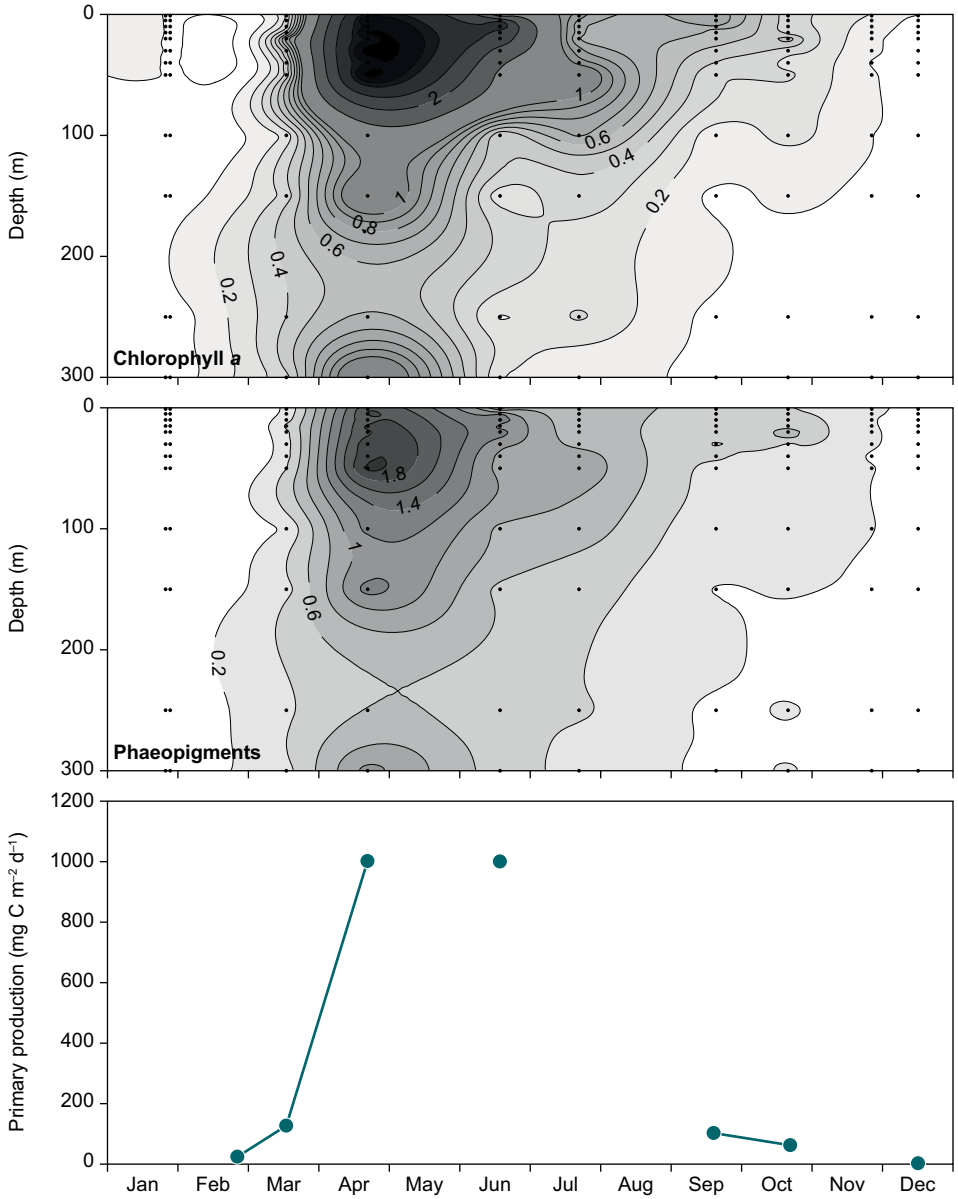

Figure 5.9 Annual variation in chlorophyll a concentration (µg l^{-1}), phaeopigments concentration (µg l^{-1}) and primary production (mg C m^{-2} d^{-1}) at the Main Station in 2013. Vertical dotted lines on chlorophyll a and phaeopigments plots represent sampling days and depths.

of warm and saline coastal water below 150 m during February (figure 5.7). The presence of dense coastal water is reoccurring annually in February/March. Decreasing surface salinities from July depicts onset of the glacial melt season, which peaks sometime in August. Air-sea heat exchange, solar heating of the surface layer and freshwater run-off strengthen the pycnocline during summer. This stratification starts to weaken in autumn mainly due to reduction in freshwater run-off. Seasonal light conditions in the water column, i.e. irradiance, generally follow the level of incoming solar radiation during the year. Particles in the water column, e.g. phytoplankton cells and silt particles, do however also influence irradiance distribution during spring and summer.

Water samples were analysed for nutrients showed highest concentrations just before the onset of the spring phytoplankton bloom in April/May (figure 5.8). Spring and summer production reduced nutrients levels particularly in the surface layer, but reduced concentrations are also observed at depth. The decreases in primary production in autumn combined with weakening of the surface stratification promote the replenishing of nutrients from below.

Biotic parameters

Phytoplankton biomass and primary production is also measured as part of the monthly sampling programme (figure 5.9). The biomass remained low during winter, primarily due to the low light levels. The highest phytoplankton biomass was observed in April (3.8 µg l^{-1}), due to the annual spring phytoplankton bloom. No sampling was conducted in May, when the spring production is often highest, due to

logistical problems. The spring bloom is triggered by improving light conditions and the weak surface stratification and initially high nutrient levels. In summer, phytoplankton is kept suspended by the stronger stratification in the outer sill region, but the pycnocline also reduces the supply of nutrients to the algae in the photic zone by reducing the transport of nutrients from deeper nutrient rich water layers. Post-bloom conditions with decreasing phytoplankton biomass and low nutrient levels characterize early-summer. In most years a distinct summer bloom is recorded between July and September, but a missing sampling in August may have overlooked the summer bloom. Due to unusually high drift velo-city of the primary production moorings and in a direction not common in previous samplings, several free-drifting primary production moorings where lost in 2013. Combined with logistical problems the primary production sampling frequency was lower than normal (n = 7; figure 5.9). Still, the maximum primary production recorded in April and July is comparable to some of the highest values recorded in previous years (approximately 1000 mg C m^{-2} d^{-1}; figure 5.9).

A cautious estimate of the integrated annual primary production (113.2 g C m^{-2} y^{-1}) is within the range of estimates from previous years (from 84.6-139.1 g C m^{-2} y^{-1} from 2006 to 2012; data not shown).

The plankton community

The phytoplankton (including heterotrophic and mixotrophic dinoflagellates with ciliates) samples were collected using vertical net (20 µm) hauls from 0-60 m at the 'Main Station' in the outer fjord.

Haptophytes, i.e. *Phaeocystis* sp. and diatoms represented the phytoplankton community throughout the year (figure 5.10). Such species composition is typical of phytoplankton blooms observed in the low Arctic and Arctic regions, particularly during spring-summer seasons. In Godthåbsfjord, *Phaeocystis* sp. dominated from March to June (average of 86.3 %) and surprisingly later this year in September (78 %; figure 5.10). Diatoms showed highest contribution in July (94.4 %) and also in winter. Silicoflagellates recorded unusually high relative abundances during winter, compared to previous years and to other regions. This phytoplankton group typically has a minor contribution to the phytoplankton communities in the North Atlantic region. Other groups, such as dinoflagellates, ciliates and chrysophytes were also observed in winter. Interestingly, the latter group represents mainly low saline summer surface waters in low Arctic and Arctic fjords. Throughout the year, *Phaeocystis* sp. contributed more than half of the phytoplankton counts, while various diatom generic groups and species comprised almost all of the remaining counts (table 5.1). *Thalassiosira* spp. and *Chaetoceros* spp. was the dominant diatom groups, similarly to previous years studied, while *Paralia sulcata* was the dominant diatom species. *P. sulcata* is a cosmopolitan species, fairly common in coastal phytoplankton of the North Atlantic region.

Vertical zooplankton net hauls (45 µm WP2 net) were conducted monthly at station GF3 from 0-100 m. In prolongation to the observations in 2012, abundances of both copepods and copepod nauplii were significantly lower during the mid-summer months compared with previous

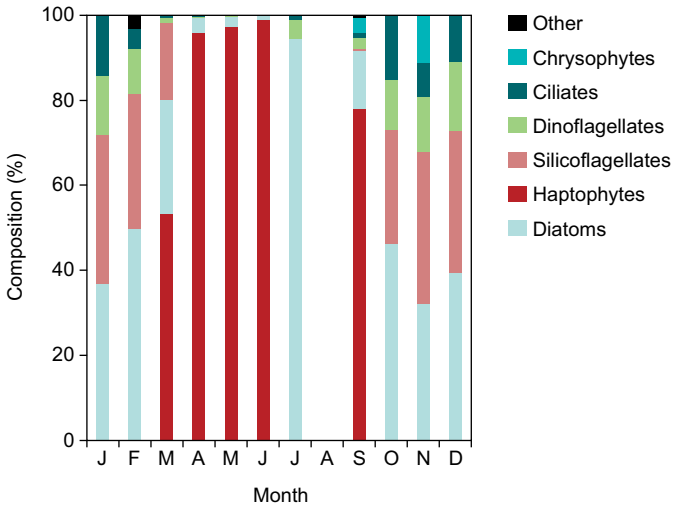

Figure 5.10 Seasonal variations in micro-plankton community composition (%) at the Main Station during 2013.

Table 5.1 Ten most dominant phytoplankton species integrated over the year as their relative accumulated proportion of total cell counts (%) at the 'Main Station' in 2013.

2013	
Phaeocystis sp.	62.6
Chaetoceros spp.	82.7
Thalassiosira spp.	88.4
Pseudo-nitzschia spp.	90.9
Paralia sulcata	93.4
Fragilariopsis spp.	94.8
Pauliella taeniata	95.8
Fragilaria sp.	96.6
Skeletonema sp.	96.9
Navicula sp.	97.1

years. However, the overall trend followed the general succession pattern.

Of the nauplii stages of copepods *Calanus* spp. nauplii dominating in June whereas *Microsetella norvegica* nauplii dominated in July both appeared in lower abundances than in previous years (figure 5.11a). The copepod community was dominated by *Microsetella norvegica*, *Oncaea* and *Oithona* spp. though the winter months. *Calanus* spp. appears with rising abundances in April and May. Whereas the copepod rise in abundances in June were due to *Microsetella norvegia* approximately. However, *M. norvegica* did not emerge in extreme numbers compare to previous years. Therefore, *Oithona* spp. comprises a relative high percentage of the total abundance (figure 5.11b) in both July and September. Unfortunately sampling was omitted in August, but the general trend during the summer months pointed towards lower abundances than in previous years.

Abundances of other zooplankton groups increased in April (figure 5.11c). Here a considerably part was due to cirripedia nauplii. A shift towards bivalve larvae and rotifers resulted in rising abundances in June and July whereas rotifers and foraminifers were abundant in September and October.

Since the beginning of the annual sampling at the Main Station (GF3) in 2008, the abundance of fish larvae varies over the years with a temporal shift in species composition during summer (figure 5.12). In general sand eel *Ammodytes* sp. larvae dominates the abundance in late winter/early spring (February/March), Arctic shanny *Stichaeus punctatus* larvae dominates the abundance in spring (April/May) followed by capelin *Mallotus villosus* larvae dominating the abundance in summer/autumn (July-September). In 2013, the abundance of sand eel larvae in February, Arctic shanny larvae in May and capelin larvae in July was the highest seen in the time series. Especially the abundance of sand eel larvae was very high with 50 individuals per 100 m^3. American plaice *Hippoglossoides platessoides* larvae peak in abundance in June and highest numbers where observed in 2011. Atlantic cod *Gadus morhua* larvae seem to peak in different months between years from May to June and highest numbers where observed in June 2011. Overall the abundance of fish larvae varies greatly between years and especially 2010 was a year with very low abundance of fish larvae in all month. Since 2010, the abundance of fish larvae has increased and 2013 was a year with highest abundance of fish larvae in the time series caused mainly by an increase in sand eel, capelin and Arctic shanny larvae in the samples.

In 2013, the highest concentration of fish larvae at the Main Station (GF3) was found in February (figure 5.13a), where sand eel larvae accounted for 99.7% of the total abundance (figure 5.13b). A second peak in abundance was observed in July where capelin larvae accounted for 96% of the total abundance. Sand eel larvae were caught from February to July and domi-

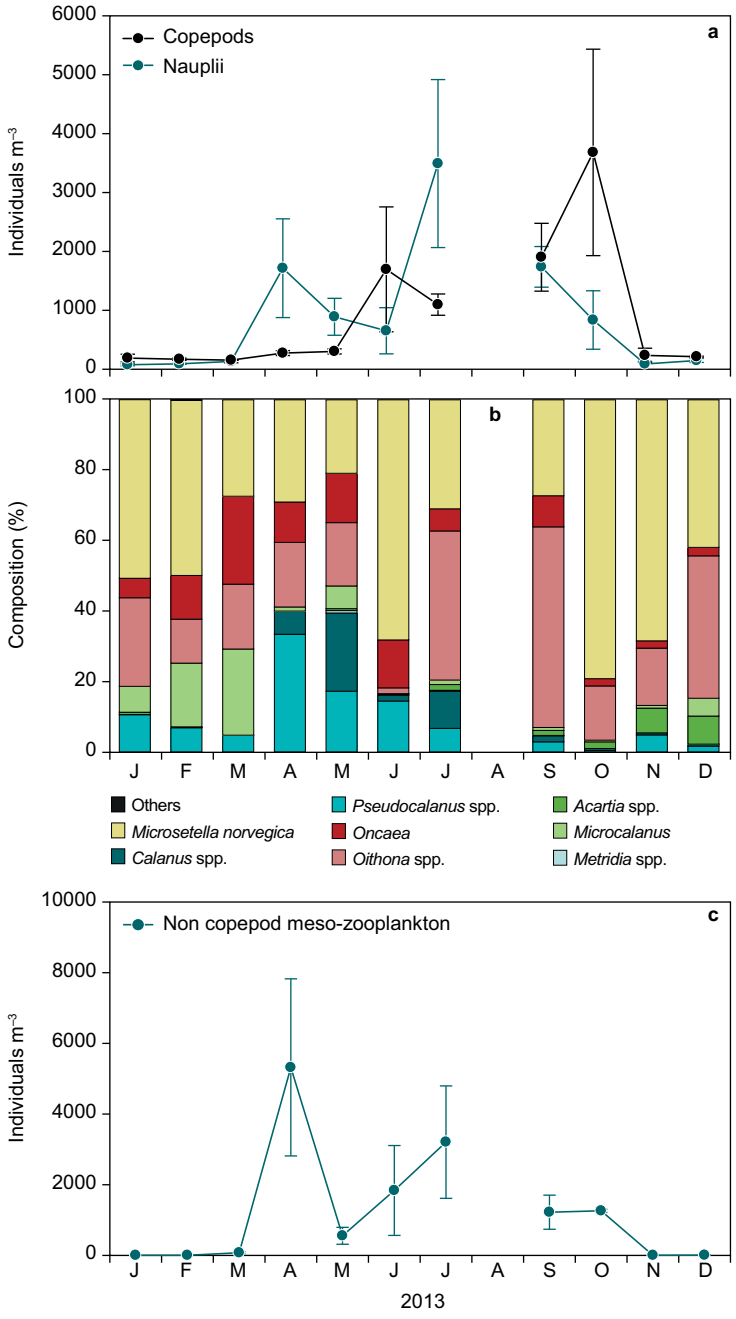

Figure 5.11 Annual variations in abundance (individuals m^{-3}) of a) copepod nauplii and copepods (i.e. copepodites and adult stages), b) copepod community composition (%) and c) abundance of other zooplankton groups (individuals m^{-3}) at the Main Station in 2013. Error bars represent standard deviation.

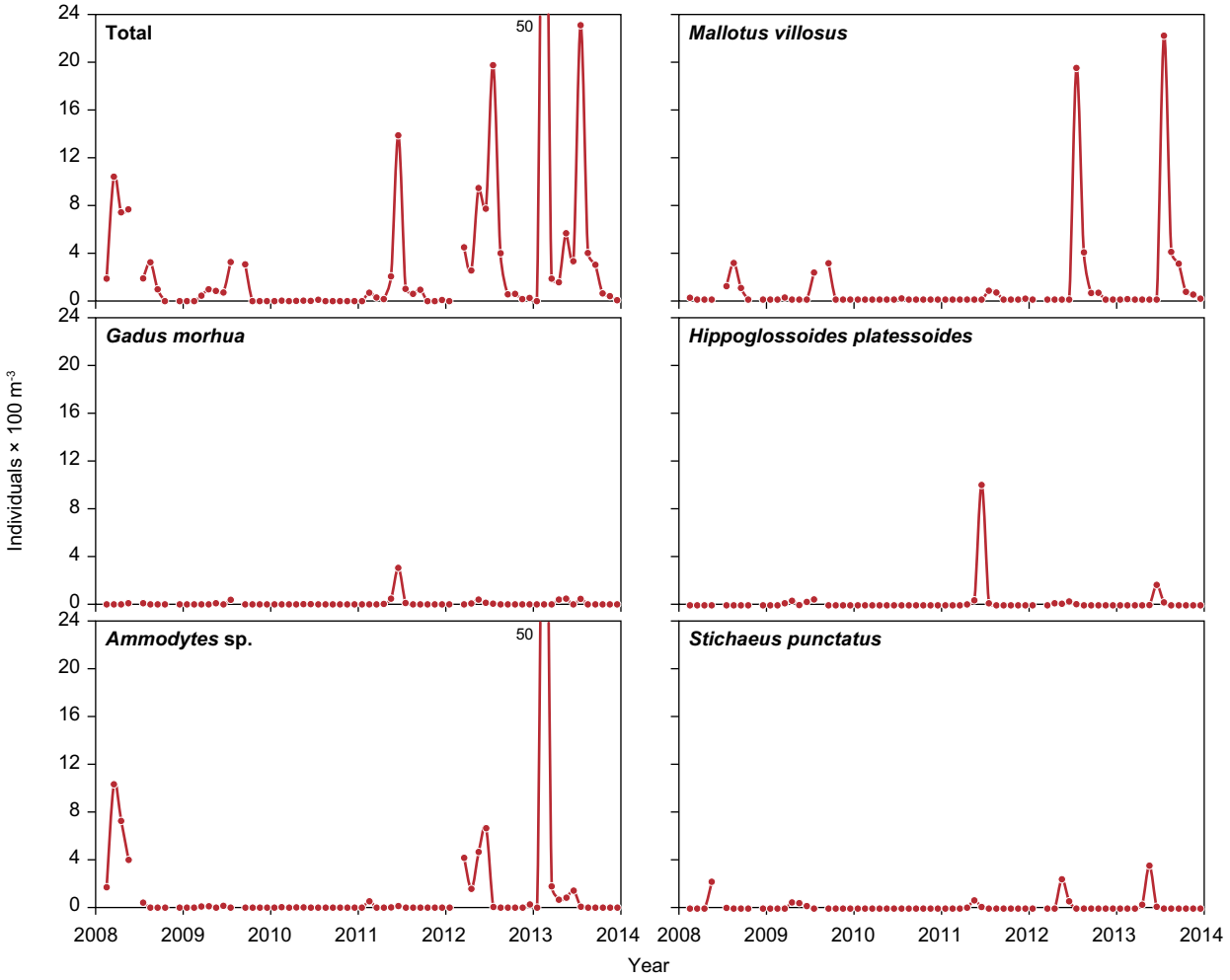

*Figure 5.12 Annual variation in abundance of fish larvae in total, capelin (*Mallotus villosus*), Atlantic cod (*Gadus morhua*), American plaice (*Hippoglossoides platessoides*), sand ell (*Ammodytes *sp.*) and Arctic shanny (*Stichaeus punctatus*) from 2008 to 2013 at the main station (GF3). Samples were collected each month except January, June and November 2008, August 2009 and February 2012.*

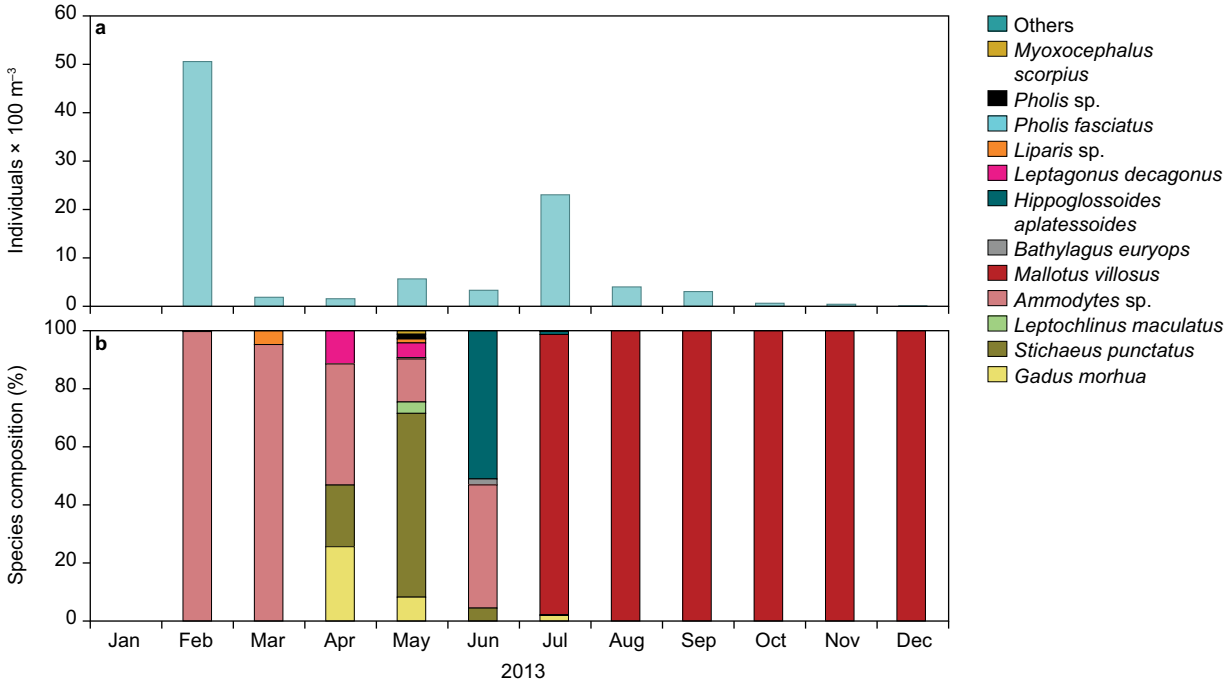

Figure 5.13 Annual variation in abundance (individuals per 100 m³) (a) and community composition (%) (b) of fish larvae at the main station (GF3) in 2013.

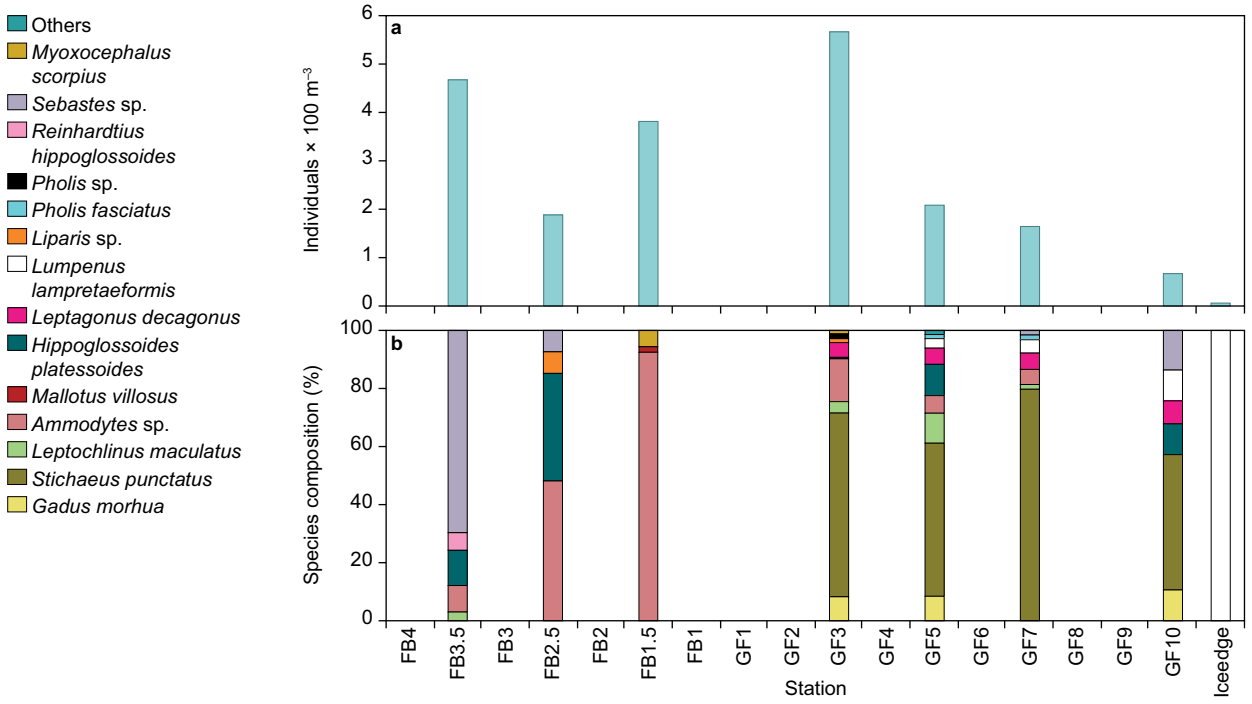

Figure 5.14 Variation in abundance (individuals per 100 m³) (a), and community composition (%) (b) of fish larvae on the longitudinal section in May 2013.

nating abundance in February and March. Arctic shanny larvae were caught from April to June and dominating the abundance in May. Capelin larvae were caught from July to December and dominating the abundance in the same months. The majority of species were caught in May.

The length section in the fjord in May 2013 show a similar pattern in fish larvae abundance and species composition as in the years 2008, 2009, 2010 and 2012 with highest abundances found closer to the inlet of the fjord at the Main Station (GF3) (figure 5.14a). In 2006, 2007 and 2011 abundance was highest on Fyllas Banke due to high numbers of sand eel larvae especially in 2006 and 2007 (112 and 35 individuals pr. 100 m^3 in 2006 and 2007 respectively at station FB2.5). In 2013, species composition varied over Fyllas Banke with redfish *Sebastes* sp. larvae dominating the abundance on the outer slope of the Banke (FB3.5), sand eel and American plaice larvae dominated on the top of the Banke (FB2.5) and sand eel larvae dominated on the inner slope of the Banke towards the fjord (FB1.5) (figure 5.14b). Greenlandic halibut *Reinhardtius hippoglossoides* larvae was only found on the outer slope of the Banke (FB3.5). Within the fjord Arctic shanny larvae dominated the abundance on all stations. Overall species composition varied on the length section with fewer species in the samples from Fyllas Banke and from deeper inside the fjord. Atlantic cod larvae were only found within the fjord.

Fish larvae species composition seems to vary between years with most species found in 2011 and 2012 (table 5.2).

The shellfish larvae community at the 'Main Station' (GF3) showed the characteristic pattern with peak abundance of *Pandalus* sp. in May. As in 2010, peak abundance of *Chionoecetes opilio* and *Hyas* spp. was observed in May, one month earlier than in previous years. The 2010 peak in density of *Pandalus* sp. declined, reaching in 2011 the lowest levels since 2009. The number of individuals m^{-3} increased by more than 82 % over 2011, but was in 2013 followed by a 34 % decline. Density of *Chionoecetes opilio* was estimated to a record high level for the time series in 2013 and was significantly (71 %) higher than 2012 observations. The continued increasing trend from 0.05 individuals m^{-3} in 2008 to 0.46 individuals m^{-3} in 2011 of *Hyas* spp., turned out to a 35 % drop from 2011 to 2012, but increased significantly (67 %) to record high level of 0.9 individuals m^{-3} (figure 5.15) in 2013. Larvae stage zoae I of *C. opilio* and *Hyas* spp. dominated samples in April to June whereas larvae stage zoae II were more prevalent in July. Low concentrations of megalope stage of *C. opilio* and *Hyas* spp. were observed in October. Abundance of *C. opilio* has been

Table 5.2 Species list of fish larvae 2006-2013.

Species list	2006	2007	2008	2009	2010	2011	2012	2013
Gadus morhua	X	X	X	X	X	X	X	X
Stichaeus punctatus	X	X	X	X	X	X	X	X
Leptochlinus maculatus	X	X	X	X	X	X	X	X
Ammodytes sp.	X	X	X	X	X	X	X	X
Mallotus villosus		X	X	X	X	X	X	X
Aspidophoroides monopterygius	X	X	X			X		
Bathylagus euryops		X	X	X	X	X	X	X
Cyclothone sp.		X						
Liparis sp.		X				X		X
Liparis gibbus					X		X	
Pholis sp.	X	X	X					X
Pholis fasciatus					X	X	X	X
Pholis gunellus							X	
Reinhardtius hippoglossoides	X		X			X	X	X
Myoxocephalus scorpius			X		X		X	X
Hippoglossoides platessoides			X	X	X	X	X	X
Sebastes sp.			X			X	X	X
Gadus ogac			X	X	X			
Leptagonus decagonus				X	X	X	X	X
Agonidae				X				
Lumpenus lampretaeformis				X	X		X	X
Triglops murrayi						X	X	
Cottidae						X		
Anarchias sp.						X		
Total	7	10	13	11	13	16	16	15

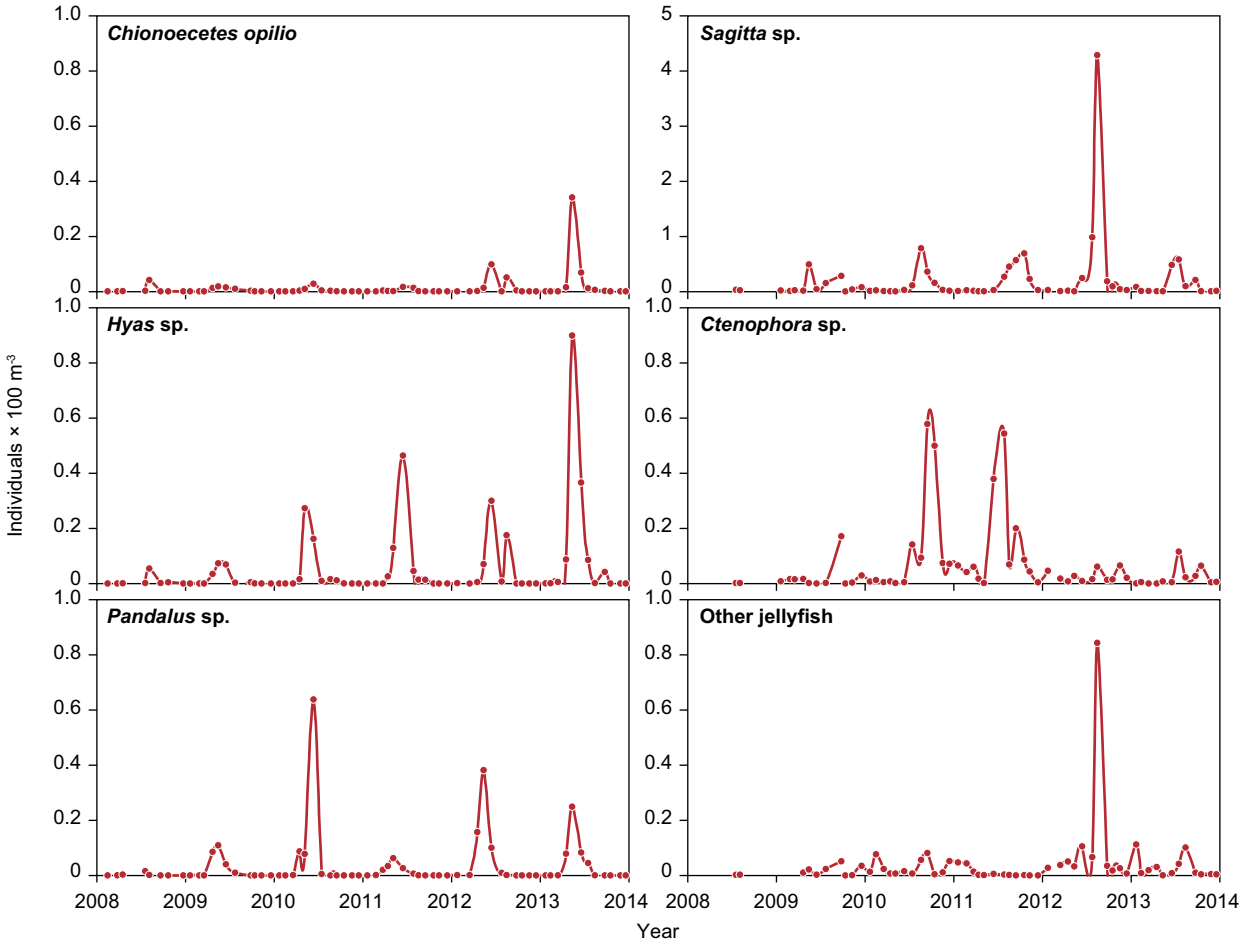

Figure 5.15 Annual variation in abundance (individuals m^{-3}) of Chionoecetes opilio, Hyas *sp.,* Pandalus *sp.* Sagitta *sp.,* Ctenophora *sp. and other jellyfish at the Main Station (GF3) from 2008 to 2013. Samples were collected each month except November 2008 and August 2009.*

low compared to *Hyas* spp. and *Pandalus* spp. throughout the years of sampling.

At the Main Station (GF3) *Ctenophora*, jellyfish and/or *Sagitta* spp. dominating the community in all months of sampling, except in the period from April to June were *Pandalus* spp., *Chionoecetes opilio* and *Hyas* spp. became more abundant. As a contrast, *Sagitta* spp. became the most dominating species in July (2012 and 2013), one month earlier than observed in the previous years (figure 5.16), but unlike in 2011, *Sagitta* spp. has been less abundant in November and in December over the past two years. Number of individuals m^{-3} of, *Sagitta* spp. was recorded in considerably high number and peaked at 4 individuals m^{-3} in August 2012, but declined significantly to levels comparable with the other years of sampling (figure 5.15). Other consistently abundant species has been Ctenophoras (39 to 55% from January to March and 62% in July 2010 and 2011), but a significantly decrease of *Ctenophores* were observed in 2012 and remain at the same low level in 2013. Density of jellyfish was record high in 2012, but 2013 observations were comparable to previous years (figure 5.15).

Along the length section from Fyllas Banke (offshore) to the inner part of the fjord (GF10) concentration of crab larvae *Hyas* spp. and *Chionoecetes opilio* were significantly higher in 2013 compared to the preceding two years (figure 5.17). In contrast to previous years, *Chionoecetes opilio* were observed at all stations along the length section, except at the outermost station (FB3.5) and the innermost station (GF10). Both *Hyas* spp. and *Pandalus* spp. are to be found at almost all stations along the length section, with variations in density among species and

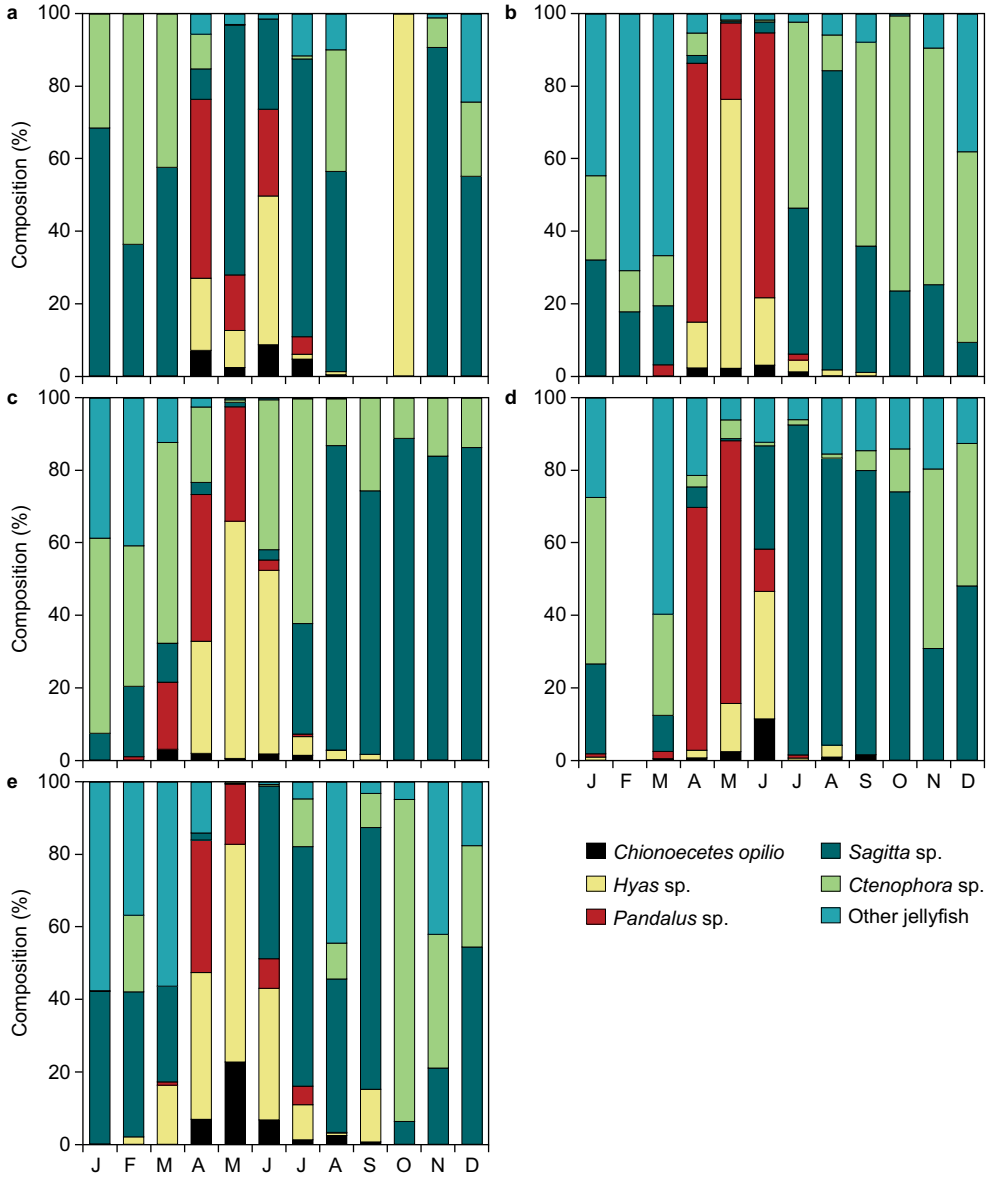

Figure 5.16 Annual variation in community composition (%) at the Main Station (GF3) from 2009-2013.a: 2009, b: 2010, c: 2011, d: 2012 and e: 2013 . Samples were collected each month except November 2008, August 2009 and February 2012.

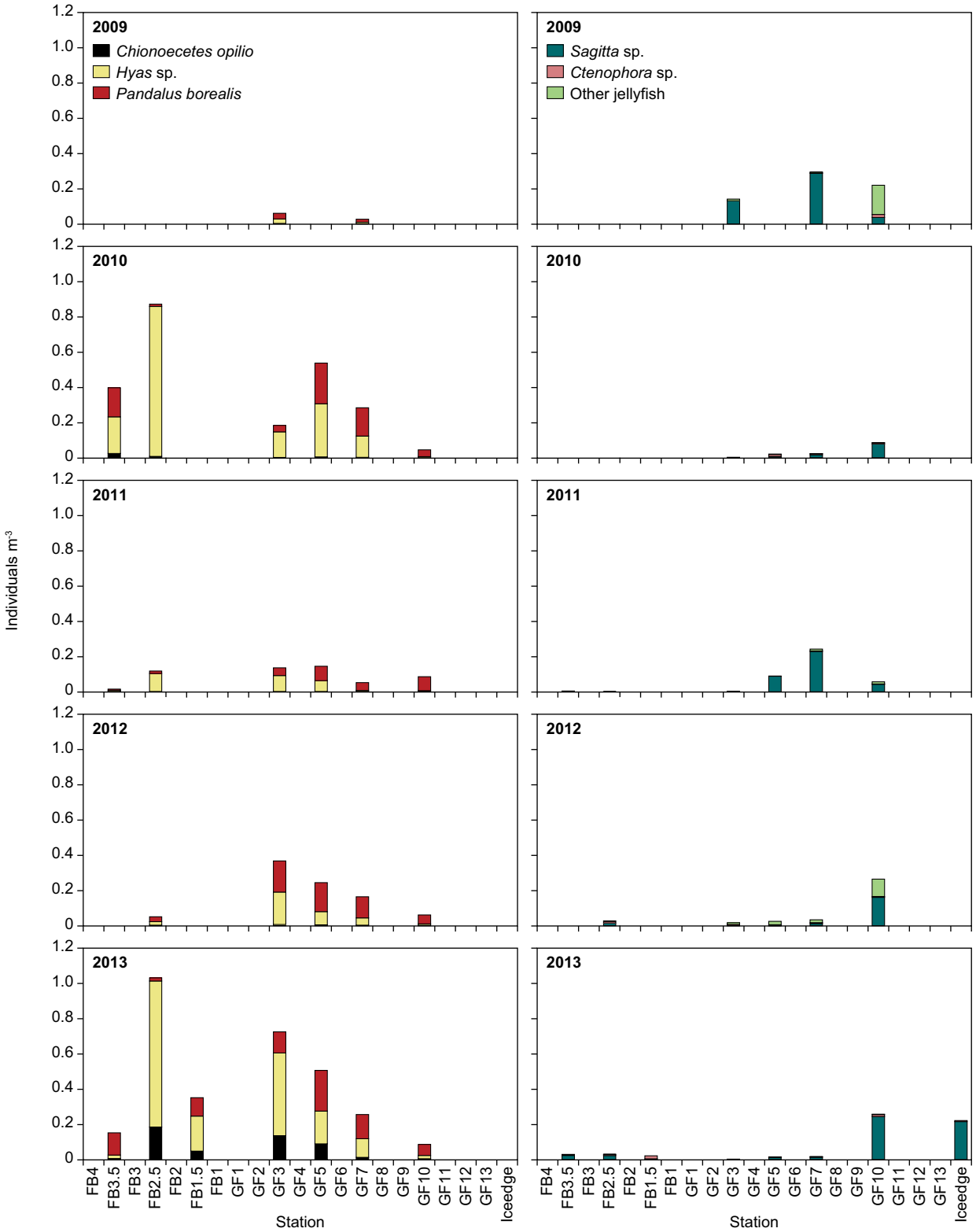

Figure 5.17 Annual variation in abundance (individuals m^{-3}) of Chionoecetes opilio, Hyas *sp.,* Pandalus *sp.* Sagitta *sp.,* Ctenophora *sp. and other jellyfish along the length section from Fyllas Banke (offshore) to the inner part of Godthåbsfjord conducted in May 2009 to 2013. In 2009, no sampling was carried out at Fyllas Banke.*

between stations. The community composition differed not only between stations but also between years (figure 5.18). In 2010 and 2011 larvae of *Chionoecetes opilio* were far more abundant at all stations, except at GF10, compared to 2012 and 2013. *Sagitta* spp. conquered the community at the inner station GF10, except with occurrence of few individuals of *Hyas* spp. and *Pandalus* spp., whereas *Sagitta* spp. were accounted for 99 % of the community at the ice edge station samples for the first time in 2013.

Vertical sinking flux

Part of the organic material produced within the euphotic zone is vertically exported and comprising the main energy sources for the benthic communities below the euphotic zone. The vertical sinking flux is measured during the monthly sampling programme using a free-drifting trap array deployed for approximately 2 hours (at 60 and 65 m, but considered the same depth). Due to unusually high drift speeds of the trap array and in a direction not common in previous samplings, several arrays where lost or grounded (i.e. samples lost) in 2013 (n = 5). The collected particulate material is analyzed for chlorophyll *a*, total particulate carbon (TPC), C:N ratio and isotopic composition. Nitrogen measurements were, however, biased during first analyses and technical problems have prevented a reanalysis in time for this report. The chlorophyll *a* sinking flux during spring followed the previously described increase in phytoplankton biomass during spring bloom (up to 6.6 mg chlorophyll *a* m^{-2} d^{-1}; figure 5.19). Similar to previous years a decrease in sinking flux of phytoplankton material (i.e. chlorophyll *a*) was observed during the post-bloom period reaching into June. Summer phytoplankton production resulted in high sinking fluxes again in September. The recorded TPC sinking fluxes was among the highest observed during the entire monitoring programme (up to 2369 mg C m^{-2} d^{-1}). Based on the limited dataset from 2013 it is not possible to estimate the integrated annual TPC sinking flux.

5.4 Sediments

Organic material produced in upper water column fuels the benthic communities in waters below the photic zone. The organic material reaching the sediments may be mineralized by benthic organisms or buried in the sediment. Mineralization is conducted using oxygen as the primary electron receptor in the upper oxic zone, while sulphate remains the main receptor in the anoxic zone below. Both processes uses oxygen either directly or indirectly, and oxygen uptake into the sediment is, therefore, used to measure the rate of remineralisation.

The seasonal monitoring include sampling and laboratory experiments on sediment cores collected at a permanent sediment sampling station in Kobbefjord

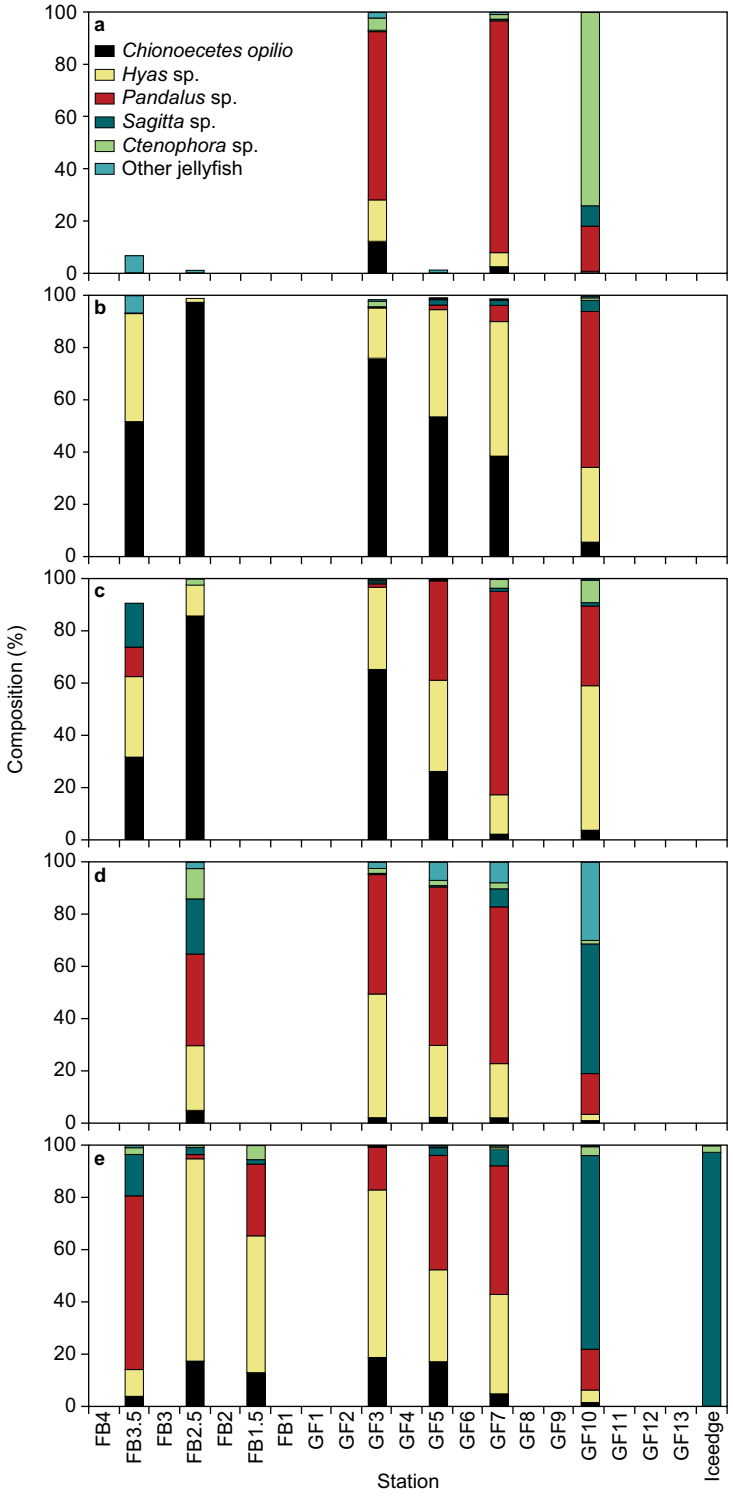

Figure 5.18 Community composition (%) along the length section from Fyllas Banke (offshore) to the inner part of Godthåbsfjord conducted in May 2009 to 2013. a) 2009, b) 2010, c) 2011, d) 2012 and e) 2013. In 2009 no sampling was carried out at Fyllas Banke.

('Sediment station', depth approximately 120 m; figure 5.1). Microprofiling is used for measuring the diffusive oxygen uptake (DOU) into the sediments. The oxygen profiles showed that the oxic zone ranged between 0.6 and 1.0 cm and that DOU ranged between 3.7 and 6.4 mmol m^{-2} d^{-1} during the three seasonal samplings (figure 5.20 and 5.21, respectively). The total oxygen uptake (TOU) ranged from 6.2 to 9.3 mmol m^{-2} d^{-1}. The highest oxygen uptake rates are generally observed du-

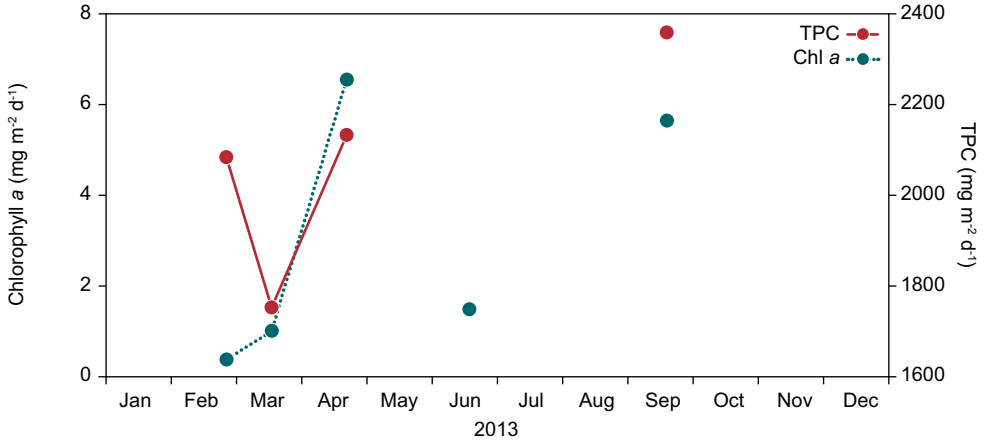

Figure 5.19 Annual variations in vertical sinking flux of total particulate carbon (mg m^{-2} d^{-1}), chlorophyll a (mg m^{-2} d^{-1}) of the sinking particulate material collected at the Main Station in 2013.

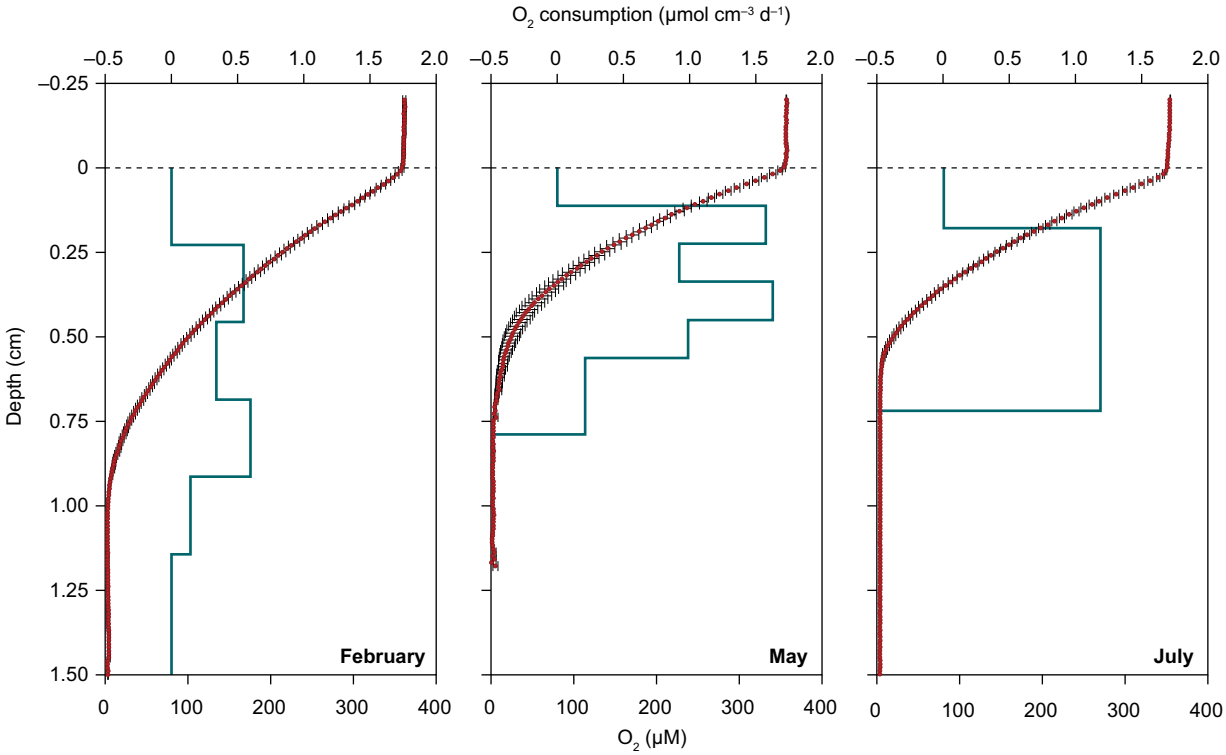

Figure 5.20 Vertical concentration profiles of oxygen (closed dots) and modelled consumption rates (solid line) from microelectrode profiles with sediment depth for each of the three sampling periods. Error bars represent standard error of the mean.

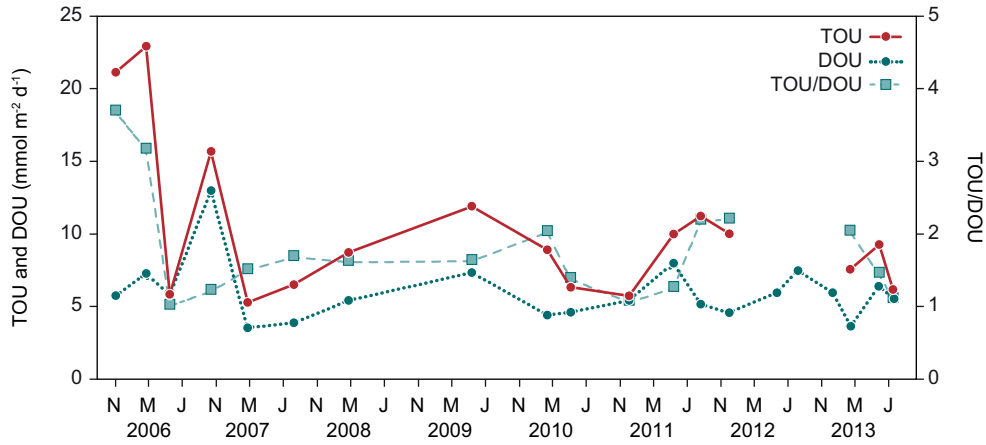

Figure 5.21 Variation in total oxygen uptake (TOU) and diffusive oxygen uptake (DOU) (mmol m^{-2} d^{-1}) and in the TOU/DOU ratio from 2005-13.

Figure 5.22 Left: Sampling in the tidal zone in inner Kobbefjord, Nuuk, where knotted wrack Ascophyllum nodosum *dominates the algal community and bladder wrack* Fucus vesiculosus *and* Fucus evanescence *are also abundant. Photo: Peter Bondo. Mid: Tips of* A. nodosum *with knots/bladders. Photo: Núria Marbà. Right: Blue mussel* Mytilus edulis. *Photo: Peter Bondo.*

ring spring and summer, when primary production and sedimentation of organic material is highest (figure 5.21).

5.5 Benthic fauna and flora

The monitoring of benthic flora and fauna has since 2012 been centred on population dynamics of key species of the intertidal zone – the brown macroalgae 'knotted wrack' *Ascophyllum nodosum* and 'blue mussel' *Mytilus edulis* – in relation to temperature, ice cover/light availability and tidal level. Knotted wrack and blue mussel are expected to respond positively to increases in water temperature in the waters around Nuuk as they are both north-temperate species with temperature optima (15-20°C for *A. nodosum*, Fortes and Lüning 1980) considerably higher than those at Nuuk during summer (10°C, Krause-Jensen et al. 2012). Therefore, they are expected to be sensitive indicators of ecological effects of Arctic warming. These species have the additional advantages as monitoring organisms that their growth rates are reflected in their morphology, which along with their presence in the tidal zone facilitates monitoring.

The coastal waters around Nuuk have a tidal range of 3-5 m and the tidal zone thus represents a broad belt along the coasts (figure 5.22). The composition of the tidal community varies markedly with exposure to ice and waves, with *Ascophyllum* being a dominant habitat former of protected inner fjords such as the monitoring site in inner Kobbefjord.

Permanent monitoring plots were established in late August/early September 2012 in the mid-intertidal zone as well as in the upper (MWL + 0.5 m) and lower intertidal (MWL –0.5 m) and revisited in early September 2013.

Population dynamics of *Ascophyllum*

Knotted wrack grows from the tip and forms a bladder/knot every year allowing an assessment of annual growth (elongation) by simply measuring the distance between consecutive bladders. Actively growing tips were sampled randomly in the population outside the permanent plots in each of the tidal zones (upper, mid, lower). In 2013, tip growth ranged from 5.3 cm y^{-1} in the upper tidal zone to 7.1 cm y^{-1} in the lower tidal zone, considerably faster than in 2012 (figure 5.23). The increased growth rates likely reflect that ice cover was extremely limited during the winter 2012/2013 and the inner part of Kobbefjord at the sampling site did not freeze at all (pers. com., Martin Blicher).

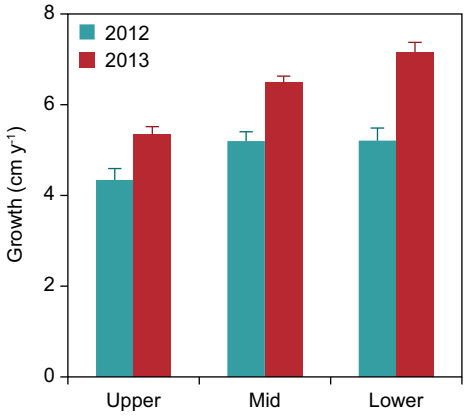

Figure 5.23 Growth of Ascophyllum *tips in the upper, mid and lower tidal zone in 2012 (blue columns) and 2013 (red columns). Data represent the length from the base of the youngest bladder to the base of the second youngest bladder. Error bars represent standard error of measurements of a total of 20 tips (with 1-3 branches) in each tidal zone.*

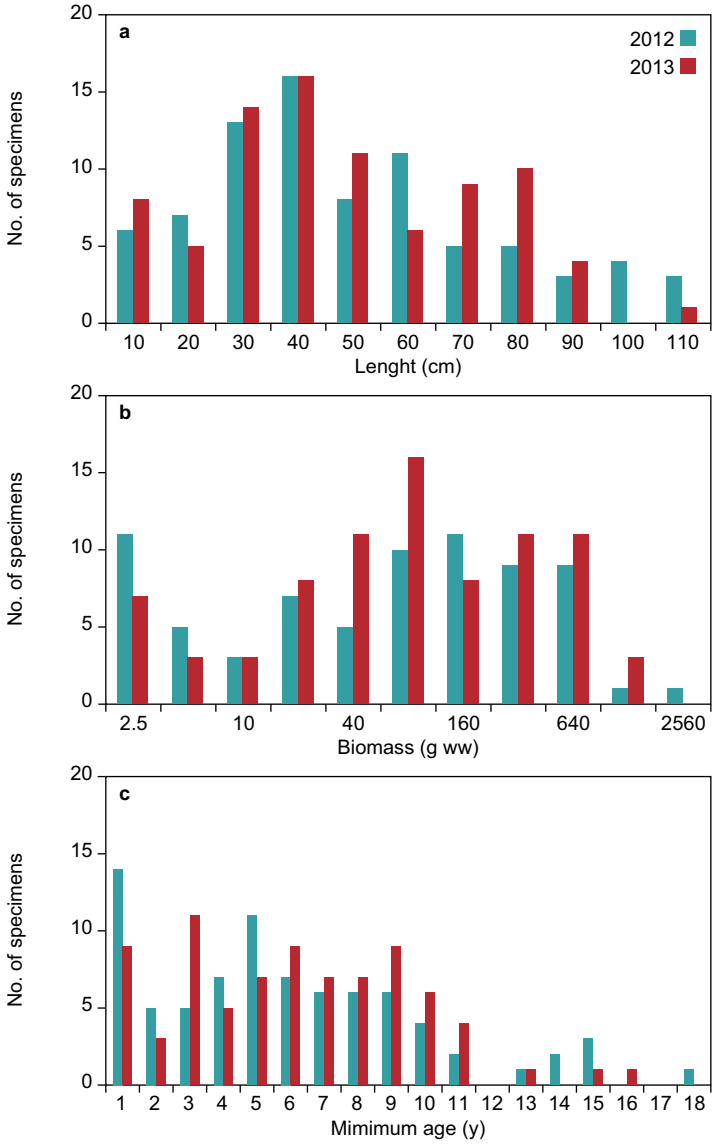

Figure 5.24 Population structure of knotted wrack Ascophyllum nododum *in 10 permanent plots located in the mid tidal zone in inner Kobbefjord. Length distribution (a), age distribution (b) and biomass distribution (c) of individuals are shown.*

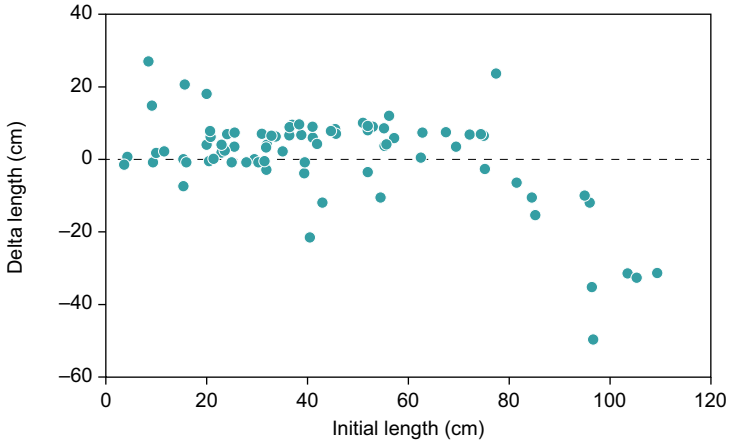

Figure 5.25 The change in length of individuals between 2012 and 2013. Individuals up to 75 cm long generally increased approximately 10 cm in length over the year while longer individuals broke. The threshold size for positive length growth was, thus, 75 cm.

Population structure of knotted wrack was quantified non-destructively in 10 permanent plots (0.25 × 0.25 m) in the mid-tidal zone. Each individual (representing one-several 'shoots' arising from a common basal disk) with bladders and exceeding a minimum length of 5-10 cm, was tagged and numbered in 2012 along with quantification of length (L), minimum age (= number of bladders) of the longest shoot and circumference (C) at the base. Based on this information population density, biomass (B) and age structure of individuals was estimated ($B=0.1057 \times LC^2$, Merzouk et al., unpublished).

The habitat was dense (128 ± 12/134 ± 13) individuals m^{-2} and 19.0 ± 2.8/15.8 ± 3 kg fw m^{-2} in 2012/2013) and completely covered the rocky shore. There was a pool of small (<10 cm), young individuals but the bulk of the rest was generally 30-60 cm long, around 3-9 years old and with a biomass of 40-640 g fw per individual (figure 5.24).

Population dynamics from 2012 to 2013 in terms of growth, mortality and recruitment was assessed based on changes in size of previously marked individuals in combination with observations of appearance and disappearance of individuals. The population was very stable, since net population growth rate was 3 ± 4 % yr^{-1}. The flow of individuals in the population was slow, as indicates the recruitment rate of 6.2 ± 5.0 individuals m^{-2} (5 %) per year and the mortality rate of 1.56 ± 1.63 individuals m^{-2} (1 %) per year. Only one (young) individual out of 81 tagged in year 2012 died during the monitoring period. The biomass tended to increase but not significantly (1761 ± 1367 g fw m^{-2} yr^{-1}). While biomass gains occurred at the tip of individuals, losses were due to breakage of primarily old (>10 bladders, >75 cm long) individuals (figure 5.25). The threshold size of losses that reflect the vulnerability of individuals may change depending on the level of disturbance and may thus also affect younger individuals during years of severe ice scour.

Population dynamics of *Mytilus edulis*

In 2012 a new approach to monitoring the benthic fauna's response to climatic conditions was initiated by quantifying annual growth and survival of *Mytilus edulis* in the intertidal zone. The *Mytilus* data will complement data on clams and sea urchins where baseline data on condition indices were obtained in May from 2007

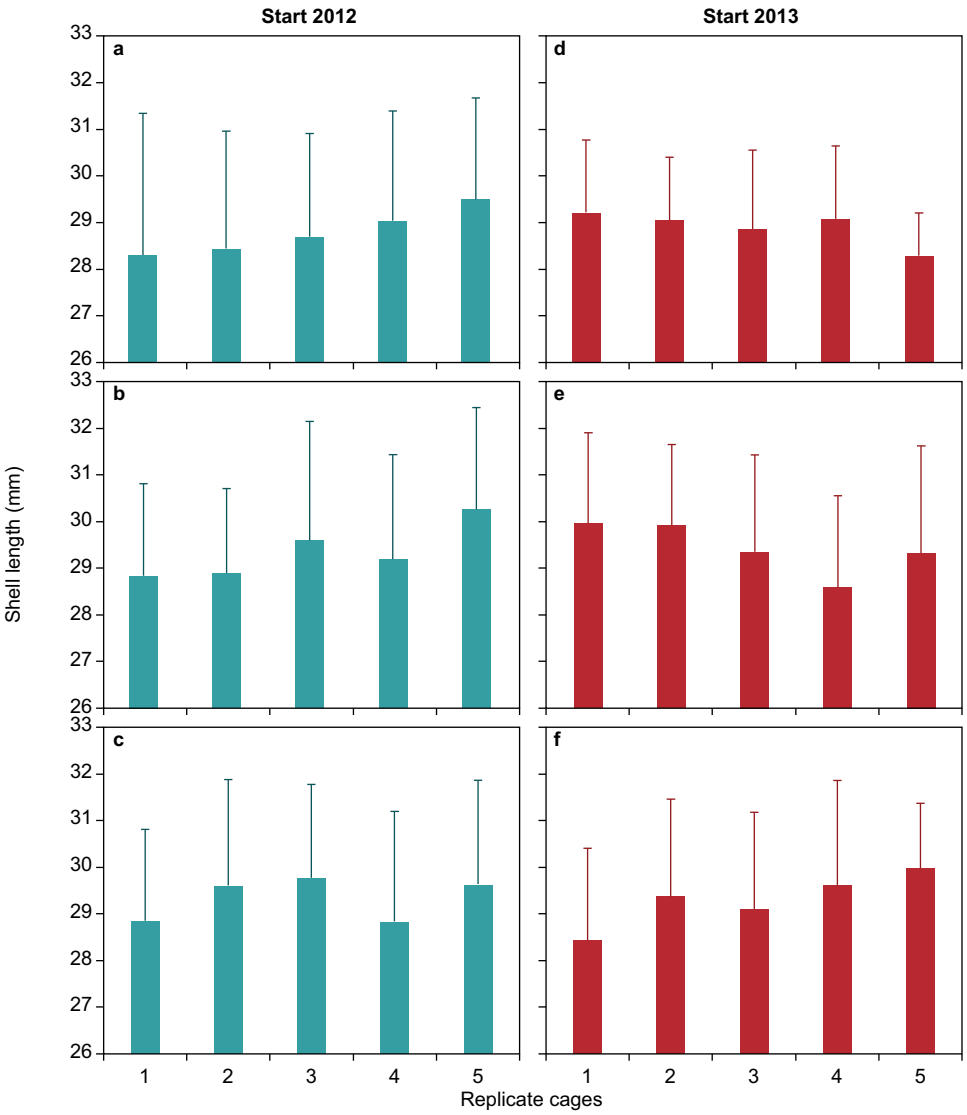

Figure 5.26 The average shell length (± SD) for mussels places in experimental cages at three intertidal levels in Kobbefjord in 2012 and 2013. Upper panel (a and d), mid (b and e) and lower (c and f) intertidal level in 2012 and 2013.

to 2010. Flora and fauna in the intertidal zone show strong response to changes in climate at lower latitudes. Studies in the intertidal zone around Nuuk have shown that abundance of *Mytilus* cf. *edulis* in the intertidal zone appears to be regulated by factors such as wave exposure, ice scouring and winter mortality due to low temperatures. Therefore, abundance in the intertidal zone is highly variable and often mussels are confined to microhabitats offering protection from both ice and wave exposure but also extreme temperatures. In an attempt to set up a monitoring protocol which allows key environmental parameters such as temperature to be collected at a level relevant for the organisms a set of five replicate cages were placed at each of three intertidal elevations; the mid-intertidal (defined as half the maximum tidal elevation) and 50 cm (vertical) above and 50 cm below. In each cage 15 individuals with known shell length (figure 5.26) was placed together with a temperature logger measuring temperature at 15 min intervals. Additionally a CTD mea-

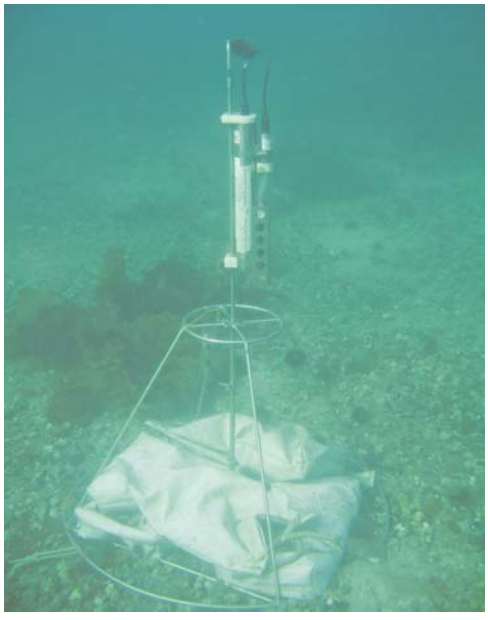

Figure 5.27 Photo of CTD deployed near experimental site measuring temperature and salinity since 2012.

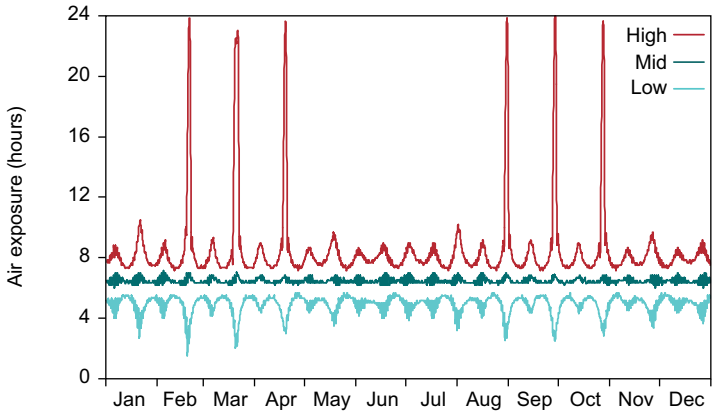

Figure 5.28 Simulated air exposure at the three intertidal levels where mussel cages where placed.

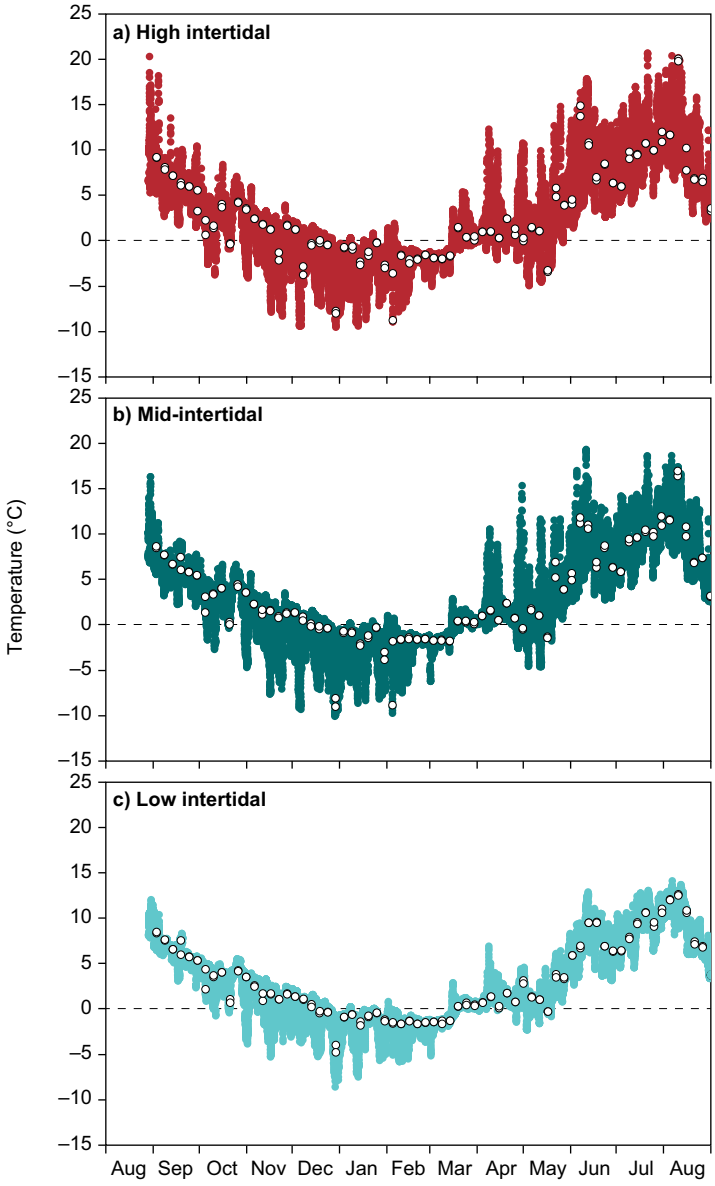

Figure 5.29 Average seasonal variation in temperature 2012-2013 in experimental cages placed at three intertidal levels.

suring pressure, temperature and salinity is placed at 3 m depth near the site (figure 5.27). The three intertidal levels represent variable levels of air exposure (figure 5.28) and especially the mussels at the highest intertidal level experience prolonged air exposure of close to 24 hours during neap tide. The extended air exposure of the two highest tidal levels results in larger temperatures fluctuations both during the daily tidal cycles and during the full year. In winter, there is a higher frequency of temperatures <5° and in summer >15° at the two higher levels compared to the lower (figure 5.29). In figure 5.30 the range of temperatures and sampling duration are showed for individual loggers together with the average temperature range observed at each of the three intertidal levels.

The cages deployed in August 2012 were collected in August 2013. Of 225 mussels deployed in cages only five survived. Deformed metal cages and crushed shells clearly indicated that the high mortality was caused by heavy ice scouring during the winter of 2012-13. This winter stands out from other years by having almost no fast ice in the inner part of the fjord (pers. obs. M. Blicher). For that reason we could not estimate annual shell growth for this batch of mussels, nor evaluate the effect of temperature extremes and air exposure. Therefore, the cage design and placement in the field has been changed in an attempt to reduce sensitivity to ice scouring. A new set of cages and loggers were deployed in August 2013 to be collected in 2014.

5.6 Seabirds

Two key seabird colonies near Nuuk are included in the MarineBasis programme. Additional seabird colonies in the Nuuk area have been visited since 2007. Amongst them, the black-legged kittiwake *Rissa tridactyla* colonies of Godthåbsfjord (five in total) have been surveyed and the results are included in this report. The seabird counts from MarineBasis are reported annually to the Greenland Seabird Colony Database maintained by the Department of Bioscience, Aarhus University.

Qeqertannguit (colony code: 64035)

Qeqertannguit in the interior parts of Godthåbsfjord (figure 5.1) is a low-lying island

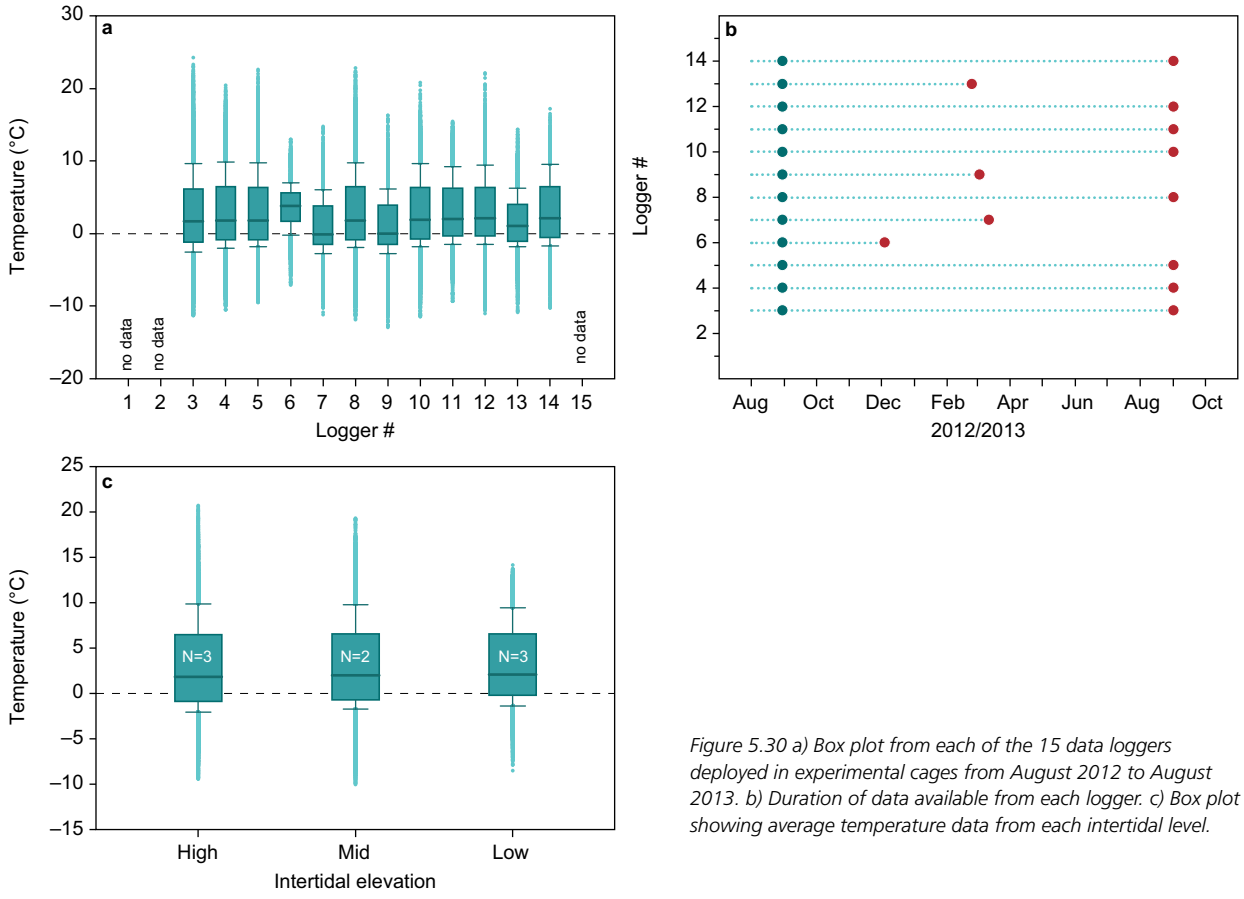

Figure 5.30 a) Box plot from each of the 15 data loggers deployed in experimental cages from August 2012 to August 2013. b) Duration of data available from each logger. c) Box plot showing average temperature data from each intertidal level.

and holds the largest diversity of breeding seabirds in the Nuuk District. Especially surface feeders such as gulls *Laridae*, kittiwake and Arctic tern *Sterna paradisaea* are usually well represented at the site (table 5.3). The steep cliff in the middle of the southeast facing side of the island (kittiwake and Iceland gull *Larus glaucoides*)

Table 5.3 Breeding seabirds (pairs (P), individuals (I) or Apparently Occupied Nests (AON)) at Qeqertannguit since 2006.

Year	2006		2007		2008		2009		2010		2011		2012		2013	
Species	**No.**	**Unit**	**No.**	**Unit**	**No.**	**Unit**	**No.**	**Unit**	**No.**	**Unit**	**No.**	**Unit**	**No.**	**Unit**	**No.**	**Unit**
Black-legged kittiwake	45	AON	45	AON	20	AON	55	AON	42	AON	80	AON	0	AON	1	AON
Iceland gull SE side	118	AON	82	AON	33	AON	40	AON	31	AON	31	AON	11	AON	17	AON
Iceland gull NV side	–	AON	**	AON	12	AON	19	AON	13	AON	20	AON	9	AON	16	AON
Great black-backed gull	46	P	38	P	44	P	24	P	40	P	17	P	16	P	18	P
Lesser black-backed gull	10	P	11	P	25	I	21	I	27	I	18	I	1	I	7	I
Glaucous gull	10	P	14	P	13	P	5	P	4	P	2	P	6	P	16	P
Herring gull	–	P	1	I	2	P	1	P	0	P	0	P	1	P	0	P
Arctic tern	150-220	I	150	I	0	I	150	I	54	I	50	I	50-100	I	0	I
Arctic skua	2	P	2	P	2	P	2	P	2	P	0	P	2	P	2	P
Black guillemot	615	I	562	I	689	I	637	I	790	I	1047	I	708	I	388	I
Red-throated diver (*Gavia stellata*)	1	P	1***	I	1	P	1	P	0	P	0	P	0	P	0	P
Red-breasted merganser (*Mergus serrator*)	*		4	P	3	P	0	P	1	P	0	P	0	P	0	P

*Observed
**These birds are included in number for SE birds
***Seen at coast, but lake was dry and no nest visible

and a smaller cliff on the northwest facing side (Iceland gull) were counted from the sea using a boat as platform. Counts of the remainder of the island were conducted by foot using direct counts of Apparently Occupied Nests (AON) or territorial behaviour as a criterion of breeding pairs. This year the island was surveyed June 8 and the SE colony was observed and photographed from boat 17 June.

Other birds observed (not considered breeding or not systematically censured) included one great cormorants *Phalacrocorax carbo* flying from the island when we arrived by boat. Snow bunting *Plectrophenax nivialis*, Lapland bunting *Calcarius lapponicus* and three mallard ducks *Anas platyrhynchos* were observed during the walk. The number of black guillemot around the island was estimated to 388 individuals.

Arctic tern was not observed at the island 8 June and no nests were found (table 5.3). Complete absence of Arctic tern on Qeqertannguit was also recorded in 2008. Small and mid-sized colonies of Arctic tern in Greenland are known to fluctuate considerably in population size and years of complete failure seems to occur regularly, but the reason is poorly understood.

No kittiwake was observed 8 June 2013, but one single pair was recorded 17 June and a large chick was observed during a visit to the island 2 August. In 2012 kittiwake was not breeding at all following a maximum of 80 pairs in 2011. The number of Iceland gull has increased to 33 in 2013 after the minimum of 20 recorded in 2012.

Qeqertannguit is influenced by legal egg harvesting (great black-backed gull *L. marinus* and glaucous gull *L. hyperboreus* prior to May 31). Illegal egg harvesting (illegal species (e.g. Iceland gull, lesser black-backed gull *L. fuscus*, herring gull *L. argentatus*) and egg harvesting after May 31 has been reported several times since the start of the monitoring programme.

Nunngarussuit (colony code: 63010)

Nunngarussuit is located approximately 40 km south of Nuuk (figure 5.1). The north facing cliff wall of the small island holds the only colony of guillemots *Uria* sp. in the Nuuk District. The colony includes both Brünnich's *Uria lomvia* and common guillemot *U. aalge*. These alcids are deep divers preying on fish and large zooplankton. Photo counts of birds present on the cliff were conducted from the sea (boat) 5 July (table 5.4). The number of guillemots (both species) on the cliff was 654 which is the highest number recorded since 2008. Due to the quality of the photos the two species could not be distinguished and no other species were counted. The number of guillemots on the water was not estimated.

In order to address the proportion of the boreal distributed common guillemot versus the Arctic Brünnich's guillemot in the colony an analysis of digital photographs is usually carried out. This is interesting in the context of climate change where the proportion of common guillemot could be expected to increase in a warmer climate (table 5.4). This analysis was not carried out this year.

Other seabird observations south of Nuuk

Simiutat consist of three smaller islands. The following was observed:

Simiutat (63011) 5 July: One puffin *Fratercula Arctica*, 20-25 black guillemots *Cepphus grylle*, one pair of great black-backed gulls, three pairs of glaucous gull, two pairs of lesser black-backed gull and

Table 5.4 Counts of breeding seabird at Nunngarussuit since 2006.

Year	2006	2007	2008	2009	2010	2011	2012	2013
Species	No.	No.	No.	No.	No.	No.	No.	No.
Guillemot unspecified	694	–			–	514	375	654
Brünnich's guillemot	–	705	388	475	–	–	–	–
Common guillemot	–	87	36	47	–	–	–	–
Guillemots on the water	2–300	450	450	–	–	500	2–400	–
Glaucous gull	20	14	14	12	–	11	4 (P)	–
Great black-backed gull	5	5	2	5	–	4	2 (P)	–
Northern fulmar	23	13	17	11	–	21	10 (P)	20 (I)

one female common eiders *Somateria mollissima*.
Simiutat (63012) 5 July: five puffins, 16 razorbills *Alca torda*, five black guillemots, 17 male and two female common eider. Six gulls of unknown species and breeding status were seen above the island.
Simiutat (63013) July 5: eight puffins, 70 razorbills, 10 Iceland or glaucous gull, four great black-backed gull, five lesser black-backed gull, 14 resting great cormorants (incl. two juveniles), nine resting Canada geese *Branta canadensis*, and 24 pairs of northern fulmar *Fulmarus glacialis*.
'The Puffin Island' at Ravneøerne (63020) July 11: 135 puffins, three razorbills, 22 black guillemots and one pair of great black-backed gull were observed at the island. A pair of Canada geese with four juveniles was observed on a neighbour island to the south.
Qarajat Qeqertaat (63019) July 5: This site consists of two islands with breeding common eiders.
West island: 15 nests of common eider (two empty nests, one with nestlings and one nest with clear signs of predation). Average of 3.6 eggs/chicks per non-empty nest. Additionally 21 eiders (20 ♀ and one ♂) were resting on the water. Otherwise 164 black guillemot, 12 pair of lesser black-backed gull, and three pair of great black-backed gull. Two nests of ducks other than eider were found.
East island: 13 nests of common eider (two empty). Average of 3.8 eggs per nest with eggs. Additionally 43 eiders (41 ♀ and one ♂) were resting on the water. Otherwise 204 black guillemots, 10 pair of lesser black-backed gull, six pair of great black-backed gulls and 70 mixed glaucous and Iceland gulls (mostly Iceland gull and juveniles) resting on skerries at the west end of the island.

Other kittiwake colonies in Godthåbsfjord (see the Seabird database for details):

The number of kittiwakes and Iceland gull at the five kittiwake colonies in the Godthåbsfjord, are listed in table 5.5 including counts since 2006.

The total number of breeding kittiwakes of all five colonies since 2007 has shown a somewhat different pattern than the Qeqertannguit numbers alone. Generally, the numbers seem to vary between the colonies – the colony with the largest number of kittiwakes has alternated between Kangiusaq and Innajuattoq, and in 2012, it appeared as all the birds from Qeqertannguit had moved to Innaarsunnguaq. However, in 2013 the number of birds in Innaarsunnguaq dropped without a corresponding increase in Qeqertannguit. Furthermore, the number of birds in Kangiusaq was reduced to about 100 breeding bird, less than half of the former minimum in 2007. Unfortunately, the Innajuattoq colony was not counted and the total number of kittiwakes cannot be calculated. But the four counted colonies was 326 breeding birds in total and unless the numbers of breeding birds in Innajuattoq has increased substantially above its former maximum,

Table 5.5 Counts of breeding kittiwakes and Iceland gulls at the five kittiwake colonies of Godthåbsfjord counted in 2013.

Year	2006	2007	2008	2009	2010	2011	2012	2013
Kittiwake								
Innaarsunnguaq (64015)	240 (I)	62	33	12	16	27	115	74
Kangiusaq (64018)	–	217	450	284	370	509	463	101
Alleruusat (64022)	–	276	369	164	260	168*	152	150
Innajuattoq (64019)	–	302	309	458	375	399*	250	–
Qeqertannguit (64035)	45	45	20	55	42	80	0	1
Sum	–	902	1181	973	1063	1183	980	–
Iceland gull								
Innaarsunnguaq (64015)	1580 (I)	–	961(I)	435	477	518	452	536
Kangiusaq (64018)	–	300	494(I)	261	277	262	242	155
Alleruusat (64022)	–	45	140	80	100	118	111	70
Innajuattoq (64019)	–	342	1497(I)	1553(I)	335/1535(I)	1538	1015	–
Qeqertannguit (64035)	118	82	45	59	44	51	20	33
Sum	–	–	–	–	1233	2487	1840	–

a new minimum of breeding kittiwakes in Godthåbsfjord was reached in 2013.

The numbers of Iceland gulls since 2007 are more difficult to compare, since they have been counted by different methods (different units (I/AON)/direct or photo counts) between years. Some of the Iceland gulls at Innajuattoq occupy areas high above sea level where nests can be difficult to see from the boat, and numbers before 2011 may have been underestimated. Innajuattoq was not counted in 2013 and as it is the largest colony in the area, the trend in total number of birds can not be interpreted. The second largest colony Innaarsunnguaq was stable, whereas the number of nesting Iceland gulls in Kangiusaq and Alleruusat were reduced by one third.

Remaining species in the kittiwake colonies observed in 2013 were:

- Innaarsunnguaq (64015): 36 razorbills June 17.
- Kangiusaq (64018): eight nests of great cormorants May 22.
- Alleruusat (64022): 10 nests of great cormorants May 22.
- Innajuattoq (64019): 61 black guillemots June 17.

5.7 Marine Mammals

West Greenland is a summer feeding ground for an estimated 3200 humpback whales, *Megaptera novaeangliae* (Heide-Jørgensen et al. 2012). Most of them stay on the off-shore banks, but some visit the fjords and bays to feed on zooplankton and capelin *Mallotus villosus* (Heide-Jørgensen and Laidre 2007). Some of these whales have a high degree of site fidelity to Godthåbsfjord and return year after year to feed but also new individuals visit the fjord annually (Boye et al. 2010). In the MarineBasis monitoring programme we use photo-identification to estimate the number of humpback whales feeding in Godthåbsfjord each summer and the turnover of whales during a season to understand how much these top-predators eat and thus affect the Godthåbsfjord ecosystem.

Photo-identification is a technique used to identify individual animals from photographs showing natural markings such as scars, nicks and coloration patterns (Katona et al. 1979). The technique can, in combination with mark-recapture analysis be used for estimating abundance of marine mammals in specific areas. Photo-identification is also used to investigate residence time (i.e. how long the animals stay in a given area) and site fidelity (i.e. individuals returning to an area in different years) (e.g. Bejder and Dawson 2001). In humpback whales, the ventral side of the fluke is used for identification as the tail contains individual colour patterns, which in a way is comparable to human fingerprints. Photo-identification pictures were taken with a 350 EOS Canon camera with a 300 mm Canon lens. In addition to dedicated surveys, guides on the local whale tourist boats and the public kindly contributed with identification-photos. Due to personnel limitation photographic material from 2013 has not been processed in time for this report, but will be processed later.

6 Research Projects

6.1 Nuuk Campaign 2013

Thomas Juul-Pedersen and Søren Rysgaard

Greenland Institute of Natural Resources, Greenland, Aarhus University, Denmark, and University of Manitoba, Canada, joined forces in July 2012 to strengthen Arctic research. The Arctic Science Partnership (ASP) was formed to study the full impact of the changes in the Arctic and the mechanisms behind these changes. This new and extensive Greenlandic-Danish-Canadian research collaboration is bringing together a number of the world's leading scientists in climate-related research in the Arctic.

The ASP partners are actively part in the Greenland Ecosystem Monitoring (GEM), and the monitoring programme plays a vital scientific and logistical role for all campaigns in Greenland. The close connection between ASP and GEM also secure exchange of data, knowledge and know-how between the two, thus improving and promoting collaboration between monitoring and research activities in the Arctic.

Coordinated field campaigns involving scientists from the ASP institutions and external institutions are planned years into the future in order to promote strong collaboration and achieve the most productive outcome (see figure 6.1). In 2013 a coordinated ASP field campaign 'Nuuk 2013' was conducted in the Nuuk region in close collaboration with the different Nuuk Basic subprogrammes. A series of projects covered the following research topics: Marine Chemistry, Marine Biology, Atmospheric Processes, Land and Freshwater Processes. The project titles in 'Nuuk 2013' were:

Marine Biology Group

- Processes determining the quantity and fate of net primary production.
- Linking primary producers to top-predators: the role of capelin and sand eel in the Godthåbsfjord area.
- Seasonal synergy between bacterial osmoprotection and algal production in sea ice.
- Seasonal dynamics of phytoplankton production in a glacier influenced fjord.
- pH and the possible buffering role of the expanding marine vegetation against ocean acidification in coastal waters of Greenland.

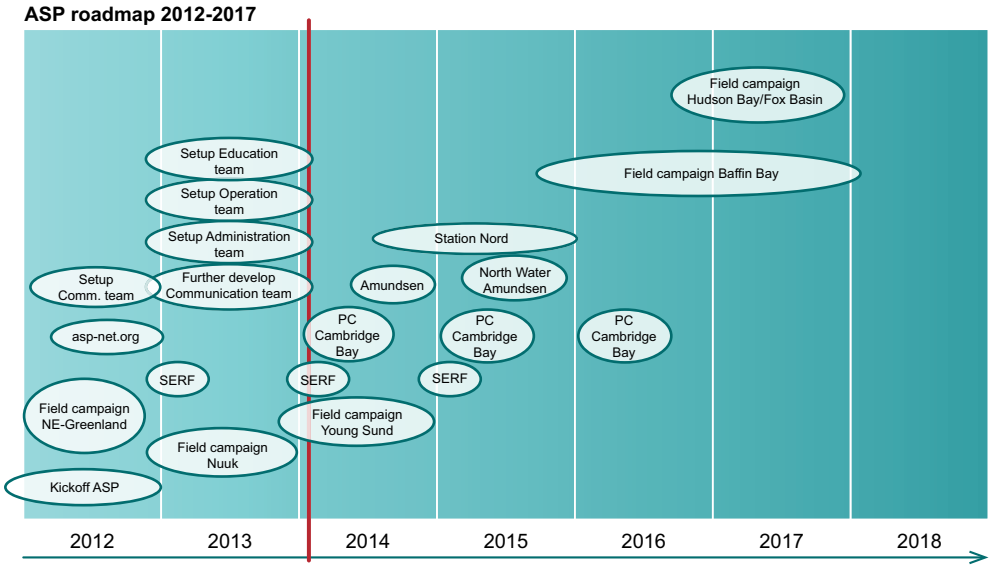

Figure 6.1 Roadmap of ASP field campaigns.

- Quantifying the influences of biogeochemical processes on carbon dynamics in Godthåbsfjord.
- Paleoclimate and sediment biogeochemistry.
- Otoliths and mussel shells as recorders of potential future pollution on a section from Nuuk to the proposed Isua iron-mine.
- Seasonality of marine mammals and background noise level in Godthåbsfjord.
- Quantifying grazing impact of krill and copepods in the Godthåbsfjord system.

Marine Chemistry Group

- Greenhouse gases (CO_2-CH_4-N_2O) dynamics within fjord sea ice.
- Underwater eddy correlation measurements of ice-ocean heat and mass exchange.
- Evolution and distribution of pH in natural first-year sea ice.
- Assessment of sea ice algae production in Kanajorusuit Fjord.
- Mercury transport and transformation across the sea ice environment.
- Circulation and exchange processes at the entrance to Godthåbsfjord.

Atmosphere Group

- Interactions between atmospheric processes and marine emissions of carbon.

Land and Freshwater Group

- Influence of environmental gradients on Arctic plant communities.
- Impact of shrub expansion and climate, and climate gradients on arthropod assemblages.
- Ecosystem patterns and processes at retreating glaciers.
- Snow cover in the Godthåbsfjord area 2007-2013.
- Fingerprints in lake sediments from retreating and expanding glaciers in a changing climate.
- Limnic ecosystem patterns and processes near retreating glaciers.
- Glacial activity and its consequences to terrestrial and limnic systems in Kobbefjord.
- Evolution potential. Arctic char and three-spined stickleback in Greenland.
- Carbon cycling in glacier forelands and the microbial terrestrial-atmospheric coupling.
- A millennium of changing environment in Godthåbsfjord.
- Permafrost – preserving the cultural heritage of Greenland in a changing climate.

For more information on the ASP partners, field campaigns and other activities please visit the website: http://asp-net.org/

6.2 Soil microarthropods collected in Kobbefjord and Zackenberg

Paul Henning Krogh, Peter Gjelstrup, Helena Wirta, Tomas Roslin, Zdenek Gavor, Elin Jørgensen, Niels Martin Schmidt, Henning Petersen, Katrine Raundrup, Josephine Nymand and Peter Aastrup

During the last few years, we have invested specific effort in generating a library of DNA barcodes *sensu* Hebert et al. (2003) for the microarthropod fauna of both BioBasis Nuuk and Zackenberg locations. Our prime objectives include generating a species identification tool for the benefit of all ecologists, creating the means for molecularly-based diet analysis and for quantifications of food web structure, and establishing the identity of microarthropod taxa encountered on both sides of Greenland.

Microarthropods collected during the barcoding campaign in 2012 were prepared according to the guidelines of BOLD (www.boldsystems.org) and submitted for sequencing in 2013 and 2014. Each specimen was photographed and subsequently placed in a well containing about 50 µl of 96% ethanol in a 96 well microplate. DNA extraction, amplification and sequencing were carried out by the Canadian Centre for DNA Barcoding (CCDB) following their standard procedures (CCDB, 2014). For both mites and collembolans, the primer set C_LepFolF/C_LepFolR was used for amplification. Collection details for each specimen together with its taxonomic assignment and its photograph are provided at the BOLD website. No physical vouchering was carried out for the sequenced specimen, but the species are in most cases available at Department of Bioscience, AU. When using the BOLD facility the Barcode Index Numbers (BIN) assigned to similar barcodes, guides the

Table 6.1 Collembola submitted for barcoding at CCDB by March 2014. Numbers in brackets indicates the number of individuals compiled from specific habitats within the Kobbefjord monitoring area (Krogh et al. 2013) or from the Zackenberg sampling location, ZA.

Order	Species	Habitats
Entomobryomorpha	*Desoria olivacea*	Kaer (5)
	Desoria tshernovi	ZA (5)
	Folsomia bisetosa	ZA (5)
	Folsomia cf. near penicula	MArt2 (5)
	Folsomia quadrioculata	Sitka Østerild DK (2)[1], Urteli (5), ZA (5)
	Folsomia sexoculata	ZA (5)
	Isotomiella minor	MArt2 (5)
	Lepidocyrtus violaceus	Urteli (5)
	Parisotoma ekmani	ZA (5)
	Parisotoma notabilis	Urteli (5)
	Tetracanthella Arctica	MArt2 (5)
Neelipleona	*Megalothorax minimus*[2]	ZA (5)
Poduromorpha	*Ceratophysella denticulata*	ZA (5)
	Friesea quinquespinosa	ZA (5)
	Hypogastrura concolor	ZA (5)
	Neanura muscorum	MArt2 (5)
	Oligaphorura groenlandica	Kaer (5), ZA (5)
	Willemia anophthalma	MArt2 (5)
	Willemia scandinavica	ZA (2)
Symphypleona	*Sminthurides schoetti*	ZA (5)
	Sminthurinus aureus	ZA (5)

[1]Two specimen from a Danish spruce forest included for reference
[2]Formerly considered a symphypleonid

Table 6.2 Acari species submitted for barcoding to CCDB by March 2014. Numbers in brackets indicate the number of individuals compiled from specific habitats within the Kobbefjord monitoring area (Krogh et al. 2013) or from the Zackenberg sampling location, ZA.

Order	Species	Habitats
Oribatida	*Ceratoppia bipilis*	ZA (4)
	Brachychthonius sp.	MArt5 (4)
	Camisia lapponica	Kaer (2), MArt3 (3), ZA (2)
	Ceratoppia sp.	ZA (1)
	Ceratozetes sp.	Snow (3)
	Ceratozetes thienemanni	MArt3 (4)
	Diapterobates sp. nov.	ZA (4)
	Dissorhina ornata	Snow (4)
	Eupelops sp.	Kaer (1), Snow (2)
	Heminothrus longisetosus	MArt2 (3), MArt3 (1), Snow (1)
	Hermannia sp.	MArt2 (3)
	Hydrozetes sp.	Kaer (1)
	Liebstadia sp.	Kaer (1)
	Liochthonius alpestris	ZA (3)
	Liochthonius muscorum	Kaer (4)
	Melanozetes cf. meridianus nov. sp	Kaer (5), Snow (3)
	Microppia minus	MArt5 (4)
	Mucronothrus nasalis	Kaer (5)
	Mycobates tridactylus	MArt7 (5), ZA (4)
	Neonothrus sp. nov.	Kaer (5)
	Neonothrus sp. nov.	Kaer (5), ZA (5)
	Nothrus cf. borussicus	MArt3 (2)
	Opiella sp.	Kaer (2)
	Oppiella clavigera spp. nov.	ZA (4)
	Oribatula tibialis	MArt3 (3), ZA (3)
	Oromurcia bicuspidata	Snow (4)
	Plathynothrus thori	Kaer (4)
	Platynothrus capillatus	Urteli (5)
	Tectocepheus alatus	MArt5 (4)
	Tectocepheus tenuis	ZA (4)
Prostigmata	*Bdella* sp. 2	MArt3 (2)
	Bryobia sp.	ZA (2)
	Callidosom (cf.)	ZA (5)
	Erythraeus sp.	ZA (4)
	Erythraeus sp. larva	ZA (5)
	Eupodes sp.	ZA (2)
	Neomolgus sp.	ZA (2)
	Penthaleus sp.	ZA (2)
	Penthaleus sp. 2	ZA (2)
	Rhagidia sp.	MArt3 (2), ZA (1)
	Trombidium sp.	Kaer (1), Krat (3), MArt3 (1), ZA (4)
	Trombidium sp. z	ZA (3)

species identification and could possibly discover errors and synonymy of the barcoded specimen (Ratnasingham and Hebert, 2013).

At the time of writing this report, sixteen of 22 collembolan species collected in 2012 (table 6.1) had been barcoded. All species seem to form well-defined and identifiable clades, with no cases of barcode-sharing among taxa (figure 6.2). Some taxa were characterised by surprisingly high levels of intraspecific variation, with sequence differences more than 5% within *Oligaphorura groenlandica* from Zackenberg, hence cryptic species diversity is suspected (figure 6.2); (Kimura 2-parameter distance). In *Folsomia quadrioculata*, individuals differed by as much as 19% (figure 6.3), which is still within the range of up to 20% (mean 14%) found for this species in BOLD[1]. Whether or not the species then corresponds to a single lineage or a larger species complex is then a topic worth further investigation. The genetically most variable species was *Megalothorax minimus* with up to 27% intraspecific

[1] www.boldsystems.org

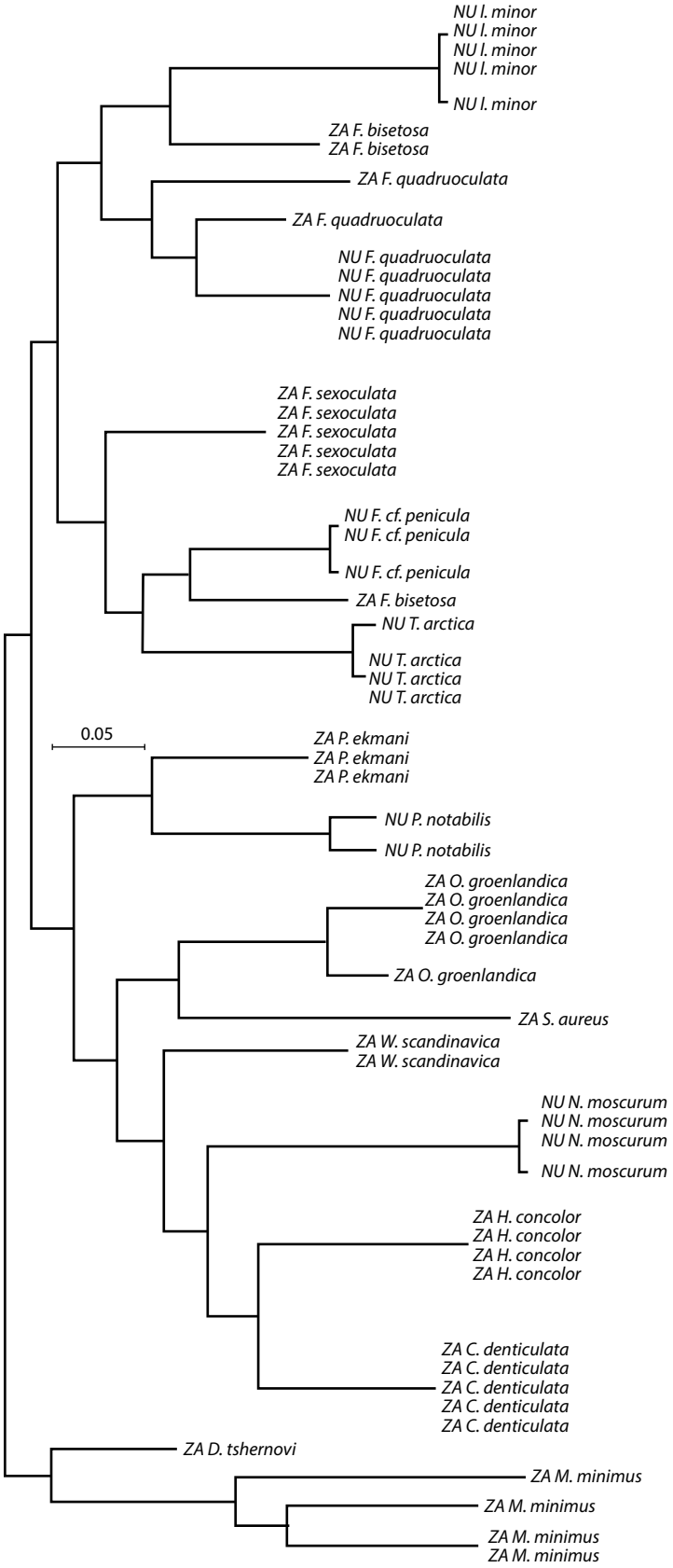

Figure 6.2 A cladogram showing the relationship among 58 COI sequences from 16 species of Collembola. The topology of the tree was reconstructed by MEGA version 6 (Tamura et al. 2013) as based on the K2P model (Kimura 1980). All nucleotide positions containing gaps and missing data were eliminated, resulting in a data set of 558 bp. Individual sequences derive from a total of 16 collembolan species identified by morphological criteria, with species designations shown at the end of each branch. ZA: Zackenberg; NU: Nuuk, Kobbefjord.

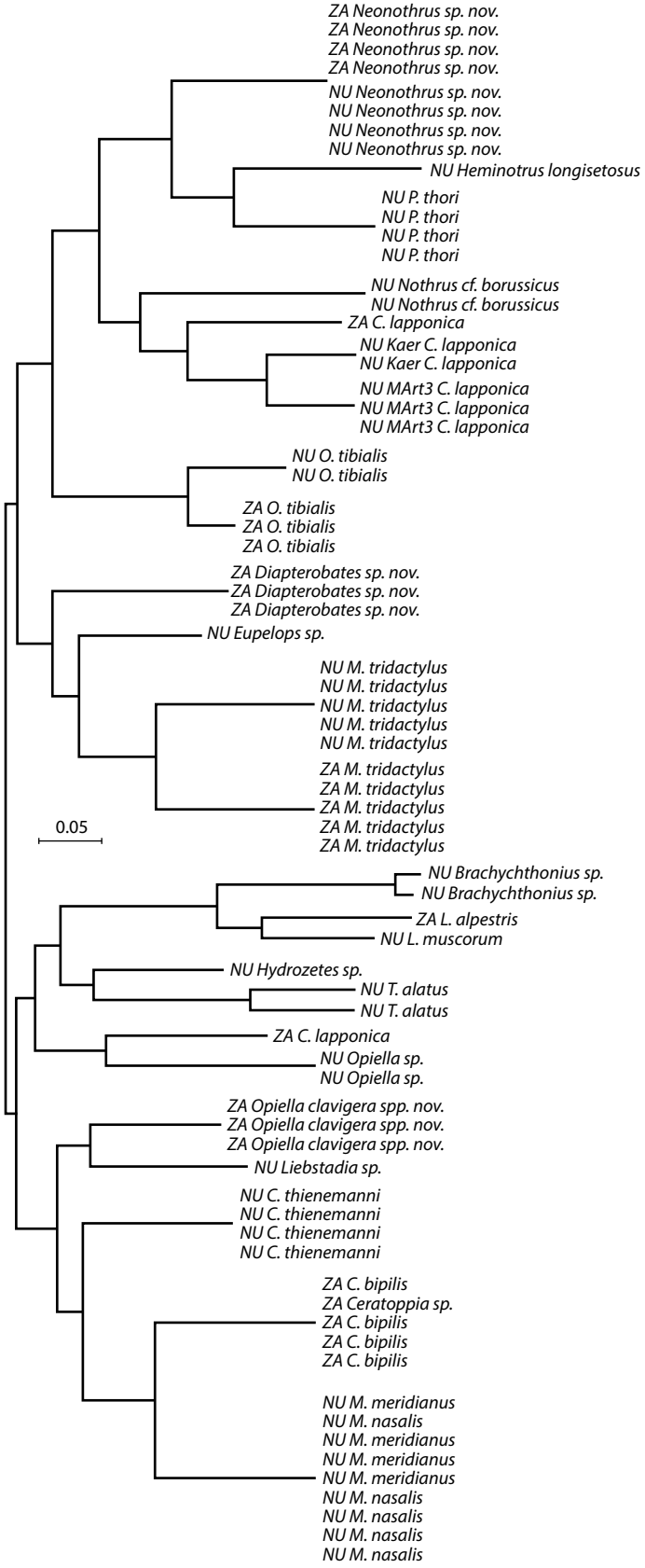

Figure 6.3 A cladogram showing the relationship among 73 COI sequences from oribatid mites. The topology of the tree was reconstructed by MEGA version 6 (Tamura et al. 2013) as based on the K2P model (Kimura 1980). All nucleotide positions containing gaps and missing data were eliminated, resulting in a data set of 606 bp. Individual sequences derive from a total of 23 mite species identified by morphological criteria, with species designations shown at the end of each branch. ZA: Zackenberg; NU: Nuuk, Kobbefjord.

variability, supporting the conclusion of Schneider et al. (2011) that this taxon is a species complex containing many species yet to be discovered. Nonetheless, as *M. minimus* is likely parthenogenetic, the variability observed may also reflect intraspecific differences between clones. Most of the collembolan species were still characterised by remarkably low levels of intraspecific variability (figure 6.2). Hence, beyond the variability mentioned above, haplotypes within species were either identical or differed by a few bp only (figure 6.2). This pattern brings confidence to our ecological investigation of these collembolan species at the Kobbefjord monitoring site, proving that morphologically-identified taxa are indeed valid species. On a more systematic note, it should be stressed that the tree shown in figure 6.2 is not providing any more generally valid phylogenetic hypothesis of Collembola, as e.g. species like the sminthurid *Sminthurinus aureus* (a symphypleonid) are here grouped together with the genetically distant poduromorph onychiurids.

Patterns observed within mites were more complex. Of the 41 mite species found in Kobbefjord and Zackenberg (table 6.2), 73 individuals have now been barcoded (figure 6.3). Here, a number of challenges were revealed by the sequencing exercise, as related partly to the morphologically-based identification of oribatids and partly to the barcoding itself. A few cases of barcode-sharing emerged, of which one was related to *Mucronothrus nasalis* – a species belonging to the primitive oribatid superfamily, Crotonoidea, of moss mites. This taxon is, from a systematic point of view, rather distant from the higher oribatids, but yet it shared its barcode with *Melanozetes meridianus* (figure 6.3) – and was grouped by BOLD into a single molecular taxonomic unit (MOTU) together with *Ghilarovizetes longisetosus* collected in Manitoba (Young et al. 2012) (BIN: BOLD:AAF907). For two other species, *Camisia lapponica* and *Mycobates tridactylus*, haplotypes encountered within the Kobbefjord area and Zackenberg proved distinctly different (figure 6.3), and only added material will show whether the taxa encountered in Western and Northeastern Greenland are indeed identical or not.

6.3 Comparing Late Holocene climate changes in low and high Arctic regions using lake sediments and annual rings of dwarf tundra shrubs records

Daniel Nývlt, Jiří Lehejček and Petra Polická

Due to lack of long instrumental climatic records and their spatial scarcity (Weijers et al. 2010) as well as missing written sources from the Arctic, paleoclimatological studies are important evidence of climatic variations in Polar Regions (AICA 2005). Our study aims to reconstruct past climate development prior instrumental measurements. We used two main approaches combining high-resolution record of responses for recent climate (dendroclimatology of dwarf tundra shrubs and record from lake sediments). In addition, soil characteristics and vegetation cover were recorded in order to display the current state of ecosystem to understand past changes better.

Multi-proxy record from lake sediments is combining litological (mainly grain-size composition), petrophysical (magnetic susceptibility), geochemical (determination of basic lithophile elements, organic and anorganic carbon and sulphur, possibly also stable isotopes), and biological proxy (pigments, biostratigraphy of different groups of organisms) approaches. Petrophysical and geochemical analysis were finalized recently. Remaining analysis is being processed at the moment. This will show climatic and environmental variability. For determination of the time development of sedimentation appropriate dating methods will be applied (AMS radiocarbon dating, OSL, ^{210}Pb and ^{137}Cs for the youngest parts of sediments accumulated in last centuries; see Nehyba et al. 2011).

Dendroclimatology of dwarf tundra shrubs (*Juniperus communis, Salix glauca, Alnus crispa*) will give up to three century long climatic record. The age of the oldest shrub (*Juniperus communis*) spans to 17th century. Using microtome knife and staining solutions the micropreparates were prepared (Gärtner and Schweingruber 2013) to obtain reliable information from this archive on the cell level. Subsequently, the digital photos were taken under microscope with 100x magnification (figure 6.4) and growth parameters (width of rings,

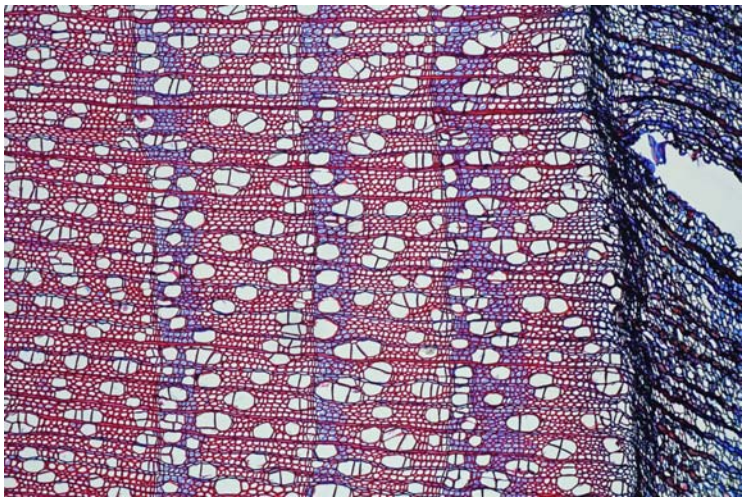

Figure 6.4 Three outer most rings and bark of Salix glauca *and its cells and vessels. Blue parts are lignified (bark and tension wood) 6100x magnified. Photo: J. Lehejček.*

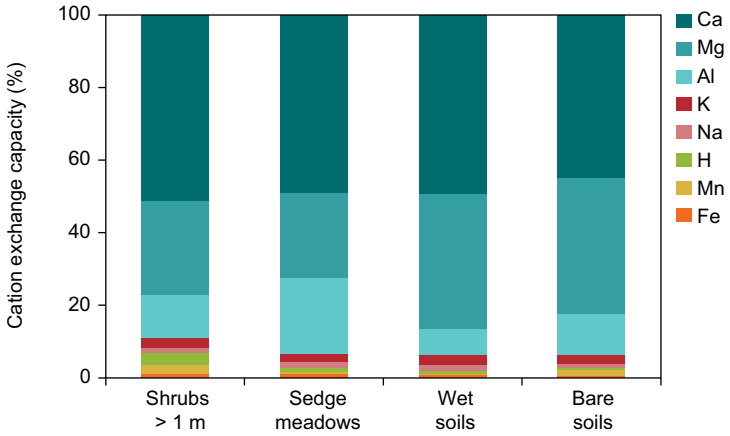

Figure 6.5. Average cation exchange capacity for particular vegetation types.

cell sizes, vessel sizes, cell wall thicknesses) were measured using programme WinCell. Above mentioned parameters are confronted with climate data from a nearby meteorological station. Those parameters, which show the best correlation with climate, are used to indirectly prolong the record of climate development.

Soil properties in the Kobbefjord in relation to vegetation cover and exposition were studied on twenty plots of 5×5 m. They were chosen to include variety of altitudes, slopes, aspects and characteristic vegetation types. The following vegetation types were mapped: (a) shrub vegetation up to 100 cm in height (b) wet soils along streams (c) meadows with sedge vegetation (d) bare soils with scattered cushion plants. One mixed soil sample from each plot was taken (a horizon 0-10 cm; b horizon if available) and plots were subdivided into twenty-five 1×1 m to map the dominant species. Mixed soil samples were analysed for pH, exchangeable cations, exchangeable acidity and major inorganic anions. Expected results should examine an influence of relief and vegetation on the soil properties, especially on cation exchange capacity, percent base saturation and quantity of negatively charged ions.

Similar research is currently undertaken in Svalbard at the Czech Polar Station in Petuniabukta. This season we will work on the border of Russia and Norway at the coast of Barents Sea. Such three field campaigns should cover key locations of Northern Atlantic with substantial shift from maritime to continental climate. Such complex study should suggest drivers, links, and implications, which might have led to the Late Holocene climatic changes with the consequences for west and mid-European climate.

Funding received from INTERACT.

6.4 MIBIPOL: ecological and evolutionary constraints on microbial biodiversity in lake ecosystems – a bipolar comparison

Elie Verleyen, Pieter Vanormelingen, Dagmar Obbels, Otakar Strunecky, Josef Elster, Annick Wilmotte, Koen Sabbe and Wim Vyverman

During summer 2013, microbial mats were sampled in about 80 lakes near Nuuk (West Greenland) and Zackenberg (Northeast Greenland). Additional live samples were taken from temporary ponds, small (melt water) streams and seepages. These campaigns were carried out in the framework of the INTERACT project MIBIPOL, which entails collaboration between the universities of Ghent and Liège (Belgium) and the Centre for Polar Ecology (Czech Republic). MIBIPOL aims at comparing and quantifying the differences in the biodiversity and community structure of bacteria, cyanobacteria and micro-eukaryotes in microbial mats from Arctic and Antarctic lakes using state-of-the-art technologies. The underlying rationale of the project is to test the traditional view that because of unlimited dispersal, most polar micro-organisms will display bipolar distributions. This view requires critical revision as there is growing evidence of dispersal limitation and endemism in these organisms. We therefore hypothesize that given the higher connectivity of Arctic

Figure 6.6 Microbial mat from lake between Nuuk and the Kobbefjord basis (June 2013, 64°12'08.1"N, 51°34' 3.9"W). Photo: Koen Sabbe.

Figure 6.7 Sampling lake sediments with the UWITEC corer near Kapisillit (July 2013, 64°21'18.4"N, 50°08'16.1"W). Photo: Koen Sabbe.

regions microbial communities will be relatively diverse, while the more isolated AntArctic communities will be species-poor and dominated by endemic species.

We sampled a total of 43 lakes near Nuuk (26 in the Nuuk/Kobbefjord area, 17 from the Kapisillit area), and 36 lakes near Zackenberg (20 in the lower Zackenberg valley area, 10 around Daneborg and six in the Kap Ehrenberg area). Microbial mats were sampled using a UWITEC corer from deeper parts of the lake and from the littoral zone. In addition, we also took water samples for limnological (pH, conductivity, temperature and dissolved oxygen) and nutrient analyses, and filters (0.22 µm GSWP) for molecular-genetic analysis of the pelagic microbial communities. Live samples were taken to isolate strains and establish cultures. The microbial mat and water samples will be analyzed in 2014 using high-throughput sequencing technologies (Illumina MiSeq). In addition, isolates were established that will be used for multigene molecular-phylogenetic and ecophysiological characterization and DNA barcoding. Special attention was paid to some known cryptic species complexes and allegedly bipolar taxa. To date, approximately 40 diatom isolates from each area were established for further study in Ghent University. A few tens of these belong to the *Eunotia bilunaris/flexuosa* species complex, for which we already have molecular data on 15 lineages from warm to cold temperate climates. These were selected for further molecular-phylogenetic characterization. All data will then be compared with results obtained within ongoing AntArctic projects and stored in open access archives.

6.5 Population and assemblage-based study of Arctic spiders (Araneae): first results from Kobbefjord

Julien Pétillon, Cyril Courtial and Philippe Vernon

The SPACEWOLF project (Spatial gradients in physiological adaptation and life history variation in Arctic wolf spiders, INTERACT founding) aims at (i) increasing the knowledge of ground-active arthropod (mainly spiders) ecology, and at (ii) investigating the effects of eleva-

Figure 6.8 Picture of a pitfall trap at 200 m a.s.l. (north-facing slope). Photo: Cyril Courtial.

tion and latitude on the fitness of wolf spiders (Lycosidae). After Iceland and Faroe Islands in 2012, this second year of founding targeted a low Arctic site (Kobbefjord), before a high Arctic site (Zackenberg) in 2014.

In Kobbefjord, we set up 30 yellow pitfall traps (figure 6.8) operating from 4-9 July 2013 in five stations up to 400 m a.s.l. Unfortunately, we could not find a proper place for the 400 m north-facing treatment (too rocky), resulting in 0 m, 200 m and 400 m south-facing, 200 m and 280 m north-facing stations (all equipped with temperature loggers). All arthropods caught by pitfall trapping were sorted to order or family levels, and all the spiders by trapping and hand-collecting were identified to species level.

Pitfall trapping yielded the collection of 1007 arthropods (and 2 annelids), dominated by Acari (40% of individuals caught), followed by *Araneae, Diptera, Coleoptera, Collembola, Hemiptera* and *Opiliones* (24%,

*Table 6.3 Spider species found in Kobbefjord during July 2013 (Number of males/Number of females, Underlined: immature) from 0 to 400 m a.s.l. (*hand-collected at an unknown altitude, n: north-facing slope, s: south-facing slope). 1: species only found by hand-collecting, 2: species only found by pitfall trapping, 3: species found by both methods.*

	*	0	200n	200s	280n	400s
Araneidae						
Hypsosinga groenlandica[3] (Simon, 1889)	2/2	4/1			1/0	1/0
Dictynidae						
Dictyna major[1] (Menge, 1869)	4/3					
Gnaphosidae						
Haplodrassus sp.[2]		1		2		0/1
Hahniidae						
Hahnia glacialis[3] (Sørensen, 1898)	1/1		0/2			
Linyphiidae						
Agyneta jacksoni[2] (Braendegaard, 1937)		1/1	0/1	2/1		
Dismodicus decemoculatus[1] (Emerton, 1882)	1/2					
Erigone sp.[1]	0/1					
Erigone whymperi[1] (O.P.-Cambridge, 1877)	1/2					
Oreoneta frigida[1] (Thorell, 1872)	0/2					
Islandiana princeps[1] (Braendegaard, 1932)	0/2					
Mecynargus morulus[2] (O.P.-Cambridge, 1873)			0/1			0/2
Mecynargus paetulus[2] (O.P.-Cambridge, 1875)						1/0
Pelecopsis mengei[2] (Simon, 1884)						0/2
Pocadicnemis americana[3] (Millidge, 1976)	0/1			0/1	0/1	
Scotinotylus evansi[1] (O.P.-Cambridge, 1894)	0/1					
Tiso aestivus[2] (L. Koch, 1872)					0/1	
Wabasso quaestio[2] (Chamberlin, 1949)		2/0				
Walckenaeria clavicornis[2] (Emerton, 1882)		0/1				0/1
Lycosidae						
Arctosa sp.[2] (cf. alpegina)			1			
Pardosa furcifera[3] (Thorell, 1875)	3/5	29/5/1	1	4/1/1		
Pardosa groenlandica[3] (Thorell, 1872)	0/1	1/0	4			2/3/2
Pardosa hyperborea[3] (Thorell, 1872)	2/1	1/1		49/17/3	7/2/1	65/16/2
Philodromidae						
Thanatus Arcticus[3] (Thorell, 1872)	0/1			1/0		2/0
Xysticus durus[2] (Sørensen, 1898)						0/1
Theridiidae						
Enoplognatha intrepida[1] (Sørensen, 1898)	0/4			0/1		0/1

Figure 6.9 Picture of Pardosa hyperborea *female carrying a cocoon. Photo: Cyril Courtial.*

22%, 7%, 3%, 2% and 1% of all individuals caught, respectively), and *Hymenoptera, Lepidoptera, Psocoptera* and *Thysanoptera* (all with less than 10 individuals). We collected a total of 297 spiders by traps and by hand, representing 25 species (including two not yet identified species: table 6.3). Eight species were collected by hand only, 10 species only by traps and seven species by both methods. Surprisingly, most spider species were found at the lowest and highest altitudes. At least one species, *Pelecopsis mengei*, is new to Greenland. This discovery is not surprising given the HolArctic distribution of that species, whereas the report of the related, but PaleArctic, *P. parallela* in Disco (West coast of Greenland) is more questionable (which was underlined by Marusik et al. 2006, who could not find the individuals).

For the fitness experiment, it first came out that two lycosid species were abundant and carrying cocoons during our stay in Kobbefjord: *Pardosa hyperborea* (figure 6.9) and *P. furcifera* (the latter being larger, with a Y-shaped drawing on the cephalothorax, and preferring wetter places). We also collected the large *P. groenlandica*, but at low numbers and in stony places only. The following design was performed: 1) comparison of body size and fitness between *P. furcifera* and *P. hyperborea* at low altitude (replicated design, 60 females per species), and 2) variation in body size and fitness of *P. hyperborea* along an altitudinal gradient (0, 50, 100, 150 and 200 m, 30 females at each altitude).

6.6 Serial sectioning applied to tundra shrubs for dendrochronological analyses

Agata Buchwal and Grzegorz Rachlewicz

The value of shrubs for dendrochronological analyses, both dendroclimatological and dendroecological reconstructions, dependents on a successful cross-dating of a single plant. For studying the growth relations of Arctic shrubs to climate and other environmental factors reliable data have to be used. Our findings from studies on *Salix polaris* from Central Spitsbergen show that there is high intra- and inter-plant variability in the annual growth pattern of shrubs, represented by high (i.e. one quarter) missing and wedging ring ratio (Buchwal et al. 2013).

Funded by INTERACT Transnational Access we were able to conduct a field work in the frame of the project titled: Serial sectioning applied to tundra shrubs for dendrochronological analyses in the high and low Arctic locations (DENDRO 2). The project aims to investigate intra-plant growth on dendrochronological scale. Specifically, we aim to investigate the annual radial increments and the proportion of partially and completely missing rings in the above ground and below ground parts of the shrub in order to determine whether and how intra-plant growth allocation varied with a changing climatic conditions.

Our study was conducted in August 2013 and focused on three shrub species which commonly grow in the Kobbefjord area, namely *Betula nana* (sampled: 23 shrubs, 153 cross-sections), *Empetrum nigrum* (26 shrubs, 190 cross-sections) and *Juniperus communis* (18 shrubs, 86 cross-sections). The sections were derived from stems (i.e., 50% of a total cross-sections), main roots and tap roots (22%) and two to three main above-ground shoots (28%).

The shrub sampling procedure consisted of serial sectioning (Kolishchuck 1990) of entire plants (figure 6.10a) within minimum two chosen locations differentiated based on the geomorphic settings of the site (i.e. valley bottom, upper marine terraces). The shrub sampling strategy was supplemented by an examination of lithological properties of plants growth substratum. Together with shrubs sampling we extracted 21 samples of surface

Figure 6.10 (A) Serial sectioning of one Empetrum nigrum *individual consisting of 13 specimens taken from the main root, stem and branches; (B) a* Juniperus communis *stem part presenting very eccentric growth form and (C) a selective radial growth marked on the cross-sectional cut in the series of wedging rings with a rotten pith visible on the bottom.*

and subsurface sediments to determine the physical and chemical characteristics, which might further help to determine the environmental conditions of shrubs growth.

Current laboratory work consists of: (i) preparation of micro-sections of shrubs' specimens by using a sledge microtome; (ii) performing image analyses of micro-sections using WinCell software and ring-width measurement (in minimum four radii per section) supplemented by wood anatomical studies of shrubs radial growth; (iii) cross-dating of growth curves from different parts of the plant (below ground versus above ground parts), presenting a single plant tree-ring growth series; cross-dating of growth curves between the plants in order to present a site chronologies of each species for Kobbefjord area.

First results from our dendrochronological analyses reveal that the age of shrubs is promising for more than a century-long retrospective analyses of tree-ring growth of most commonly growing shrubs in the Kobbefjorden area. Although some of the species (esp. *Juniperus communis)* presents very eccentric growth (figures 6.10b, 6.10c and 6.11a), we found some specimens being older than 200 years (figure 6.12). The oldest parts of dwarf birch individuals were often rotten and therefore not useful in further analyses. Nevertheless, one of

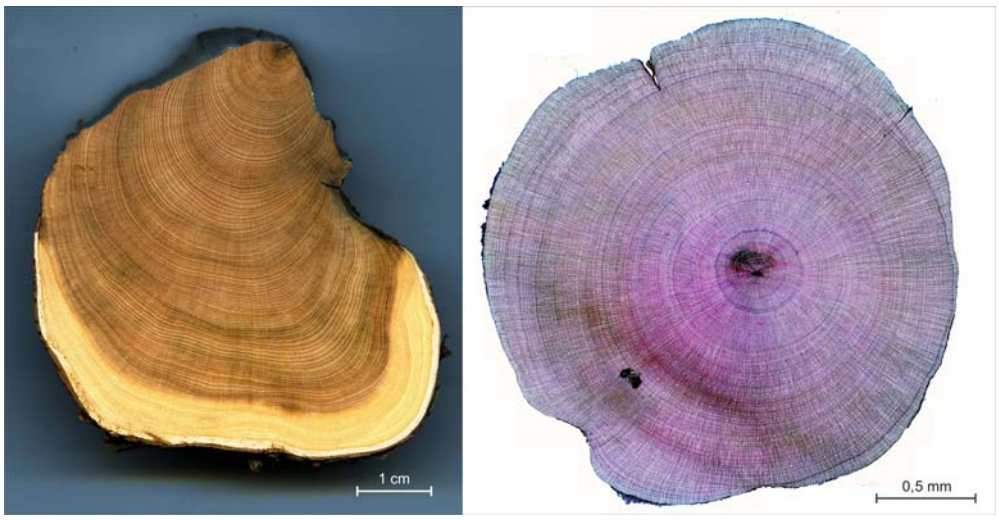

Figure 6.11 An example of shrubs sections analyzed: (left) Eccentric Juniperus communis *stem cross-section (a polished disc) with 229 tree-ring widths (TRW) measured (1785-2013); (right)* Betula nana *stem specimen (a stained micro-section of 20-30 µm thickness) from Kobbefjord with 114 tree-ring widths (TRW) measured (1900-2013), mean TRW= 98 µm (min TRW=12 µm; max TRW=290 µm).*

the oldest healthy specimen of *Betula nana* was dated for being more than 100 years old (figure 6.11b). The determined on the spot a weight moisture content in soil revealed variation in the range from 0.6 to 17.2%, showing high diversity in water availability between shrub sampling sites, i.e. from dry habitats undergoing transformation into moist sites. Mean radial growth and missing rings ratio comparisons between the sites will help us to verify if tree-ring growth of investigated shrubs species is water-limited.

Final stage of Arctic shrubs investigation will focus on a correlation of shrub chronologies and anatomical parameters with accessible climatic data from the NERO (Kobbefjord) station and Nuuk. Through climate-growth relationship analyses we will be able to correlate different factors like temperature with the annual growth rate of shrubs to determine the dominant factor or a group of factors, which stimulate or limit the intra-plant growth of Arctic shrubs. Moreover, a correlation of obtained chronologies from Eastern and Western Greenland will be performed, in order to determine climate induced and species-specific growth response in the Arctic shrubs zone.

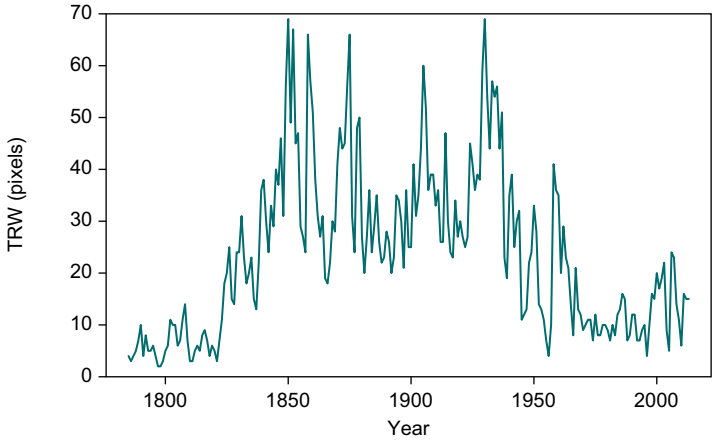

Figure 6.12 Raw ring widths measurements of 229-years old stem part of Juniperus communis *(see figure 6.10a) from Kobbefjord.*

We aim to integrate previously gathered data in Disko Island with those collected in Kobbefjord area and Zackenberg (planned for summer 2014) in order to establish West-East and North-South transect in dendrochronological studies of shrub in Greenland. Comparative studies of the same species from different locations with diverse climatic settings will help us to understand the annual growth allocation in chosen Arctic shrub species. Dendrochronological studies on dwarf shrubs supplemented by detailed wood anatomical analyses might significantly improve our knowledge about ongoing changes in the Arctic.

7 Disturbance in the study area

Maia Olsen

The study area at Kobbefjord is situated approximately 20 km south east of Nuuk and can be reached by boat within half an hour. It is a public area and admittance is free to anyone. Public disturbance falls in the following categories:

- Visits by boat in the bottom, of the fjord – no landing.
- Visits by boats in the bottom of the fjord – the persons take a short walk inland and returns within a few hours or less.
- Visits by boats in the head of the fjord – the persons go on land and spend the night in a tent close to the coast.
- Hiking through the area – there is a hiking route from Nuuk to the inland passing through the area.
- Visits by snowmobile – during winter people visit the area from Nuuk.
- The electrical power transmission line between Nuuk and the hydropower plant in Buksefjord runs through the area.
- Ordinary flights by fixed winged aircrafts passing over the study area in cruising altitude or in ascent or descent to or from Nuuk.
- Helicopter flights at cruising altitude passing over the study area or following the transmission line at low altitude.

There have been only few interactions between visitors in the study area and the different setups and the cabin. On 30 June a small plane landed on the fjord and took off again shortly after. In July a large group of people camped in the area between the cabin and the gas-flux setup for one night, putting up a number of tents. Foxes have been moving and taken pit-fall traps and laid droppings in the pit-fall traps.

The monitoring programme itself has brought disturbance to the area i.e. transportation between Nuuk and the bottom of the fjord, housing of personnel, walking between study plots and around study plots. Especially around the permanent plots on *Empetrum* heath and the fens have signs of wear. Furthermore, the wear around and between the C-flux measuring plots has become increasingly noticeable. The area close to the cabin, where most visitors put up their tents, is showing signs of erosion, as is the trail between the boat landing and the cabin.

Transportation between Nuuk and the study site in Kobbefjord has been conducted on an irregular basis, but during most of the season, there was transportation two to three times a week (Tuesdays and Thursdays, or Mondays, Wednesdays, and Fridays). During most of the season, the cabin was used temporarily by two to four persons. On a few occasions more than 10 people stayed overnight for one to two nights, in tents close to the cabin. This year also had several groups staying in the area for prolonged periods of time, thus there were several instances when staying in tents were necessary.

Walking around the study plots has had a wearing effect on the vegetation and it should be considered to mark permanent trails between reseach house and study plots. Portable boardwalks will be used in the future, especially around the C-flux measuring plots.

In conclusion, it is estimated that monitoring activities only had minor impact on the vegetation and terrain.

8 Logistics

Henrik Philipsen

In 2013, Greenland Institute of Natural Resources (GINR) took care of the logistics related to Nuuk Basic in the Kobbefjord area.

The 2013 field season in the Kobbefjord area started 10 January and continued until 11 December. During this period 47 scientists and logisticians spent 534 and 36 'man-days' in the study area, respectively.

The winter 2012/2013 was not particularly hard with ice two to four kilometres out from the bottom of the fjord during the period 27 February to 4 April. It was possible to sail to the bottom of Kobbefjord from 22 May to 17 October. From 22 October the ice was back in the fjord and an 'airboat' from GINR was used together with 'Erisaalik' until 11 December.

GINR carried out transportation of staff, technicians, scientists and guests from Nuuk to the Kobbefjord area with the boats 'Erisaalik' and 'Aage V. Jensen II Nuuk'. The total number of sailing days to the Kobbefjord area used by logisticians, BioBasis, GeoBasis and ClimateBasis were 74. MarineBasis used 28 sailing days to go to the study areas in Kobbefjord and Godthåbsfjord.

In 2013, scientists spend 328 'bed nights' in the research house and in tents in the Kobbefjord area. In Nuuk, Nuuk Basic scientists were accommodated in the annex of GINR, with 450 'bed nights'.

The research house and the generator hut were tar painted and minor repair work was carried out.

Water for drinking and other purposes were taken from the nearby river.

Electrical power was provided by two portable gasoline generators (3 and 4 kW) and a 5 kW diesel generator. A new 3.5 kW gasoline generator were bought in 2013.

Communication to/from Nuuk was made by Irridium satellite telephones, while local communication within the study area was by portable VHF-radios. Two new portable VHF-radios were bought, and a long-range stationary VHF-radio was installed in the research house.

Fuel consumption for the generators was 50 litres of diesel and 771 litres of gasoline. Fuel consumption for the oven in the research house was 100 litres diesel.

Freshwater consumption was 15.000 litres.

A drainpipe for grey household water was connected from early June until late September.

All garbage (450 kg) was removed by ship to Nuuk during the season.

Six helicopter trips were made by Air Greenland to the area.

13 May: Three scientists from Asiaq – Greenland Survey made a trip to a nearby glacier.

26 June: Three technicians from Asiaq – Greenland Survey carried out maintenance work at the climate station.

2 August: Ulrich Gosewinkel, Department of Environmental Science, Aarhus University, made a trip to a nearby mountain to pick up equipment.

12 August: Torben Lauridsen, Department of Bioscience, Aarhus University and his group were picked up at Langsø and flown to the research house.

3 September: Three scientists from Asiaq – Greenland Survey made a trip to the M1000 station at the nearby mountain.

4 October: Three scientists from Asiaq – Greenland Survey made a trip to a nearby glacier and the M1000 station at the nearby mountain.

The study area in Kobbefjord was during 2013 visited by several honourable guests (see chapter 10).

9 Acknowledgements

MarineBasis wish to acknowledge the crew onboard the R/V Sanna for their valuable assistance during this year's May Cruise. We also thank Thomas Krogh, Jens Weinell, Louise Mølgaard, Gabriela Garcia, Rebecca Scheuerlein, Maia Olsen, Lars Heilmann, Flemming Heinrich, Kunuk Lennert, Sofie R. Jerimiassen, Signe Jeremiassen, Jørgen Sethsen, Andrzej Witkowski and Marek Zajaczkowski for field and technical assistance. We would also like to acknowledge Paul Batty, Morten S. Frederiksen, Anna Haxen, Winnie Martinsen, Peter B. Christensen, Carsten Egevang, Bo Bergstrøm and Ditte M. Mikkelsen for their contribution to the programme in previous years.

10 Personnel and visitors

Compiled by Lillian Magelund Jensen

Agate Buchwal, Adam Mickiewicz University, Poland
Albin Brönmark, Photographer, Sweden
Andreas Schramm, Department of Bioscience, Aarhus University, Denmark
Anker Christensen, Department of Geosciences and Natural Resource Management, University of Copenhagen, Denmark
Anne-Laure Ferchaud, Department of Bioscience, Aarhus University, Denmark
Anton Bøge Holm, Department of Geosciences and Natural Resource Management, University of Copenhagen, Denmark
Birger Ulf Hansen, Department of Geosciences and Natural Resource Management, University of Copenhagen, Denmark
Birgit Olesen, Department of Bioscience, Aarhus University, Denmark
Bjarne Jensen, Department of Bioscience, Aarhus University, Denmark
Carl Isaksen, Greenland Institute of Natural Resources, Greenland
Cathrine Chapman, Journalist, Canada
Cyril Courtial, Université de Rennes, France
Dagmar Obbels, Department of Biology, Ghent University, Belgium
Daniel Nyvlt, Czech Geology Survey, Czech Republic
Emilia Söelund, Journalist, Sweden
Ewan Shillard, Aarhus University, Denmark
Feizhou Zen, Aarhus University, Denmark
Flemming Heinrich, Greenland Institute of Natural Resources, Greenland
Gaba Egede, Greenland Institute of Natural Resources, Greenland
Gróa Pétursdóttir, Marine Research Institute, Iceland
Guðrún Finnbogadóttir, Marine Research Institute, Iceland
Grzegorz Rachlewicz, Adam Mickiewicz University, Poland
Heidi Sørensen, Greenland Institute of Natural Resources, Greenland
Helge Ro-Poulsen, Department of Biology, University of Copenhagen, Denmark
Helle Gosewinkel, Department of Environmental Science, Aarhus University, Denmark
Henrik Lund, Greenland Institute of Natural Resources, Greenland
Henrik Philipsen, Greenland Institute of Natural Resources, Greenland
Ida Vedel-Petersen, Department of Biology, University of Copenhagen, Denmark
Ivali Lennert, Greenland Institute of Natural Resources, Greenland
Jacob Abermann, Asiaq – Greenland Survey, Greenland
Jakob Sievers, Department of Bioscience, Aarhus University, Denmark
Jens Gammeltoft, Department of Geosciences and Natural Resource Management, University of Copenhagen, Denmark
Jens Gottlieb, Asiaq – Greenland Survey, Greenland
Jesper Olsen, Department of Physics and Astronomy, Aarhus University, Denmark
Jiri Lehejcek, Česká zemědělská univerzita v Praze, Czech Republic
John Renner Hansen, Dean, University of Copenhagen, Denmark
Josephine Nymand, Greenland Institute of Natural Resources, Greenland
Julien Pétillon, Université de Rennes, France
Jørgen Sethsen, Greenland Institute of Natural Resources, Greenland
Kathrine Lund Olsen, Greenland Institute of Natural Resources, Greenland
Katrine Raundrup, Greenland Institute of Natural Resources, Greenland
Keld H. Svendsen, Asiaq – Greenland Survey, Greenland
Kim Mouritsen, Department of Bioscience, Aarhus University, Denmark
Kisser Thorsøe, Asiaq – Greenland Survey, Greenland
Koen Sabbe, Department of Biology, Ghent University, Belgium

Kristine Arendt, Greenland Institute of Natural Resources, Greenland
Kunuk Lennert, Greenland Institute of Natural Resources, Greenland
Kurt Møller Pedersen, University of Greenland, Nuuk, Greenland
Lars Heilmann, Greenland Institute of Natural Resources, Greenland
Laurits M. Bernitt, Asiaq - Greenland Survey, Greenland
Lene Holm Kleist, Greenland Institute of Natural Resources, Greenland
Lise-Lotte Sørensen, Department of Bioscience, Aarhus University, Denmark
Lorenz Meire, Department of Biology, Ghent University, Belgium
Louise Holm Christensen, Asiaq – Greenland Survey, Greenland
Magnus Kramshøj, University of Copenhagen, Denmark
Magnus Lund, Department of Bioscience, Aarhus University, Denmark
Maia Olsen, Greenland Institute of Natural Resources, Greenland
Majbritt Westring Sørensen, Asiaq - Greenland Survey, Greenland
Malene Simon, Greenland Institute of Natural Resources, Greenland
Malik Naamansen, Asiaq – Greenland Survey, Greenland
Marcin Jackowicz-Korczynski, Department of Physical Geography and Ecosystems Analysis, Lund University, Sweden
Maria L. Burup, Department of Geosciences and Natural Resource Management, University of Copenhagen, Denmark
Marion Jaussi, Department of Bioscience, Aarhus University, Denmark
Marti Pujolar, Department of Bioscience, Aarhus University, Denmark
Mathias Madsen, Department of Geosciences and Natural Resource Management, University of Copenhagen, Denmark
Mathilde Borg Dahl, Department of Biology, University of Copenhagen, Denmark
Michael Magee, Greenland Institute of Natural Resources, Greenland
Michael Møller Hansen, Department of Bioscience, Aarhus University, Denmark
Mikhail Mastepanov, Department of Physical Geography and Ecosystems Science, Lund University, Sweden
Naja Christensen, Greenland Institute of Natural Resources, Greenland
Naja O. Lennert, Greenland Institute of Natural Resources, Greenland
Ole Geertz-Hansen, Greenland Institute of Natural Resources, Greenland
Paaviaaraq Ludvigsen, Greenland Institute of Natural Resources, Greenland
Per Hangaard, Asiaq – Greenland Survey, Greenland
Peter Brusvang, Department of Biology, University of Copenhagen, Denmark
Peter Hegelund, Greenland Institute of Natural Resources, Greenland
Peter Stief, Max Planck Institute for Marine Microbiology, Germany
Petra Policka, Česká Zemědělská univerzita v Praze, Czech Republic
Rasmus Egede, Asiaq – Greenland Survey, Greenland
Rebecca Dorph Berg, Greenland Institute of Natural Resources, Greenland
Scott Hillier, Journalist, Australia
Signe Jeremiassen, Greenland Institute of Natural Resources, Greenland
Sofie Ruth Jeremiassen, Greenland Institute of Natural Resources, Greenland
Stine Højlund Pedersen, Department of Bioscience, Aarhus University, Denmark
Susanne Sass Hvass, Greenland Institute of Natural Resources, Greenland
Søren Post, Greenland Institute of Natural Resources, Greenland
Thomas Skotte, Asiaq – Greenland Survey, Greenland
Tina S. Temkiv, Department of Bioscience, Aarhus University, Denmark
Tor Lund, Nuuk, Greenland
Torben L. Lauridsen, Department of Bioscience, Aarhus University, Denmark
Torben Røjle Christensen, Department of Physical Geography and Ecosystems Science, Lund University, Sweden and Arctic Research Centre, Aarhus University, Denmark
Ulrich Gosewinkel, Department of Environmental Science, Aarhus University, Denmark

Eleven Government officers from the Nordic Council of Ministers, Climate and Air Pollution Group (KoL)
Nineteen PhD students and six teachers from the "NordFrost travelling workshop/PhD training course"
Nine journalist students, University of Greenland, Greenland
One carpenter, to change broken window
Six PhD students from the IGERT-programme, Dartmouth College, US

Twenty-one high school students and one teacher from GU, Nuuk, Greenland
Two painters, for painting the cabin

Further contributors to the annual report

Aili L. Labansen, Greenland Institute of Natural Resources, Greenland
Andreas Westergaard, Department of Geosciences and Natural Resource Management, University of Copenhagen, Denmark
Annick Wilmotte, Centre for Protein Engineering, University of Liège, Belgium
Anja Retzel, Greenland Institute of Natural Resources, Greenland
AnnDorte Burmeister, Greenland Institute of Natural Resources, Greenland
Diana Krawczyk, Greenland Institute of Natural Resources, Greenland
Dorte Krause-Jensen, Department of Bioscience, Aarhus University, Denmark
Dorthe Petersen, Asiaq-Greenland Survey, Greenland
Elie Verleyen, Laboratory of Protistology and Aquatic Ecology, Department of Biology, Ghent University, Belgium
Elin Jørgensen, Department of Bioscience, Aarhus University, Denmark
Helena Wirta, Department of Agricultural Sciences, University of Helsinki, Finland
Henning Petersen, Mols Laboratory, Natural History Museum, Denmark
John Mortensen, Greenland Institute of Natural Resources, Greenland
Jonathan N.K. Petersen, Asiaq – Greenland Survey, Greenland
Josef Elster, Centre for Polar Ecology, Department of Ecosystem Biology, University of South Bohemia, Czech Republic
Kristian Albert (not affiliated)
Martin E. Blicher, Greenland Institute of Natural Resources, Greenland
Mikael K. Sejr, Department of Bioscience, Aarhus University, Denmark
Mikkel P. Tamstorf, Department of Bioscience, Aarhus University, Denmark
Niels Martin Schmidt, Department of Bioscience, Aarhus University, Denmark
Núria Marbà, Department of Bioscience, Aarhus University, Denmark
Ole Geertz-Hansen, Greenland Institute of Natural Resources, Greenland
Otakar Strunecky, Centre for Polar Ecology, Department of Ecosystem Biology, University of South Bohemia, Czech Republic
Paul Henning Krogh, Department of Bioscience, Aarhus University
Peter Aastrup, Department of Bioscience, Aarhus University
Peter Gjelstrup, Knebel, Denmark
Philippe Vernon, Université de Rennes, France
Pieter Vanormelingen, Laboratory of Protistology and Aquatic Ecology, Department of Biology, Ghent University, Belgium
Rasmus Nygaard, Greenland Institute of Natural Resources, Greenland
Søren Rysgaard, University of Manitoba, Canada and Arctic Research Centre, Aarhus University, Denmark
Tenna Boye, Department of Bioscience, Aarhus University, Denmark
Thomas Juul-Pedersen, Greenland Institute of Natural Resources, Greenland
Tomas Roslin, Department of Agricultural Sciences, University of Helsinki, Finland
Wim Vyverman, Laboratory of Protistology and Aquatic Ecology, Dept. Biology, Ghent University, Belgium
Zdenek Gavor, Department of Bioscience, Aarhus University, Denmark

Publications

Compiled by Lillian Magelund Jensen

Scientific papers

Arendt, K.E., Juul-Pedersen, T., Mortensen, J., Blicher, M.E. and Rysgaard, S. 2013. A five years study of seasonal patterns in me-sozooplankton community structure in a sub-Arctic fjord reveals dominance of *Microsetella norvegica* (Crustacea, Copepoda). Journal of Plankton Research 35: 105-120.

Blicher, M.E., Sejr, M.K. and Høgslund, S. 2013. Population structure of *Mytilus edulis* in the intertidal zone in a sub-Arctic fjord, SW Greenland. Marine Ecology Progress Series 487:89-100.

Ekici, A., Beer, C., Hagemann, S., Boike, J., Langer, M. and Hauck, C. 2014. Simulating high-latitude permafrost regions by the JSBACH terrestrial ecosystem model. Geoscientific Model Development 7: 631-647.

Kaartokallio, H., Søgaard, D., Norman, L., Rysgaard, S., Tison, J.-L., Delille, B. and Thomas, D.N. 2013. Short- term variability in bacterial abundance, cell properties, leucine and thymidine incorporation in sub-Arctic sea ice. Aquatic Microbial Ecology 71: 57-73.

Kjeldsen, K.K., Mortensen, J., Kjær, K.H., Bendtsen, J., Lennert, K. and Rysgaard, S. 2014. Ice-dammed lake drainage cools raises surface salinities in a tidewater outlet glacier fjord, West Greenland. Journal of Geophysical Research Earth Surface. Doi:10.1002/2013JF003034.

Mbufong, H.N., Lund, M.1, Aurela, M., Christensen, T.R.1, Eugster, W., Friborg, T., Hansen, B.U., Humphreys, E.R., Jackowicz-Korczynski, M., Kutzbach, L., Lafleur, P.M., Oechel, W.C., Parmentier, F.J.W., Rasse, D.P., Rocha, A.V., Sachs,T., van der Molen, M.M. and Tamstorf, M.P. 2014. Assessing the spatial variability in peak season CO_2 exchange characteristics across the Arctic tundra using a light response curve parameterization. Biogeosciences Discussion 11: 6419-6460.

Mortensen, J., Bendtsen, J., Motyka, R.J., Lennert, K., Truffer, M., Fahnestock, M. and Rysgaard, S. 2013. On the seasonal freshwater stratification in the proximity of fast-flowing tidewater outlet glaciers in a sub-Arctic sill fjord. Journal of Geophysical Research Oceans 118: 1382-1395.

Parmentier, F.J.W., Christensen, T.R., Sørensen, L.L., Rysgaard, S., McGuire, A.D., Miller, P.A. and Walker, D.A. 2013. The impact of a lower sea-ice extent on Arctic greenhouse-gas exchange. Nature Climate Change 3: 195-202.

Rysgaard, S., Søgaard, D., Cooper, M., Pucko, M., Lennert, K., Papakyriakou, T.N., Wang, F., Geilfus, N.X., Glud, R.N., Ehn, J., McGinnes, D., Attard, K., Siverts, J., Deming, J.W. and Barber, D. 2013. Ikaite crystal distribution in Arctic winter sea ice and its implications for CO_2 system dynamics. The Cryosphere 7: 1-12.

Søgaard, D.H., Thomas, D., Rysgaard, S., Glud, R.N., Norman, L., Kaartokallio, H., Juul-Pedersen, T. and Geilfus, N.-X. 2013. The relative contributions of biological and abiotic processes to the carbon dynamics in subArctic sea ice during the transition from winter to spring. Polar Biology. Doi: 10.1007/s00300-013-1396-3.

Westergaard-Nielsen, A., Lund, M., Hansen, B.U. and Tamstorf, M.P. 2013. Camera derived vegetation greenness index as proxy for gross primary production in a low Arctic wetland area. ISPRS Journal of Photogrammetry and Remote Sensing 86: 89-99.

Zamora-Terol, S., Nielsen, T.G and Saiz, E. 2013. Plankton community structure and role of *Oithona similis* on the western coast of Greenland during the winter-spring transition. Marine Ecology Progress Series 483: 85-102.

Reports

Jensen, L.M., Rasch, M. and Schmidt, N.M. (eds.) 2013. Nuuk Ecological Research Operations, 6th Annual Report, 2012. Aarhus University, DCE – Danish Centre for Environment and Energy. 92 pp.

Rysgaard, S., Pucko, M. and Mundy, C.J. 2013. Arctic geomicrobiology and climate change. ArcticNet Annual Progress Report (2012-13). 18 pp.

Presentation at symposiums, workshops, meetings and conferences

Arendt, K.E. 2013. Are small copepods important? GCRC 4th Annual Meeting, 13-14 November, Nuuk, Greenland.

Attard, K., Glud, R.N., McGinnis, D. and Rysgaard, S. 2013. Aquatic oxygen eddy-covariance measurements in Arctic and Sub-Arctic environments – a case study from Godthåbsfjord, SW Greenland. GRS/GRC for Polar Marine Science, 9-15 March, Ventura, California, USA.

Bendtsen, J., Mortensen, J., Lennert, K. and Rysgaard, S. 2013. Cirkulation og energitransport i Godthåbsfjorden og påvirkning fra intermediære vandmasser på issmelt. 17. Danske Havforskermøde, 21 January, Roskilde, Denmark.

Bendtsen, J., Mortensen, J., Lennert, K. and Rysgaard, S. 2013. Modelling of intermediate water formation and subsurface heat transport in Godthåbsfjord. U. S. CLIVAR international workshop on understanding the response of Greenland's marine terminating glaciers to oceanic and atmospheric forcing. 4-7 June, Boston, USA.

Christensen, T.R., Lund, M., Mastepanov, M., Rysgaard, S., Tamstorf, M.P., Sejr, M.K. and Juul-Pedersen, T. 2013. Arctic carbon storage and greenhouse gas exchange – a measurement based integrated assessment of two coupled terrestrial and marine ecosystems. Pergamon Symposium, GEOMAR Helmholtz Centre for ocean research, 5-7 November, Kiel, Germany.

Juul-Pedersen, T., Arendt, K.E., Mortensen, J., Blicher, M., Krawczyk, D. and Rysgaard, S. 2013. A 6-year study of pelagic primary production in a freshwater influenced sub-Arctic fjord system – with a view to the past. 45th International Liège Colloquium on Ocean Dynamics, 13-17 May, Liège, Belgium.

Juul-Pedersen, T., Arendt, K.E., Mortensen, J., Blicher, M. and Rysgaard, S. 2013. Pelagic Primary Production in a freshwater influenced sub-Arctic fjord system – with a view to the past. Arctic Frontiers, 20-25 January, Tromsø, Norway.

Meire, L., Sørensen, H.L., Petersen, T.J., Thamdrup, B., Rysgaard, S., Glud, R.N. and Meysman, F. 2013. Seasonal study of carbon dynamics in a subArctic fjord (Kobbefjord, Greenland). GRS/GRC for Polar Marine Science, 9-15 March, Ventura, USA.

Mortensen, J., Bendtsen, J., Rysgaard, S. and Lennert, K. 2013. Circulation and heat sources for glacial melt in a sub-Arctic sill fjord (Godthåbsfjord). U.S. CLIVAR international workshop on understanding the response of Greenland's marine terminating glaciers to oceanic and atmospheric forcing. 4-7 June, Boston, USA.

Ribeiro, S., Ellegaard, M., Andersen, T.J., Kuijpers, A., Mikkelsen, N., Pedersen, N.N. and Rysgaard, S. 2013. Climate variability in the Godthåbsfjord ares (SW Greenland) since the little ice age: a multiproxy approach. 9-13 December, San Francisco, USA.

Rysgaard, S. 2013. Arctic Science Partnership infrastructure. Logistic workshop on research infrastructure in the Arctic. Danish Technical University, 7 November, Denmark.

Rysgaard, S. 2013. Arctic Science Partnership Research infrastructure. ERA-Can II Rome Symposium on Arctic and Marine Research Infrastructure Embassy of Canada, 19-20 September, Rome, Italy.

Rysgaard, S. 2013. Arctic geomicrobiology and climate change. Canada Excellence Research Chairs presentations. 13 May, University of Alberta, Canada.

Rysgaard, S. 2013. Biogeochemistry and sea ice – an overlooked factor in the carbon cycle? ArcticNet seminar course on climate change and the Arctic marine system. University of Manitoba, 20 March, Winnipeg, Canada.

General information

Juul-Pedersen, T. 2013. TV Documentary Interview to 'Melting Point Greenland' (National Emmy Award Nominee), 18 June, Nuuk, Greenland.

Juul-Pedersen, T. 2013. Greenland Ecosystem Monitoring. Presentation for the Oak Foundation, 24 May, Nuuk, Greenland.

Juul-Pedersen, T. 2013. Greenland Ecosystem Monitoring. Presentation for Rigsrevisionen, 19 February, Nuuk, Greenland.

Mikkelsen, P.S. 2013. Klimaforskning i Grønland. Presentation for Defence Attaché accredited to Denmark, 28 May, Nuuk, Greenland.

Mikkelsen, P.S. 2013. Klimaforskning i Grønland. Presentation for the Oak Foundation, 24 May, Nuuk, Greenland.

Mikkelsen, P.S. 2013. Klimaforskning i Grønland. Presentation for Nuuk Rotary Club, 26 February, Nuuk, Greenland.

Mikkelsen, P.S. 2013. Klimaforskning i Grønland. Presentation for Rigsrevisionen, 19 February, Nuuk, Greenland.

Mikkelsen, P.S. 2013. Klimaforskning i Grønland. Ekstrabladet, 18 April, Nuuk, Greenland.

Mikkelsen, P.S. 2013. Klimaforskning i Grønland. 10 A from Kangillinnguit Atuarfiat, 24 January, Nuuk, Greenland.

Rysgaard, S. 2013. Status of research and education during the first year of Arctic Research Centre, 13 June, Aarhus, Denmark.

11 References

Compiled by Lillian Magelund Jensen

Aastrup, P., Nymand, J., Raundrup, K., Lauridsen, T.L., Krogh, P.H., Schmidt, N.M., Illeris, L. and Ro-Poulsen, H. 2009. Conceptual design and sampling procedures of the biological programme of Nuuk Basic. National Environmental Research Institute, Aarhus University, Denmark. NERI Technical Report No. 745. 77 pp.

ACIA 2005. Impacts of a warming Arctic. In Arctic Climate Impact Assessment. NY, USA, Cambridge University Press. 1042 pp.

Bejder, L. and Dawson, S. 2001. Abundance, residency and habitat utilisation of Hector's dolphins (*Cephalorhynchushectori*) in Porpoise Bay, New Zealand. New Zealand Journal of Marine and Freshwater Research 35: 277-287.

Boye, T.K., Simon, M.J. and Madsen, P.T. 2010. Habitat use of humpback whales in Godthåbsfjord, West Greenland, with implications for commercial exploitation. Journal of the Marine Biological Association of the United Kingdom 90: 1529-1538.

Buchwal A. et al. 2013. Temperature modulates intra-plant growth of *Salix polaris* from a high Arctic site (Svalbard). Polar Biology 36(9): 1305-1318.

Cappelen, John, 2013. Greenland – DMI Historical Climate Data Collection 1873-2012 – with Danish Abstracts, DMI, Technical report 13-04.

CCDB, 2014. CCDB Documents. CCDB Protocols. Biodiversity Institute of Ontario. http://ccdb.ca/resources.php.

Fortes, M.D. and Lüning, K. 1980. Growth rates of North Sea macroalgae in relation to temperature, irradiance and photoperiod. Helgoländer-Meeresunters 34: 15-29.

Gärtner, H. and Schweingruber, F.H. 2013. Microscopic preparation techniques for plant stem analysis. Kessel Publishing House, Remagen. 78 p.

Hansen B.U., Christensen, L.H., Tamstorf, M.P., Lund, M., Højlund, S., Burup, M.L., Raundrup, K., Mastepanov, M., Westergaard-Nielsen, A. and Christensen, T.R. 2013. Nuuk Basic: The GeoBasis Programme. In Jensen, L.M., Rasch, M. and Schmidt, N.M. (eds.). Nuuk Ecological Research Operations, 6th Annual Report, 2012. Aarhus University, DCE – Danish Centre for Environment and Energy. 92 pp.

Hansen, B.U., Hill, K., Pedersen, S.H., Christensen, L.H., Tamstorf, M.P., Sigsgaard, C., Fruergaard, M., Lund, M., Raundrup, K., Mastepanov, M., Westergaard-Nielsen, A. and Christensen, T.R. 2012. Nuuk Basic: The GeoBasis Programme. In Jensen, L.M. (ed). Nuuk Ecological Research Operations, 5th Annual Report, 2011. Aarhus University, DCE – Danish Centre for Environment and Energy. 84 pp.

Hansen, B.U., Iversen, K.M., Tamstorf, M.P., Sigsgaard, C., Fruergaard, M., Højlund, S., Lund, M., Raundrup, K., Mastepanov, M., Falk, J.M., Ström, L., Westergaard, A., Rasmussen, B.H. and Christensen, T.R. 2010. Nuuk Basic: The GeoBasis Programme. In Jensen, L.M. and Rasch, M. (eds.). Nuuk Ecological Research Operations, 3rd Annual Report, 2009. National Environmental Research Institute, Aarhus University, Denmark. 80 pp.

Hebert, P.D.N., Cywinska, A., Ball, S.L. and de Waard, J.R. 2003. Biological identifications through DNA barcodes. Proceedings of the Royal Society of London. Series B: Biological Sciences 270: 313-321.

Heide-Jørgensen, M.P. and Laidre, K.L. 2007. Autumn space-use patterns of humpback whales (*Megapteranovaeangliae*) in West Greenland. Journal of Cetacean Research and Management 9: 121-126.

Heide-Jørgensen, M.P., Laidre, K.L., Hansen, R.G., Burt, M.L., Simon, M., Borchers, D.L., Hansen, J., Harding, K., Rasmussen, M., Dietz, R. and Teilmann, J. 2012. Rate of increase and current abundance of humpback whales in West Greenland. Journal of Cetacean Research and Management 12: 1-14.

ISO 1100-2 1998. Measurement of liquid flow in open channels – Part 2: Determination of stage-discharge relation, ISO 1100-2, International Organization for Standardization, Switzerland.

Iversen, K., Rasmussen, S. and Thorsøe, K. 2008. The ClimateBasis programme. In Jensen, L.M and Rasch, M. (eds.) Nuuk Ecological Research Operations, 1st Annual Report, 2007. Copenhagen, Danish Polar Centre, Danish Agency for Science, Technology and Innovation, Ministry of Science, Technology and Innovation. 111 pp.

Katona, S.K., Baxter, B., Brazier, O., Kraus, S., Perkins, J. and Whitehead, H. 1979. Identification of humpback whales by fluke photographs. The behavior of marine mammals. Pages 33-44 in Winn, H.E. and Olla, B.L. (eds). Behavior of marine mammal science. Volume 3. Cetaceans. Plenum press, New York, NY. 438 pp.

Kimura, M. 1980. A simple method for estimating evolutionary rates of base substitutions through comparative studies of nucleotide sequences. Journal of Molecular Evolution 16: 111-120.

Kolishchuk, V. 1990. Dendroclimatological study of prostrate woody plant. In Cook, E.R. and Kairiukstis, L.A. (eds). Methods of dendrochronology applications in the environmental sciences. Kluwer Academic Publishers, Dordrecht. 394 pp.

Krause-Jensen, D., Marbà, N., Olesen, B., Sejr, M.K., Christensen, P.B., Rodrigues, J., Renaud, P.E., Balsby, T.J.S. and Rysgaard, S. 2012. Seasonal sea ice cover as principal driver of spatial and temporal variation in depth extension and annual production of kelp in Greenland. Global Change Biology 18: 2981-2994.

Krogh, P.H., Wirta, H., Roslin, T., Gjelstrup, P., Gavor, Z., Jørgensen, E., Schmidt, N.M., Petersen, H., Raundrup, K., Nymand, J. and Aastrup, P. 2013. Barcoding of soil microarthropods in Kobbefjord. In Jensen, L.M., Rasch, M. and Schmidt, N.M. (eds.). Nuuk Ecological Research Operations, 6th Annual Report, 2012, Aarhus University, DCE – Danish Centre for Environment and Energy. 84 pp.

Marusik Y.M., Böcher J. and Koponen S. 2006. The collection of Greenland spiders (Aranei) kept in the Zoological Museum, University of Copenhagen. Arthropoda Selecta 15: 59-80.

Nehyba, S., Nývlt, D., Schkade, U., Kirchner, G. and Francu, E. 2011. Depositional rates and dating techniques of modern deposits in the Brno reservoir (Czech Republic) during the last 70 years. Journal of Paleolimnology 45: 41-55.

Pernosky, M., Hill, K., Hangaard, P., Larsen, M., Thorsøe, K., Knudsen, M. and Petersen, D. 2012. ClimateBasis programme. In Jensen, L.M and Rasch, M. (eds.). Nuuk Ecological Research Operations, 5th Annual Report, 2011. Aarhus University, DCE – Danish Centre for Environment and Energy. 92 pp.

Ratnasingham, S. and Hebert, P.D.N. 2013. A DNA-Based Registry for All Animal Species: The Barcode Index Number (BIN) System. PLoS ONE 8, e66213.

Schneider, C., Cruaud, C. and D'Haese, C.A. 2011. Unexpected diversity in Neelipleona revealed by molecular phylogeny approach (Hexapoda, Collembola). Soil Organisms 83: 383-398.

Strasser, R.J., Tsimilli-Micheal, M. and Srivastava, A. 2004. Analysis of the chlorophyll-a fluorescence transient. In Papageorgiou, G.C., Govindjee (eds.) Advances in Photosynthesis and Respiration, Springer, Berlin. Volume 19. 793 pp.

Tamstorf, M.P., Iversen, K.M., Hansen B.U., Sigsgaard, C., Fruergaard, M., Højlund, S., Andreasen, R.H., Mastepanov, M., Falk, J.M., Ström, L. and Christensen, T.R. 2009. Nuuk Basic: The GeoBasis Programme. In Jensen, L.M. and Rasch, M. (eds.). Nuuk Ecological Research Operations, 2nd Annual Report, 2008. National Environmental Research Institute, Aarhus University, Denmark. 80 pp.

Tamstorf, M. et al. 2008. Nuuk Basic: The GeoBasis programme. In Jensen, L.M. and Rasch, M. (eds). Nuuk Ecological Research Operations 1st Annual Report, 2007. Copenhagen, Danish Polar Centre, Danish Agency for Science, Technology and Innovation, Ministry of Science, Technology and Innovation. 112 pp.

Tamura, K., Stecher, G., Peterson, D., Filipski, A. and Kumar, S. 2013. MEGA6: Molecular Evolutionary Genetics Analysis Version 6.0. Molecular Biology and Evolution 30: 2725-2729.

Weijers, S., Broekman, R. and Rozema, J. 2010. Dendrochronology in the High Arctic: July air temperatures reconstructed from annual shoot length growth of the circumArctic dwarf shrub *Cassiope tetragona*. Quaternary Science Reviews 29: 3831-3842.

Young, M.R., Behan-Pelletier, V.M. and Hebert, P.D.N. 2012. Revealing the hyperdiverse mite fauna of subArctic Canada through DNA barcoding. Plos One 7(11): e48755.

Appendix

Day of Year

Regular years	Jan	Feb	Mar	Apr	May	Jun	Jul	Aug	Sep	Oct	Nov	Dec
1	1	32	60	91	121	152	182	213	244	274	305	335
2	2	33	61	92	122	153	183	214	245	275	306	336
3	3	34	62	93	123	154	184	215	246	276	307	337
4	4	35	63	94	124	155	185	216	247	277	308	338
5	5	36	64	95	125	156	186	217	248	278	309	339
6	6	37	65	96	126	157	187	218	249	279	310	340
7	7	38	66	97	127	158	188	219	250	280	311	341
8	8	39	67	98	128	159	189	220	251	281	312	342
9	9	40	68	99	129	160	190	221	252	282	313	343
10	10	41	69	100	130	161	191	222	253	283	314	344
11	11	42	70	101	131	162	192	223	254	284	315	345
12	12	43	71	102	132	163	193	224	255	285	316	346
13	13	44	72	103	133	164	194	225	256	286	317	347
14	14	45	73	104	134	165	195	226	257	287	318	348
15	15	46	74	105	135	166	196	227	258	288	319	349
16	16	47	75	106	136	167	197	228	259	289	320	350
17	17	48	76	107	137	168	198	229	260	290	321	351
18	18	49	77	108	138	169	199	230	261	291	322	352
19	19	50	78	109	139	170	200	231	262	292	323	353
20	20	51	79	110	140	171	201	232	263	293	324	354
21	21	52	80	111	141	172	202	233	264	294	325	355
22	22	53	81	112	142	173	203	234	265	295	326	356
23	23	54	82	113	143	174	204	235	266	296	327	357
24	24	55	83	114	144	175	205	236	267	297	328	358
25	25	56	84	115	145	176	206	237	268	298	329	359
26	26	57	85	116	146	177	207	238	269	299	330	360
27	27	58	86	117	147	178	208	239	270	300	331	361
28	28	59	87	118	148	179	209	240	271	301	332	362
29	29		88	119	149	180	210	241	272	302	333	363
30	30		89	120	150	181	211	242	273	303	334	364
31	31		90		151		212	243		304		365

Day of Year

Leap years	Jan	Feb	Mar	Apr	May	Jun	Jul	Aug	Sep	Oct	Nov	Dec
1	1	32	61	92	122	153	183	214	245	275	306	336
2	2	33	62	93	123	154	184	215	246	276	307	337
3	3	34	63	94	124	155	185	216	247	277	308	338
4	4	35	64	95	125	156	186	217	248	278	309	339
5	5	36	65	96	126	157	187	218	249	279	310	340
6	6	37	66	97	127	158	188	219	250	280	311	341
7	7	38	67	98	128	159	189	220	251	281	312	342
8	8	39	68	99	129	160	190	221	252	282	313	343
9	9	40	69	100	130	161	191	222	253	283	314	344
10	10	41	70	101	131	162	192	223	254	284	315	345
11	11	42	71	102	132	163	193	224	255	285	316	346
12	12	43	72	103	133	164	194	225	256	286	317	347
13	13	44	73	104	134	165	195	226	257	287	318	348
14	14	45	74	105	135	166	196	227	258	288	319	349
15	15	46	75	106	136	167	197	228	259	289	320	350
16	16	47	76	107	137	168	198	229	260	290	321	351
17	17	48	77	108	138	169	199	230	261	291	322	352
18	18	49	78	109	139	170	200	231	262	292	323	353
19	19	50	79	110	140	171	201	232	263	293	324	354
20	20	51	80	111	141	172	202	233	264	294	325	355
21	21	52	81	112	142	173	203	234	265	295	326	356
22	22	53	82	113	143	174	204	235	266	296	327	357
23	23	54	83	114	144	175	205	236	267	297	328	358
24	24	55	84	115	145	176	206	237	268	298	329	359
25	25	56	85	116	146	177	207	238	269	299	330	360
26	26	57	86	117	147	178	208	239	270	300	331	361
27	27	58	87	118	148	179	209	240	271	301	332	362
28	28	59	88	119	149	180	210	241	272	302	333	363
29	29	60	89	120	150	181	211	242	273	303	334	364
30	30		90	121	151	182	212	243	274	304	335	365
31	31		91		152		213	244		305		366